Angewandte Chemie
Eine Zeitschrift der Gesellschaft Deutscher Chemiker

Supporting Information

Phenotypic Discovery of Neuroprotective Agents by Regulation of Tau Proteostasis via Stress-Responsive Activation of PERK Signaling

*Young-Hee Shin, Hana Cho, Bo Young Choi, Jonghoon Kim, Jaeyoung Ha, Sang Won Suh, and Seung Bum Park**

anie_202013915_sm_miscellaneous_information.pdf
anie_202013915_sm_Movie_1.mp4
anie_202013915_sm_Movie_2.mp4
anie_202013915_sm_Movie_3.mp4
anie_202013915_sm_Movie_4.mp4
anie_202013915_sm_video_1.pptx

< Supporting Information >

Contents

Materials and Methods

Cell culture

BiFC-tau stable HEK293 human embryonic kidney cell line was kindly provided by Dr. Yun Kyung Kim, Korea Institute of Science and Technology (KIST), and was cultured in Dulbecco's Modified Eagle's Medium (DMEM) [Gibco] supplemented with 10% fetal bovine serum (FBS) [Gibco], 1% penicillin (100 units/mL)/streptomycin (100 μg/mL) [Gibco], Fungizone (0.25 μg/mL) [Gibco], and Geneticin (100 μg/mL) [Gibco]. SH-SY5Y human neuroblastoma cells (CRL-226, ATCC) were cultured in advanced DMEM/F12 [Gibco] supplemented with 10 % FBS, 1% penicillin/streptomycin, and Fungizone. All cells were maintained at 5% CO_2 in a 37 ℃ incubator and confirmed to be mycoplasma negative using EZ-Mycoplasma detection kit [DoGenBio].

Stable cell line generation using viral production and transduction

Lentiviral- and retroviral-expression systems were used to stably express DsRed_IRES_Tau-EGFP and mCherry-GFP-Tau in HEK293 cell line, respectively. The mCherry-GFP-Tau expression vector was constructed by insertion of the MAPT gene into the retroviral expression vector pBABE-puro mCherry-GFP-LC3 (gifted from Dr. Heesun Cheong, Division of Chemical Biology, Research Institute, National Cancer Center, Korea). For virus production, HEK293 cells were seeded in 100-mm culture dishes and co-transfected with 3 μg of lentiviral transfer plasmid encoding pLenti-DsRed_IRES_MAPT:EGFP (Addgene, #92196), 3 μg of pCMV-VSV-G envelope plasmid (Addgene, #8454), and 3 μg of psPAX2 packaging plasmid (Addgene, #12260) using Lipofectamine [ThermoFisher Scientific]. For virus production of the retroviral system, HEK293 cells were co-transfected with 3 μg of retroviral transfer plasmid encoding pBABE-puro mCherry-GFP-MAPT, 3 μg of pCMV-VSV-G envelope plasmid (Addgene, #8454), and 3 μg of pUMVC packaging plasmid (Addgene, #8449) using Lipofectamine [ThermoFisher Scientific]. HEK293 cells were infected by the addition of viral stock in six-well cell culture dishes overnight. Following the infection, cells were subjected to selection by addition of Geneticin or puromycin for 7–10 days. Cells were then further sorted by a double-positive (DsRed and EGFP, or mCherry and GFP) gating using FACS Aria II [BD Bioscience]. HEK293-DsRed-EGFP-Tau stable cell lines were cultured in DMEM supplemented with 10% FBS, 1% penicillin/streptomycin, Fungizone (0.25 μg/mL), and Geneticin (100 μg/mL), and maintained at 5% CO_2 in a 37 ℃ incubator.

siRNA transfection

For PDIA3 and DNAJC3 knockdown experiments, short interfering RNA (siRNA) duplex against PDIA3 and DNAJC3 were purchased from BIONEER. siRNA oligonucleotides were transfected in BiFC-tau stably expressing HEK293 cells using Lipofectamine RNAiMAX

[ThermoFisher Scientific] and Opti-MEM [Gibco] on the basis of manufacturer's instructions. Oligonucleotide sequences for PDIA3 and DNAJC3 are as follows:

siPDIA3 #1	sense	5′- CGUCCUUCACAUCUCACUA -3′
	antisense	5′- UAGUGAGAUGUGAAGGACG -3′
siPDIA3 #2	sense	5′- GAAAUACCAGGACCAGUUU -3′
	antisense	5′- AAACUGGUCCUGGUAUUUC -3′
siDNAJC3 #1	sense	5′- CUGCUAUAGCCUUCCUUGA -3′
	antisense	5′- UCAAGGAAGGCUAUAGCAG -3′
siDNAJC3 #2	sense	5′- GUGAUGGCUUUUACCUACU -3′
	antisense	5′- AGUAGGUAAAAGCCAUCAC -3′

Tau assembly monitoring and compound screening using BiFC-tau Venus HEK293 cell line

Phenotype-based screening to monitor tau assembly was performed using HEK293 BiFC-tau Venus cells in a high-throughput manner. Cells were seeded into 384-well plates at a density of 2.8×10^3 cells/well in 40 µL media for 24 h. Cells were treated with 80 nM thapsigargin [Sigma-Aldrich] in 10 µL media, then ~3,000-membered pDOS library compounds (10 µM) were treated using a 0.1 µL pinning tool. For the knockdown experiments, cells were transfected with 5 or 10 nM siRNAs using Lipofectamine RNAiMAX and incubated for 48 h, followed by thapsigargin treatment. After 24 h of incubation in a 37 ºC, 5% CO_2 incubator, nuclei were stained by medium-diluted Hoechst 33342 (2 µg/mL) [ThermoFisher] for 20 min. Plates were scanned in an INCell Analyzer 2000 [GE Healthcare] at $\lambda_{ex}/\lambda_{em}$ = 490/525 nm (for FITC channel) for Venus fluorescence and at $\lambda_{ex}/\lambda_{em}$ = 350/455 nm (for DAPI channel) for nuclei. Bright-field images were also taken to check the cell morphologies and images were analyzed to quantify Venus intensity per cell using Developer software [GE Healthcare].

Flow cytometry analysis using HEK293 DsRed−IRES−tau-EGFP cell line

HEK293 DsRed-IRES-tau-EGFP cells were treated with each compound for the designated time or were transfected with siRNAs using Lipofectamine RNAiMAX. The cells were trypsinized, suspended in phosphate-buffered saline (PBS), and subjected to FACS analysis using Aria II. Data were analyzed to measure the fluorescence intensity ratio of EGFP to DsRed per cell using flowing software 2.5.1. Mean values of GFP and DsRed fluorescence intensity per cell with double-positive gating were used for the analysis.

Immunoblotting

Cells were collected and lysed in modified radioimmunoprecipitation assay (RIPA) buffer (50 mM Tris–HCl, pH 7.8, 150 mM NaCl, 1% NP-40, 0.5% deoxycholate, 5 mM NaF, 2 mM Na_3VO_4, 1× Protease Inhibitor Cocktail [Roche]), followed by centrifugation at 200 g for 10 min at 4 ℃ for the whole-cell analysis and the determination of total protein concentration in each lysate using Pierce BCA Protein Assay Kit [ThermoFisher Scientific]. Equal amounts of each lysate were fractionated by PAGE, transferred to PVDF membrane [Bio-Rad], and blocked with 2% bovine serum albumin (BSA) [MP Biomedicals] in Tris Buffered Saline with Tween20 (TBS_T) [Sigma] for 1 h at room temperature. Membranes were probed with protein-specific antibodies overnight at 4 ℃. The next day, membranes were washed three times in TBS_T and incubated for 1 h at room temperature with anti-rabbit or anti-mouse horseradish peroxidase secondary antibody [Cell Signaling Technology] in 2% BSA in TBS_T. After washing, membranes were exposed to detection reagent [GE Healthcare] and quantified using chemiluminescence [Bio-Rad].

The following antibodies were purchased as primary antibodies for immunoblot studies: Rabbit anti-ph(T982)-PERK polyclonal antibody (Abcam, ab192591); rabbit anti-PERK monoclonal antibody (Cell Signaling Technology, 3192); rabbit anti-EIF2S1 (phospho S51) polyclonal antibody (Abcam, Ab32157); rabbit anti-ph-eIF2α (Ser51) monoclonal antibody (Cell Signaling Technology, 3597); mouse anti-eIF2α monoclonal antibody (santa cruz, sc-133132); rabbit anti-ATF4 monoclonal antibody (Cell Signaling Technology, 11815); mouse anti-CHOP monoclonal antibody (Cell Signaling Technology, 2895); mouse anti-Tau-5 monoclonal antibody (Abcam, ab80579); mouse anti-Tau-5 monoclonal antibody (Invitrogen, AHB0042); rabbit anti-Tau (phospho S199) monoclonal antibody (Abcam, ab81268); rabbit anti-Tau (phospho T231) monoclonal antibody (Abcam, ab151559); rabbit anti-Tau (phospho S396) monoclonal antibody (Abcam, ab109390); rabbit anti-DNAJC3 monoclonal antibody (Cell Signaling Technology, 2940); rabbit anti-ERp57 polyclonal antibody (Abcam, ab10287); mouse anti-P4HB monoclonal antibody (Abcam, ab2792); mouse anti-GFP monoclonal antibody (Cell Signaling Technology, 2955); rabbit anti-SQSTM1/p62 polyclonal antibody (Cell Signaling Technology, 51145); rabbit anti-LC3B polyclonal antibody (Abcam, ab51520); rabbit anti-BDNF monoclonal antibody (Abcam, ab108319); rabbit anti-GAPDH monoclonal antibody (Cell Signaling Technology, 2118).

TS-FITGE

Procedures for TS-FITGE was previously described.[1] Briefly, HEK293 BiFC-tau cells or SH-SY5Y cells were treated with dimethylsulfoxide (DMSO, 0.1 %), SB1607 (10 μM), and SB1617 (10 μM), respectively, in the absence or presence of thapsigargin (200 nM) for 3 h. Application of SB1607, a significantly less active compound comparing to SB1617, to TS-FITGE as a partial negative control enabled us to avoid a great number of protein lists that are non-specifically stabilized by SB16xx compounds during the target identification process. The cell suspension was heated at a range of the designated temperatures for 3 min, followed by 25

°C for 3 min. The heated cell was washed with PBS and resuspended in lysis buffer A (0.4 % NP-40 in PBS supplemented with Protease Inhibitor Cocktail). The cell suspension was freeze-thawed 3 times in liquid nitrogen for cell lysis. The cell lysate was clarified by centrifugation for 20 min at 20000 g, 4 °C. The protein concentration of the soluble fraction was quantified with Pierce BCA protein assay. 50 μg of the protein was precipitated with cold acetone followed by centrifugation for 7 min at 20000 g, 4 °C. The residual pellet was resuspended with 10 μl of conjugation buffer (30 mM Tris-HCl at pH 8.6, 2 M thiourea, 7 M urea, and 4% w/v CHAPS). 1 μl of 0.4 mM Cy2-*N*-hydroxysuccinimide (NHS) (for DMSO-treated group), Cy3-NHS (for SB1607-treated group), or Cy5-NHS (for SB1617-treated group) was mixed to the proteins and incubated at 4 °C for 45 min. The dye-conjugated proteomes were precipitated with cold acetone and resuspended with 50 μl of rehydration buffer (7 M urea, 2 M thiourea, 2% w/v CHAPS, 40 mM DTT, and 1% IPG buffer). The same amount of DMSO-treated, SB1607-treated, and SB1617-treated samples were mixed, then a total of 150 μg (50 μg for Cy2-, Cy3-, and Cy5-labeled each) of proteomes was loaded on a 24-cm Immobiline Drystrip gel [GE Healthcare]. Isoelectric focusing was done by Ettan IPGphor 3 [GE Healthcare] followed by polyacrylamide gel electrophoresis (PAGE) with Ettan DALTsix system [GE Healthcare]. The gel was scanned with Typhoon Trio [GE Healthcare]. The protein spot location and fluorescence signals were analyzed by Melanie [GE Healthcare, Version 9.2.3]. The Cy2- (DMSO), Cy3- (SB1607), and Cy5- (SB1617) fluorescent intensity of each protein spot on TS-FITGE images were quantified and normalized by Melanie. Normalized Cy5/Cy2 and Cy5/Cy3 were used for a scatter plot to visualize thermal stabilization only by SB1617. Experimentally reproducible spots from the double-positive area on the scatter plot (Cy5/Cy2 and Cy5/Cy3) were analyzed by LC-MS/MS analysis.

In-gel digestion and mass spectrometry. The protein spots from the silver-stained gel were excised, destained, and digested with trypsin. The mixture was evaporated in SpeedVac and then dissolved in 10% acetonitrile with 0.1% formic acid. The resulting peptides were desalted in a trap column (180 μm × 20 mm, Symmetry C18) and separated on a C18 reversed-phase analytical column (75 μm × 200 mm, 1.7 μm, BEH130 C18) [Waters]. Mass spectrometry was done by nanoAcquity UPLC-ESI-QTOF/MS (SYNAPT G2-Si HDMS) [Waters] with an electrospray ionization PicoTip (±10 μm i.d., New Objective). The data were converted to .pkl files by Protein Lynx Global Server and searched by MASCOT engine with the SwissProt database.

CETSA

HEK293 BiFC-tau cells were treated with DMSO (0.1%), SB1607 (10 μM), or SB1617 (10 μM), respectively, in the presence of thapsigargin (200 nM) for 3 h. The cell suspension was heated at a range of the designated temperatures for 3 min, followed by 25 °C for 3 min. The heated cell was washed with PBS and resuspended in lysis buffer A. The cell suspension

was freeze-thawed 3 times in liquid nitrogen for cell lysis. The cell lysate was clarified by centrifugation for 20 min at 20000 g, 4 °C. The same volume of clarified cell lysate was combined with SDS buffer, then subjected to immunoblotting.

Pulldown assay

SH-SY5Y cells were seeded on 6-well plates, then treated with 1 μM thapsigargin and 5 μM SB1624 (probe compound) in the presence or absence of 40 μM SB1617 for 2.5 h. Cells were exposed to 356 nm UV irradiation for 30 min on ice. After washing with cold PBS, cells were lysed in RIPA buffer and cleared by centrifugation at 20000 g for 15 min, 4 °C. The protein concentration of supernatants was determined by Pierce BCA Protein Assay Kit and the protein concentration was adjusted to 1 mg/mL. Click reaction was pursued on the proteome with biotin-azide (50 μM, Sigma Aldrich), TBTA (100 μM, Sigma Aldrich), $CuSO_4$ (1 mM, Sigma Aldrich), TCEP (1 mM, Sigma Aldrich), and *t*BuOH (5%) for 1 h. Cold acetone was added to the mixture for 20 min at –20 °C for the protein precipitation. After the centrifugation at 15000 g for 10 min, 4 °C, the pellet was dissolved in PBS containing 1.2% SDS by sonication and diluted to 0.2% sodium dodecyl sulfate (SDS) by adding PBS. The samples were incubated with 20 μL streptavidin agarose beads [Sigma Aldrich] by rotating for 3 h at room temperature. The beads were washed with PBS containing 0.2% SDS four times. The proteins were eluted by boiling with a 3× SDS sample buffer and analyzed by SDS-PAGE and western blot.

Surface plasmon resonance (SPR) assay

SPR experiments were performed using a Biacore T100 instrument [GE Healthcare]. Recombinant PDIA3 or DNAJC3 proteins were immobilized through amide bonds to a CM5 sensor chip [GE Healthcare] by activating the carboxyl group on the CM5 chip with a 1:1 mixture of *N*-ethyl-*N'*-(3-dimethylaminopropyl)-carbodiimide and *N*-hydroxysuccinimide. The protein immobilization reactions were carried out in PBS with 0.005% Tween 20 at pH 4.7 and pH 5.0 for PDIA3 and DNAJC3, respectively. Bindings between the compounds and proteins were monitored by flowing various concentrations of compounds in PBS (pH 7.3) containing 3% DMSO and 0.005% Tween 20 at 25 °C. Data were analyzed to calculate kinetic parameters by fitting sensorgrams with the 1:1 binding model using Biacore T100 Evaluation software [GE Healthcare].

PEG maleimide modification assay

Cysteine modification assay using PEG maleimide was carried out by following a paper.[2] After compound treatment, BiFC-tau HEK293 cells were washed with cold PBS and incubated with 20 mM *N*-ethylmaleimide (NEM, Sigma Aldrich) in PBS for 20 min on ice to alkylate the reduced form of cysteines. After washing with cold PBS, the cells were lysed in RIPA buffer. For the whole-cell analysis, lysates were centrifuged with 200 g for 5 min at 4 °C

to remove insoluble matters. The protein concentration of supernatants was determined by Pierce BCA Protein Assay Kit. Equal amounts of each lysate were treated with 12 mM tris(2-carboxyethyl)phosphine (TCEP, Sigma Aldrich) for 20 min at room temperature to reduce the oxidized forms of PDI. Lysates were incubated with 15 mM of methoxy polyethylene glycol 5000 maleimide (mPEG-mal_{5000}, Sigma Aldrich) for 1 h at room temperature. After adding with the SDS sample buffer to the lysates and brief vortex, SDS samples were directly used for SDS-PAGE and western blot.

RNA extraction and quantitative real-time PCR

To analyze the levels of autophagy-related genes, SH-SY5Y cells were treated with 1 μM thapsigargin in the presence or absence of 5 μM SB1617 for 8 h. Total RNA was extracted using the RNeasy kit [Qiagen] according to the manufacturer's instructions. RNA was quantified using NanoVue [GE Healthcare] and cDNAs were prepared with AccuPower CycleScript RT PreMix dT20 [Bioneer] according to the manufacturer's instructions. Quantitative RT-polymerase chain reaction (qRT-PCR) experiments were conducted with KAPA SYBR FAST ABI Prism qPCR Master Mix [KAPA Biosystems]. The data were analyzed by the comparative Ct method and normalized against housekeeping genes.

Live-cell imaging for mCherry-GFP-Tau fluorescence

DeltaVision Elite imaging system [GE Healthcare] was used for imaging of HEK293T cells stably expressing mCherry-GFP-Tau. For live-cell imaging, the chamber was maintained with 37 ºC, 5% CO_2 condition. Cells were treated with 100 nM thapsigargin and 40 μM SB1617 and monitored by real-time imaging. Images were obtained with a 60× scale, using mCherry/mCherry (excitation: 575/25 nm, emission: 625/45 nm), GFP/GFP (excitation: 475/28 nm, emission: 525/48 nm) filter sets. Images were analyzed and merged with SoftWorks deconvolution software.

Animals and ethics statement

CD-1 (ICR) male mice (2–3 months old, weight 25–35 g; DBL, Korea) were used for the TBI study. Mice were kept in an adjusted environment (22 ± 2 ℃, 55 ± 5% humidity, 12-h light/dark cycle with lights on at 8:00 am) and received a standard diet by Purina, Korea. All rats were given *ad libitum* access to water and food. To avert and minimize stress related to transportation, experiments were initiated after the animals were allowed 1 week of acclimatization to environmental conditions. The animal care protocol and experimental procedure were approved by the Committee on Animal Use for Research and Education at Hallym University (protocol # Hallym 2018-82), following the National Institutes of Health guidelines. This manuscript was also written in compliance with the Animal Research: Reporting In Vivo Experiments guidelines.[3]

Pharmacokinetic study

CD-1 (ICR) male mice (7 weeks old, KOATECH, Korea) were administrated with SB1617 (5% DMSO/35% PEG-400/65% DW) intravenously (5 mg/kg, 3.3 mL/kg) or intraperitoneally (5 mg/kg, 3.3 mL/kg), and blood was collected at the designated time points from orbital venous plexus. The concentration of SB1617 was investigated by LC-MS/MS analysis (Agilent 1200, 4000 Qtrap) from the plasma samples. Pharmacokinetic parameters were obtained from the plasma concentration−time plot using WinNonlin software [Pharsight, USA].

Blood-brain barrier penetration study

CD-1 (ICR) male mice (7 weeks old, KOATECH, Korea) were intraperitoneally (5 mg/kg, 3.3 mL/kg) administrated with SB1617 (5% DMSO/50% PEG-400/45% DW). Blood samples were collected in heparin-treated tubes at the designated time points (0.5 h and 3 h) from orbital venous plexus and the mice were sacrificed followed by the brain tissue harvest. Plasma and brain homogenate samples were analyzed by LC-MS/MS (Agilent 1260, Agilent 6460). The ratio of SB1617 in the brain to that in the plasma were calculated.

Experimental controlled cortical impact model for traumatic brain injury (TBI)

A controlled cortical impact (CCI) model of experimental TBI was performed as previously described.[4] Briefly, mice were deeply anesthetized with 3% inhaled isoflurane in a 70:30 mixture of nitrous oxide and oxygen using an isoflurane vaporizer [VetEquip], positioned in a stereotaxic apparatus [David Kopf Instruments], and maintained on 1–1.5% isoflurane. A craniotomy was made approximately 4 mm over the right hemisphere using a portable drill (2 mm lateral to the midline and 1 mm posterior to the bregma). Using a controlled cortical impact device (Leica Impact One, Leica Biosystems), a 2 mm flat-tip impactor was accelerated down to a 1.4 mm depth at a velocity of 5 m/sec. All rats were maintained at a core temperature of 36–37.5 °C with a homeothermic blanket control unit [Harvard Bioscience] during and after surgery, until ambulatory. Animals were assigned randomly to traumatic brain injury according to an online randomization tool (randomizer.org). Sham-operated groups only received craniotomy.

SB1617 administration for TBI experiments

To investigate the neuroprotective effects of SB1617 against brain injury after TBI, SB1617 was intraperitoneally administered twice per day at a dose of 5 mg/kg (5% DMSO/50% PEG-400/45% DW). Control group mice were treated intraperitoneally with equal volumes of vehicle.

Tissue preparation

Mice were deeply anesthetized with urethane (1.5 g/kg, intraperitoneal) in saline (0.9% NaCl) at a volume of 0.01 mL/g body weight. A toe pinch was used to evaluate the effectiveness of anesthesia. Then, mice were intracardially perfused with saline, followed by 4% paraformaldehyde in PBS. The brains were post-fixed with 4% paraformaldehyde for 1 h and immersed in 30% sucrose for cryoprotection. Thereafter, the entire brain was frozen and coronally sectioned on a cryostat microtome (CM1850, Leica) at 30 μm thickness.

Immunohistochemistry

Sections were immersed in 1.2% H_2O_2 for 20 min at room temperature to inhibit endogenous peroxidase activity. After washing in PBS, the sections were incubated with a mouse monoclonal anti-NeuN antibody (diluted 1:500; Millipore) in PBS containing 0.3% Triton X-100 at 4 ºC overnight to evaluate neuronal loss after TBI. After washing in PBS, the sections were incubated in biotinylated anti-mouse IgG (diluted 1:250; Vector) to detect NeuN antibody and biotinylated anti-rat IgG (diluted 1:250; Vector) to investigate the degree of leakage of endogenous immunoglobulin G after TBI for 2 h at room temperature. Thereafter, sections were immersed in the avidin-biotin-peroxidase complex [Vector] for 2 h at room temperature. Between incubations, the sections were washed with PBS. The immune reaction was visualized with 3,3'-diaminobenzidine [Sigma-Aldrich] in 0.01 M PBS containing 0.015% H_2O_2, and the sections were mounted on gelatin-coated slides. The immunoreactions were observed under an Olympus IX70 inverted microscope.

Immunofluorescence analysis

Immunofluorescence labeling was performed from routine immunostaining protocols as previously reported.[4b] Sections were immersed in 1.2% hydrogen peroxide for 15 min at room temperature to inhibit endogenous peroxidase activity. After washing in PBS, the sections were incubated with each specific type of polyclonal or monoclonal primary antibody in PBS containing 0.3% Triton X-100 at 4 ℃ overnight. Primary antibodies used in this study were as follows: mouse monoclonal anti-4-hydroxynonenal (4-HNE; diluted 1:500; Alpha Diagnostic International), mouse monoclonal anti-Tau (Tau5; diluted 1:500; Abcam), mouse monoclonal anti-phospho Tau (Ser202, Thr205; AT8; diluted 1:200; Invitrogen), and mouse monoclonal anti-PDI (diluted 1:100; Abcam). After washing in PBS, sections were applied with fluorescent-conjugated secondary antibodies (diluted 1:250; Invitrogen). Sections were counterstained with 4,6-diamidino-2-phenylindole (DAPI; diluted 1:1000; Invitrogen). Fluorescence-stained sections were mounted on gelatin-coated slides and coverslipped with DPX [Sigma-Aldrich]. The sections were photographed using a confocal microscope (LSM 710; Carl Zeiss).

Quantification of IHC/IF data

To count the NeuN-positive cells, every 6th sections were collected at an interval of 180 μm from 1.2 to 2.1 mm, posterior to the bregma. Five coronal sections were analyzed from each mouse using the microscope with a 20× objective. These sections were then coded and given to a blinded experimenter who counted the total number of NeuN-positive cells in the hippocampal CA1 and cortex from the ipsilateral hemisphere. Data were expressed as the average number of NeuN-positive cells per each region. To quantify PDI-, Tau5-, AT8-, 4HNE-immunofluorescence intensity, five coronal sections were evaluated by a blinded experimenter using ImageJ [National Institute of Health]. Briefly, the image was loaded into ImageJ and changed into 8-bit via the menu option (Image/Color/Split Channels). The image was binarized, and the menu option (Analyze/Measure) was selected, and then each immunofluorescence signal was expressed as the mean gray value.

Assessment of neurological deficits

To assess whether SB1617 administration attenuated TBI-induced neurological deficits, neurological function was evaluated by using a neurological severity score (NSS).[6] These tests were performed at 1, 12, 24, 48, 72 h, and 7 days after TBI or Sham surgery. The NSS assesses the functional neurological status of mice based on the presence of reflexes and the ability to perform motor (muscle status, abnormal movement) and behavioral tasks such as beam walking, beam balance, and spontaneous locomotion. This is graded from o to 10 (0 = normal function: 10 = maximal deficit). One point is awarded for failing to perform a particular task or for the lack of a tested reflex. Thus, a higher score implies a more severe injury.

Pole climbing test

Pole climbing test was performed to analyze the motor coordination of the mice.[7] Mice were placed head upward on the tip of the vertical pole (60 cm high with a rough surface). Thereafter, both time taken to orientate the body completely downwards (time to turn) and to reach the bottom with all four paws (time to finish) were recorded. The maximal testing time was 60 s. Each mouse was tested three times at the time points given followed by a calculation of means that were used for statistical analysis.

Statistical analysis

All statistical analyses were performed using the GraphPad Prism software (GraphPad, San Diego, CA, USA). For Figure 2E, statistical relevance was assessed using the one-way analysis of variance (ANOVA) test with Bonferroni's post hoc analysis. For Figure 2G, the statistical relevance of siRNA-treated groups compared to the scRNA-treated control was assessed using the one-way ANOVA test with Dunnett's post hoc analysis. For Figure 3F, statistical relevance was assessed using the two-way ANOVA test with Bonferroni's post hoc

analysis. For Figure 3G, multiple comparisons were performed within sets for each gene using the one-way ANOVA test with Bonferroni's post hoc analysis. For the *in vivo* results (Figure 4), comparisons were conducted using the repeated measures ANOVA test with Student-Newman-Keuls post hoc analysis. All data are presented per group as the mean ± standard error of the mean (SEM). A P value < 0.05 was considered significant.

Supplementary Figures

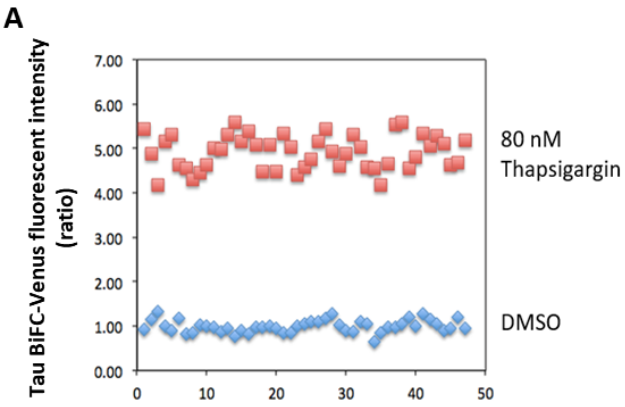

	avg	stdv	Z'
DMSO	1.0	0.1	
thapsigargin	4.9	0.4	0.6

$$\text{Z-factor} = 1 - \frac{3(\sigma_p + \sigma_n)}{|\mu_p - \mu_n|}$$

mean (μ), standard deviation (σ),
positive controls (μ_p, σ_p),
negative controls (μ_n,σ_n)

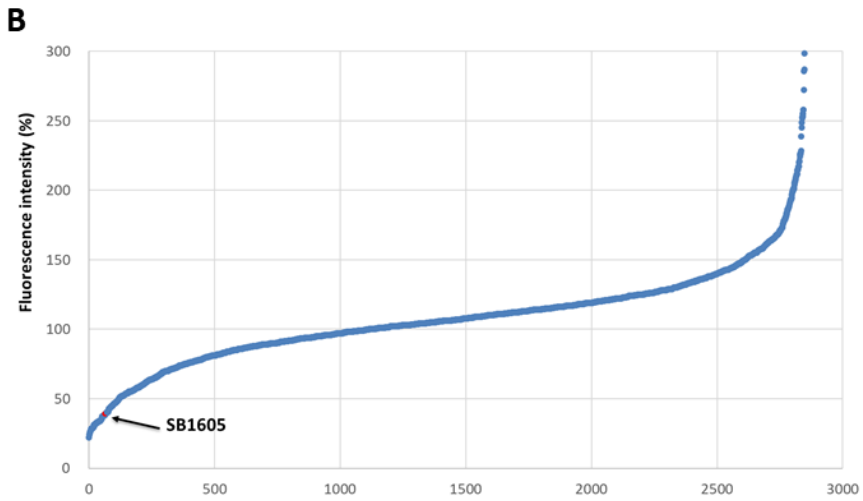

Figure S1. BiFC-tau screening system validation (Z′ factor > 0.5) and screening data. (A) The robustness of the high-throughput BiFC-tau screening system was validated by obtaining Z′-factor as higher than 0.5. Fold chances of fluorescent intensity in BiFC-tau Venus HEK293 cells were plotted and Z′- factor was calculated by applying the equation shown in (A). (B) Screening data using HEK293 BiFC-tau Venus cells. Hit compounds were selected below 50% of fluorescence intensity induced by thapsigargin treatment with >90% viability during the screening.

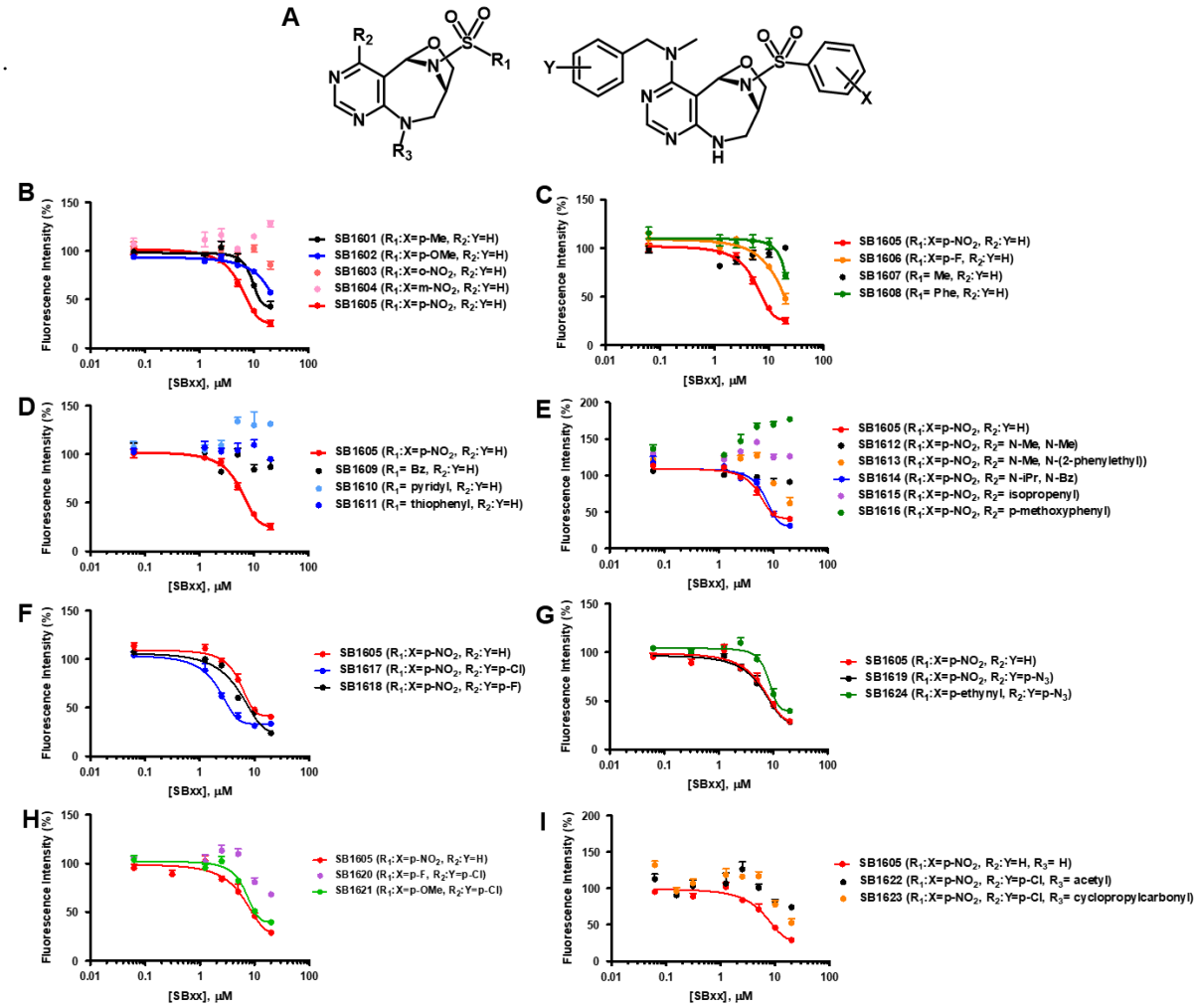

Figure S2. Structure-activity relationship study data. (A) Schematic representation of chemical structures of the pyrimidodiazepine analogues investigated for structure-activity relationship study. (B–I) Dose-dependency data of the compounds shown in (A) and Table S1 for the inhibition of BiFC-tau-Venus assembly. The varying concentrations of the compounds were co-treated with 80 nM thapsigargin to HEK293-BiFC-tau-Venus cells for 24 h. Data are shown as the mean ± SEM. IC_{50} values are listed in Table S1.

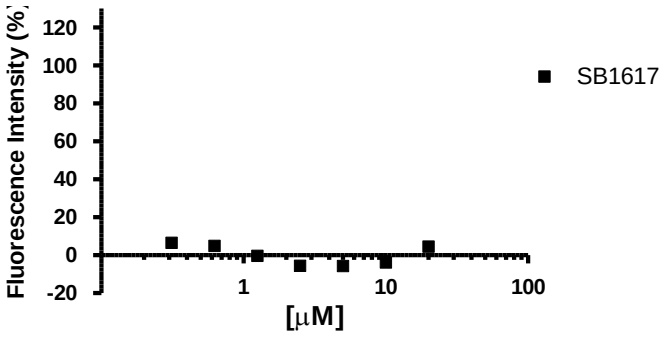

Figure S3. SB1617 treatment without thapsigargin did not alter BiFC-tau Venus-fluorescence intensity. The varying concentrations of SB1617 were treated to HEK293 BiFC-tau-Venus cells without thapsigargin for 24 h. Data are shown as the mean ± SEM.

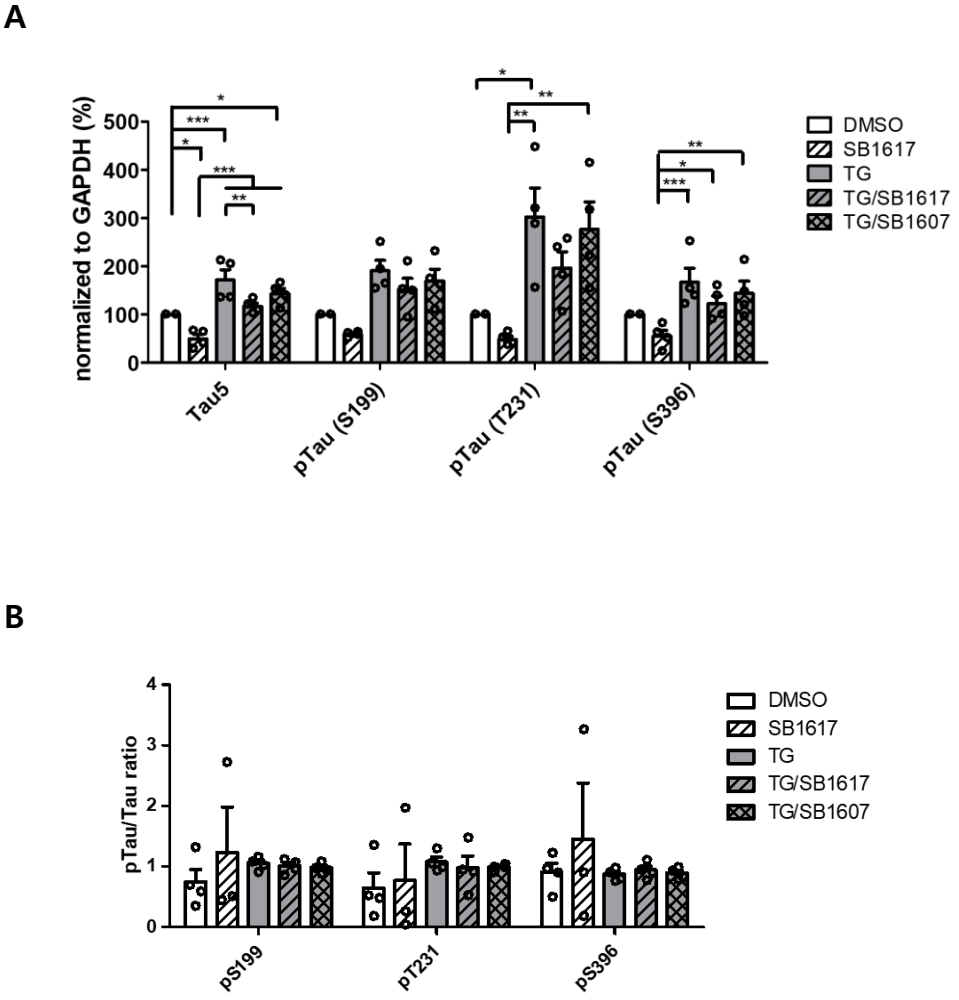

Figure S4. Quantification data of Figure 1C for total tau (Tau5) and phospho-tau (S199, T231, S396) levels (A), and for the ratio of p-tau to total tau (B) by western blot analysis upon treatment of 80 nM thapsigargin (TG) with either 5 μM of SB1617 or SB1607 for 20 h in BiFC-tau Venus HEK293 cells. TG treatment increased the levels of total tau as well as p-tau, whereas SB1617 treatment reduced the levels of both tau and p-tau increased by TG. However, there was no significant change in the ratio of p-tau to total-tau upon SB1617 treatment. Data are shown as the mean ± SEM. Multiple group comparisons were performed by one-way ANOVA with Bonferroni's multiple comparison analysis, * $P \leq 0.05$, ** $P \leq 0.01$, *** $P \leq 0.001$.

HEK293 DsRed-IRES-EGFP-Tau stable cells

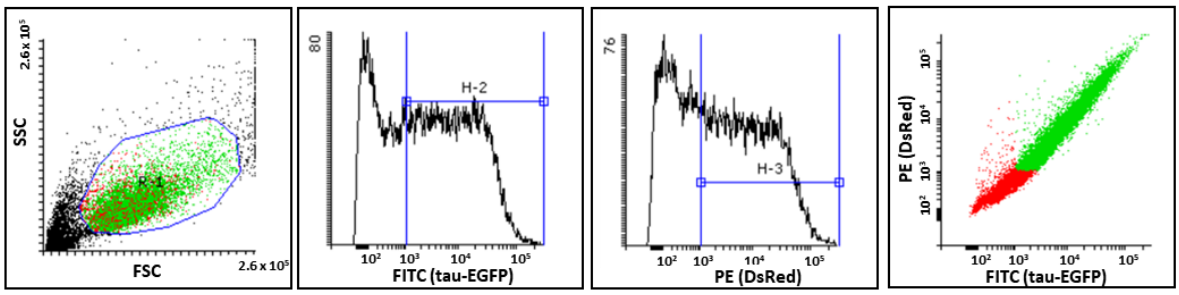

HEK293 cells

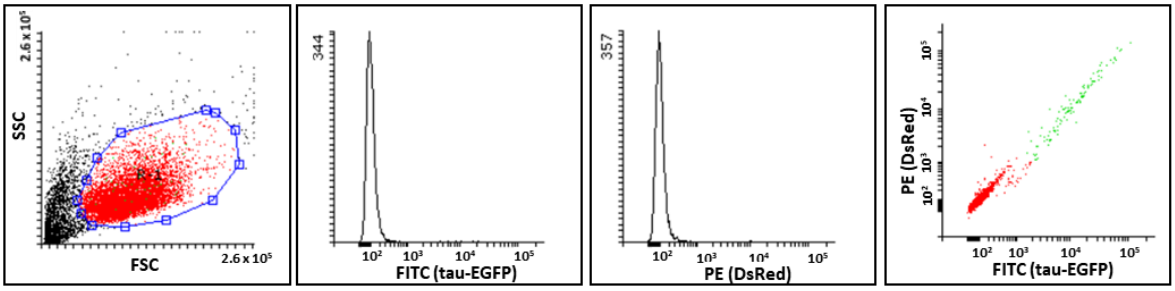

R-1 (red color, live cells), H-2 (FITC-positive), H-3 (PE-positive)
Green color: live and double-positive (FITC and PE)

Negative	events	% total	% Live
All events	10000	100	
R-1 (Live)	7623	76.23	100
R-1 and H-2 and H-3	116	1.16	**1.52**

Stable	Events	% total	% Live
All events	16879	100	
R-1	11637	68.94	100
R-1 and H-2 and H-3	8757	51.94	**75.34**

Figure S5. Post-sorted cell populations within HEK293 DsRed-IRES-EGFP-Tau stable cells were used for tau analysis. The stable cells showed more than 50-times population of double-positive cells (FITC- and PE-positive) compared to that of the negative cells (HEK293, not transfected). FITC channel: EGFP-tau; PE channel: DsRed.

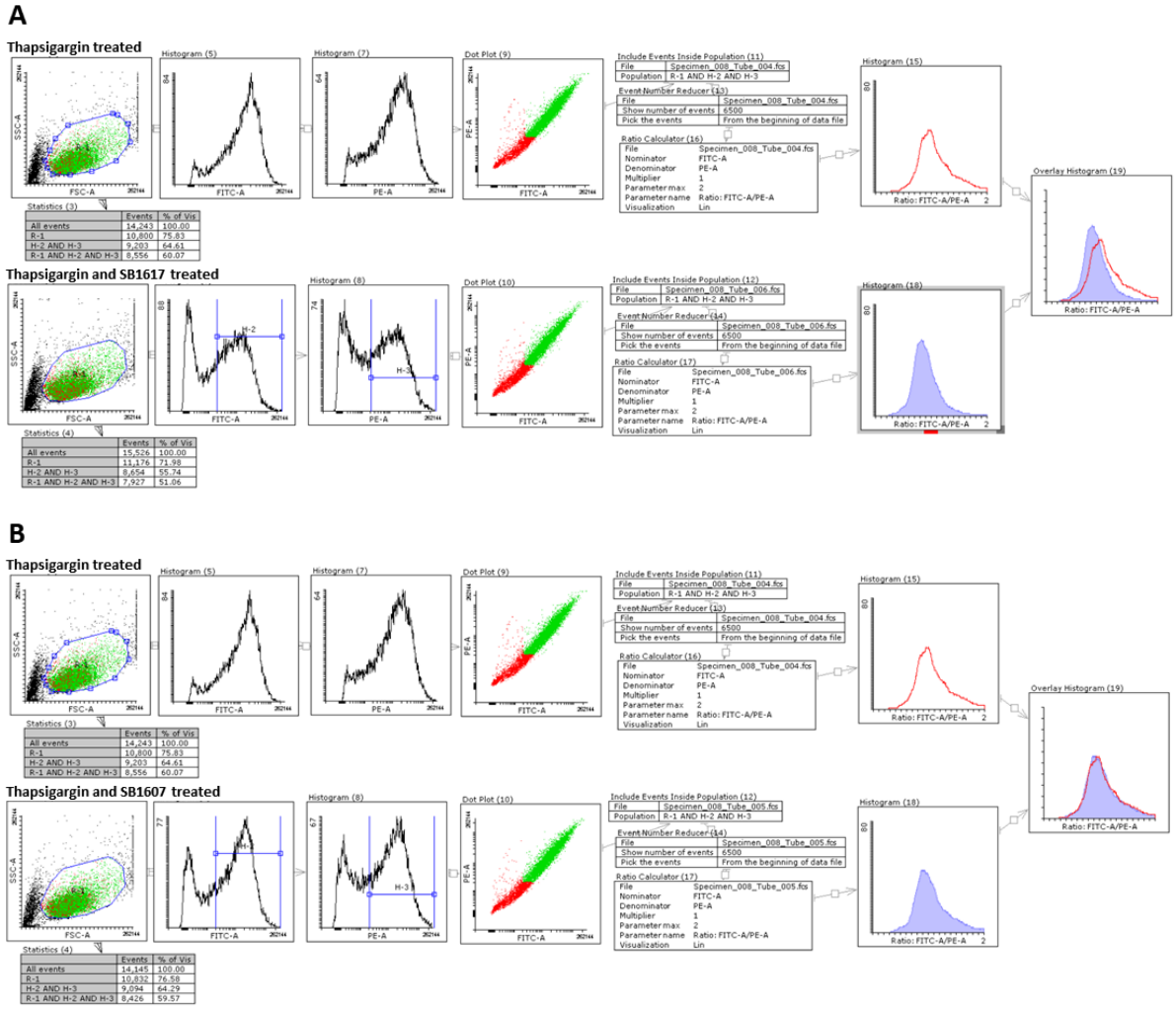

R-1 (red color, live cells), H-2 (FITC-positive), H-3 (PE-positive), **Green color**: live and double-positive (FITC and PE)

Figure S6. Gating strategy used for the investigation of tau proteostasis alterations in DsRed-IRES-EGFP-tau HEK293 cells. FITC-positive and PE-positive areas were determined as higher than 2×10^3 based on the signals from the negative cells (See Figure S4). We matched the total number of double-positive cells in each condition for fair comparison in FACS histogram, of which x-axis indicates FITC/PE intensity per cell (FITC channel: EGFP-tau; PE channel: DsRed). Representative data comparing thapsigargin-treated versus thapsigargin & SB1617-treated (A) or thapsigargin & SB1607-treated (B) cells are shown as overlaid histograms. Mean values of FITC/PE for each condition were converted to percentage values, then plotted as bar-graphs for statistical analysis.

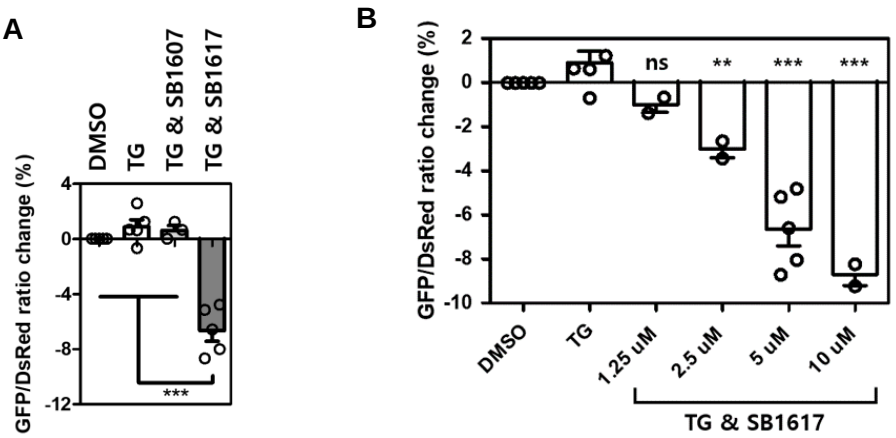

Figure S7. (A) Quantitative data of flow cytometry data in Figure 1G. DsRed-IRES-EGFP-tau HEK293 cells were treated with 100 nM TG together with either 5 μM of SB1617 or SB1607 for 20 h ($n \geq 4$). Multiple group comparisons were performed using one-way analysis of variance (ANOVA) with Bonferroni's post hoc analysis, ***$P \leq 0.001$. (B) Dose-dependency data of SB1617 in DsRed-IRES-GFP-tau HEK293 cells. Cells were treated with varying concentrations of SB1617 in the presence of 100 nM thapsigargin (TG) for 20 h. The fluorescence ratio of GFP to DsRed per cell was measured by FACS. Statistical significance for TG & SB1617-treated groups compared to the TG-treated group was assessed by one-way ANOVA with Dunnett's multiple comparison analysis., ns. $P > 0.05$, * $P \leq 0.05$, ** $P \leq 0.01$, *** $P \leq 0.001$. Data in (A) and (B) are shown as the mean ± SEM.

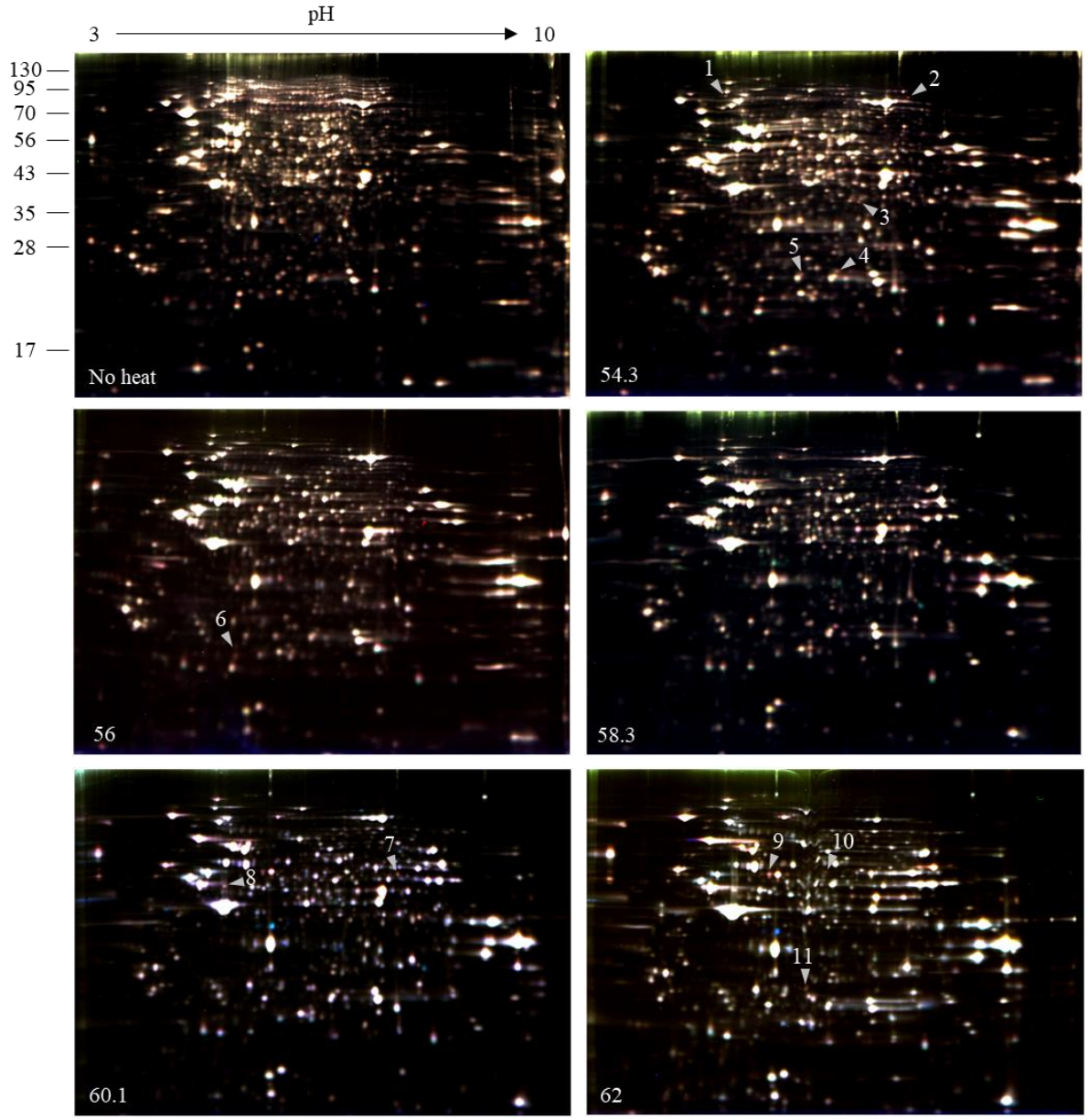

Figure S8. Full-range images of TS-FITGE 2D gels shown in Figure 2A. Merged gel images of Cy2- (blue, DMSO), Cy3- (green, SB1607), and Cy5- (red, SB1617) channels at the designated temperature. Reproducible red spots are marked with numbers (from 1 to 11). The identity of proteins from those spots are listed in Table S2.

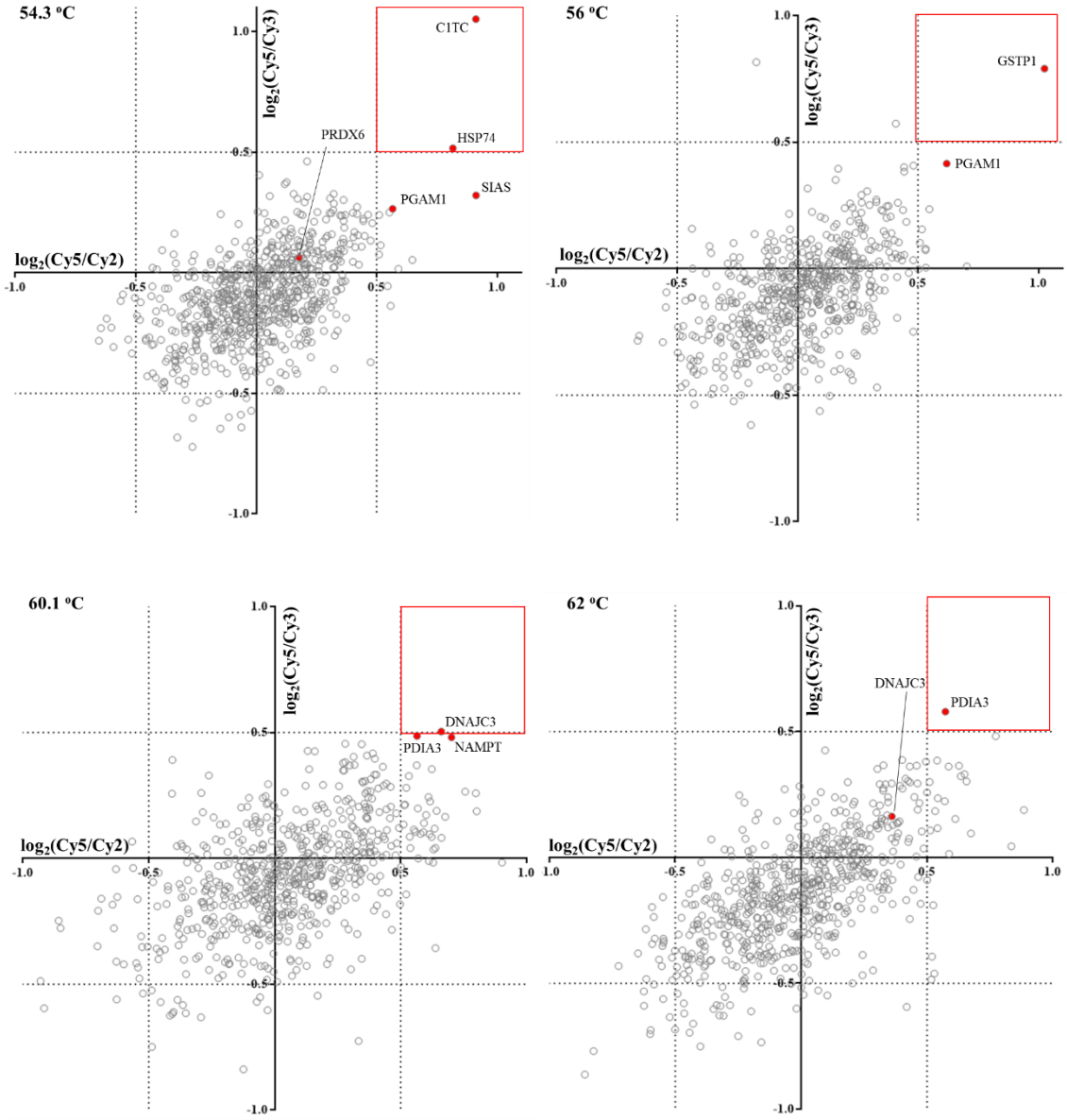

Figure S9. Quantification data of TS-FITGE in Figure S8. The Cy2- (DMSO, vehicle), Cy3- (SB1607, weakly active compound), and Cy5- (SB1617, active compound) fluorescent intensity of each protein spot on TS-FITGE images were quantified and normalized by Melanie (GE Healthcare, Version 9.2.3). Normalized Cy5/Cy2 and Cy5/Cy3 signals were used for the scatter plots to visualize the thermal stabilization only by SB1617. The red box in each scatter plot is the quadrant with protein spots with significant thermal stabilization. Red dots are the protein spots quantitatively selected from 2D gels at the dedicated temperature by Melanie software and confirmed their protein identity by LC-MS/MS analysis.

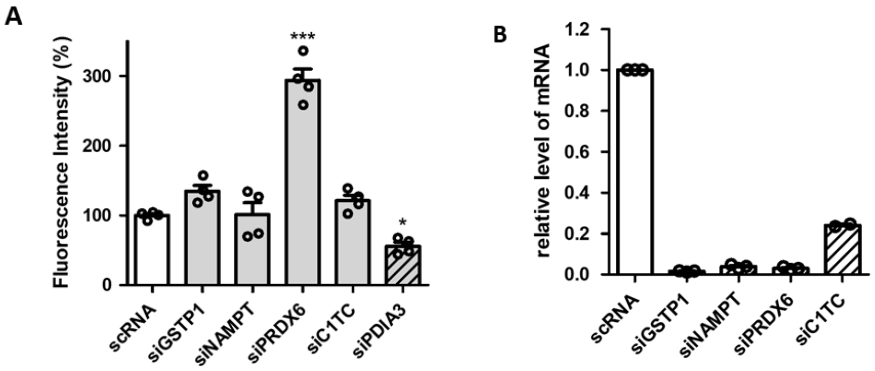

Figure S10. Target validation for candidate proteins identified from TS-FITGE results shown in Table S2. (A) BiFC-tau Venus HEK293 cells were transfected with siRNAs of each target candidate protein for 48 h then were treated with 80 nM thapsigargin for 20 h. Compared to the siPDIA3 (si1-PDIA3)-treated condition, other gene knockdown conditions did not reduce the BiFC-tau-Venus fluorescence intensity. Statistical significance of siRNA-treated groups compared to the scRNA-treated control was assessed by one-way ANOVA with Dunnett's multiple comparison analysis., ns. $P > 0.05$, * $P \leq 0.05$, ** $P \leq 0.01$, *** $P \leq 0.001$. Data are shown as the mean ± SEM. (B) The protein knockdown efficiency was demonstrated by qRT-PCR data. Cells were transfected with siRNAs for 48 h. Data are shown as the mean ± SEM.

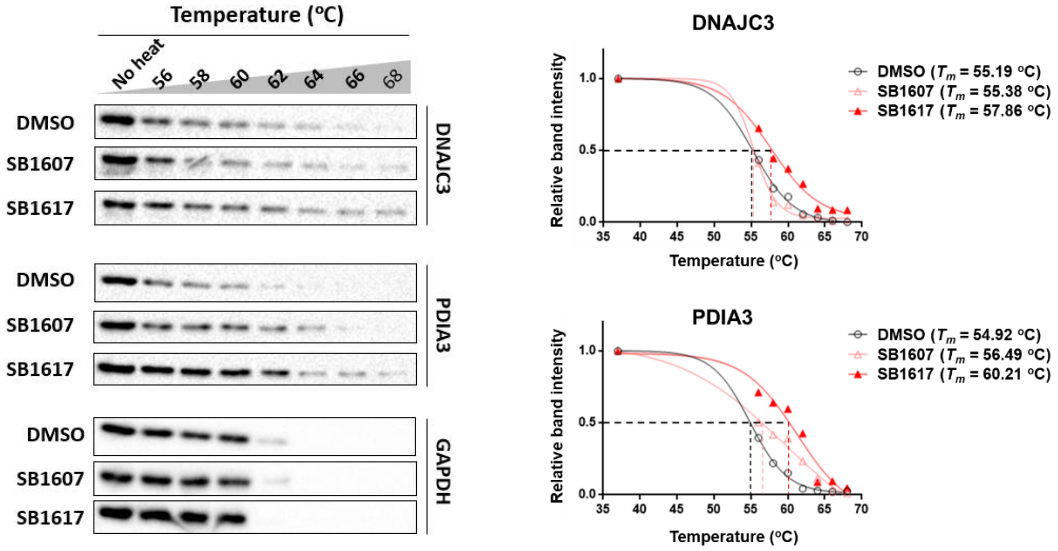

Figure S11. Representative images of cellular thermal stability shift assay (CETSA) data of SB1607- and SB1617-treated BiFC-tau Venus HEK293 cells toward DNAJC3, PDIA3, and GAPDH, visualized by immunoblotting. Quantified data are shown on the right side with T_m values. Both DNAJC3 and PDIA3 are thermally stabilized upon SB1617 treatment compared to the conditions with a vehicle or SB1607 treatment.

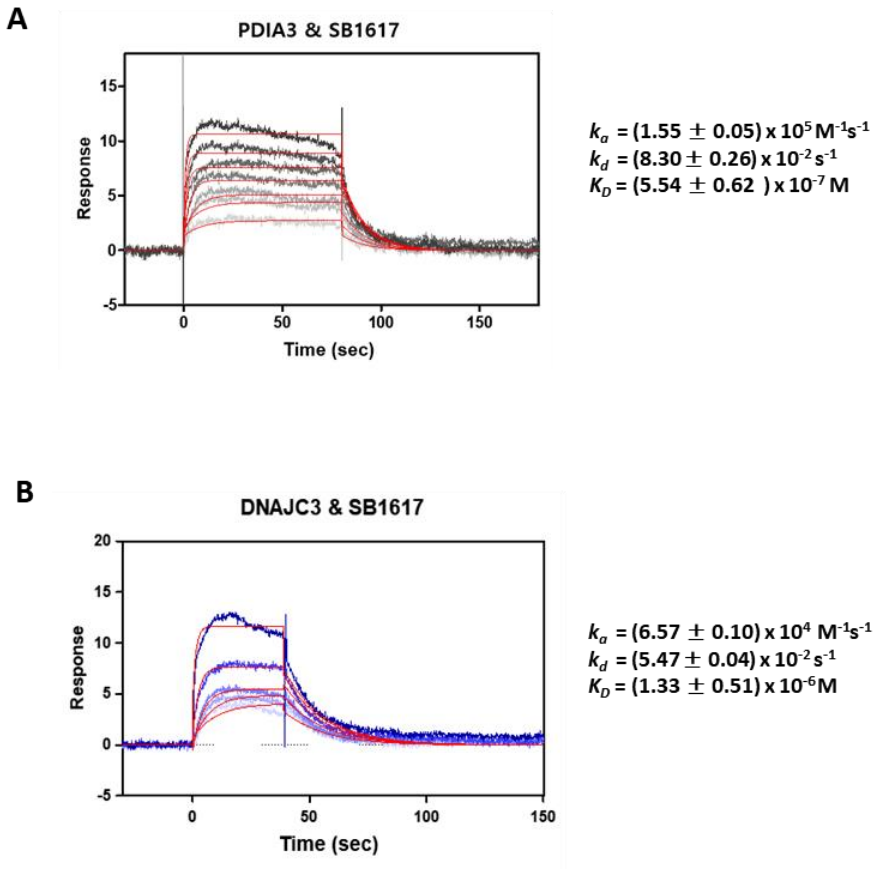

Figure S12. The biophysical kinetic studies of SB1617 toward the interactions with PDIA3 or DNAJC using surface plasmon resonance (SPR) spectroscopy. SPR data were used to investigate biophysical kinetics for the association (k_a), the dissociation (k_d), and the binding affinity (K_D) of SB1617 toward immobilized PDIA3 (A) and DNAJC3 (B) (n = 3). The overlaid SPR sensorgrams are from 0.125, 0.25, 0.5, 1.5, 3, 4, 6 μM of SB1617 in (A) and 0.625, 1.25, 2.5, 5, 10 μM of SB1617 in (B) in an order of increasing responses.

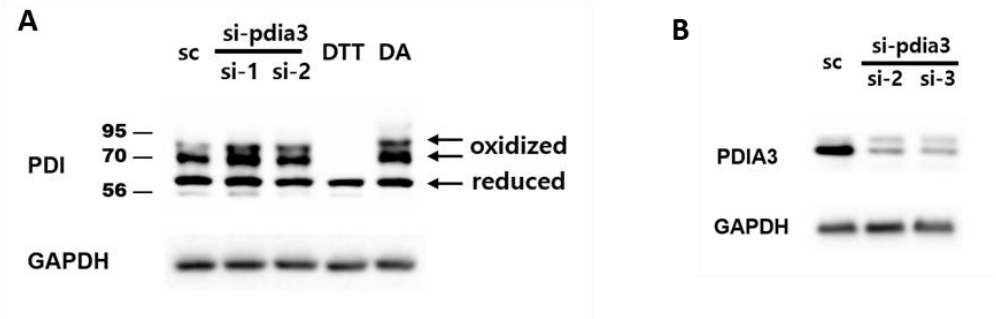

Figure S13. PEG-maleimide modification assay to monitor the oxidation status of PDI upon siRNA-based PDIA3 depletion. (A) Immunoblot data for PDI and GAPDH after PEG-maleimide modification upon siRNA treatment. Cells were treated with 10 mM 1,4-dithiothreitol (DTT) and 5 mM tetramethylazodicarboxamide (DA) for 15 min to obtain the reduced and oxidized forms of PDI, respectively. Oxidized forms of PDI were detected at the higher molecular weight than reduced PDI shown at 57 kDa. (B) Knockdown efficiency for PDIA3 was observed by anti-PDIA3 antibody. The data were taken from the cells depleted with PDIA3 using siRNAs but were not processed for the PEG-maleimide modification steps. Data shown in (A) and (B) were obtained from parallel experiments.

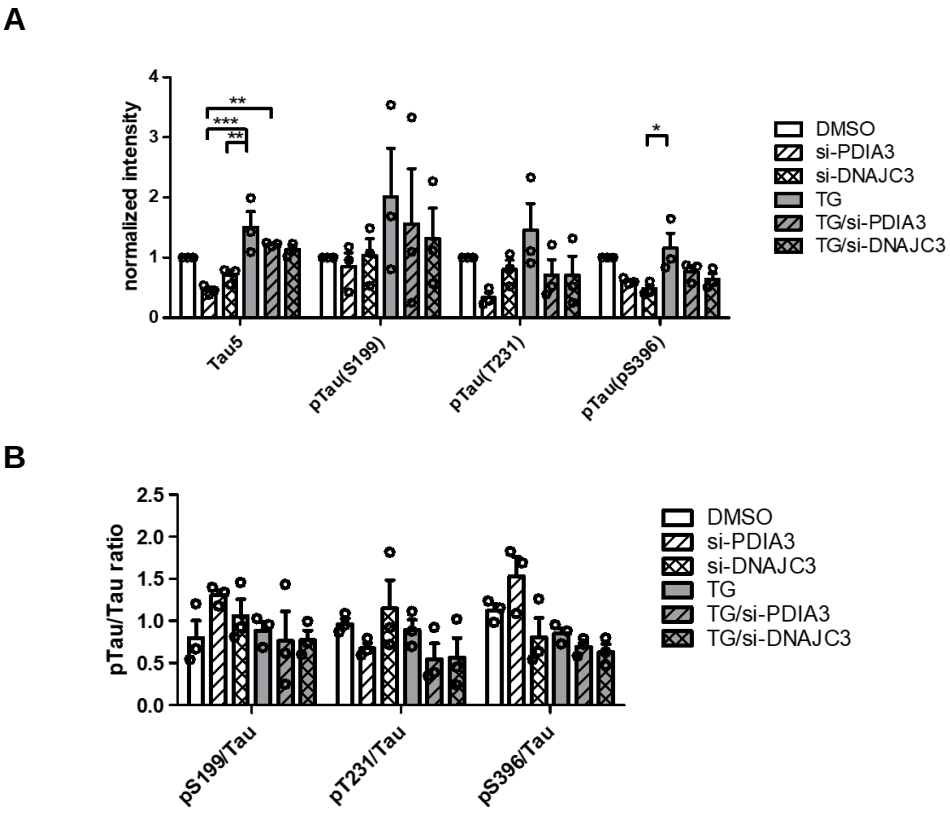

Figure S14. Quantification data of Figure 3A for total tau (Tau5) and phospho-tau (S199, T231, S396) levels (A), and for the ratio of p-tau to total tau (B) by western blot analysis. Depletion of either PDIA3 or DNAJC3 suppressed total-tau and p-tau levels in tau-overexpressing cells, whereas the depletion of either PDIA3 or DNAJC3 induced no significant changes in a ratio of p-tau to total-tau. Data are shown as the mean ± SEM. Multiple group comparisons were performed by one-way ANOVA with Bonferroni's multiple comparison analysis, * $P \leq 0.05$, ** $P \leq 0.01$, *** $P \leq 0.001$.

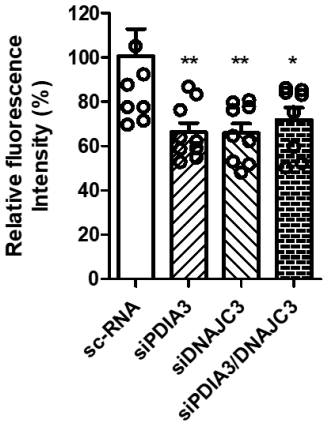

Figure S15. *PDIA3* and *DNAJC3* double knockdown effects on tau assembly inhibition in BiFC-tau Venus HEK293 cells. BiFC-tau cells were transfected with si1-PDIA3 and/or si1-DNAJC3 for 48 h, then treated with 80 nM thapsigargin for 20 h. For double knockdown experiments, a half concentration of siRNAs (5 nM) was used compared to that used in Figure 2E. Statistical significance of siRNA-treated groups compared to the scRNA-treated control was assessed by one-way ANOVA with Dunnett's multiple comparison analysis., * $P \leq 0.05$, ** $P \leq 0.01$. Data are shown as the mean ± SEM.

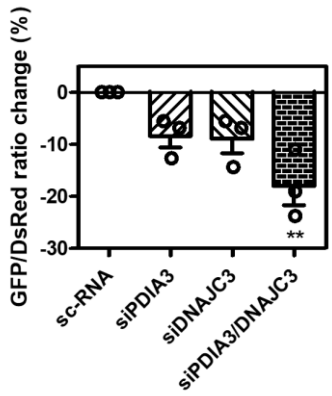

Figure S16. *PDIA3* and *DNAJC3* double knockdown effects on tau clearance in DsRed-IRES-EGFP-tau HEK293 cells. Cells were transfected with si2-PDIA3 and/or si1-DNAJC3 for 48 h, then treated with 100 nM thapsigargin for 20 h. The ratio between GFP/DsRed fluorescence intensity per cell was measured by FACS analysis. For double knockdown experiments, a half concentration of siRNAs (5 nM) was used compared to that used in Figure 2G. Statistical significance of siRNA-treated groups compared to the scRNA-treated control was assessed by one-way ANOVA with Dunnett's multiple comparison analysis., * $P \leq 0.05$, ** $P \leq 0.01$. Data are shown as the mean ± SEM.

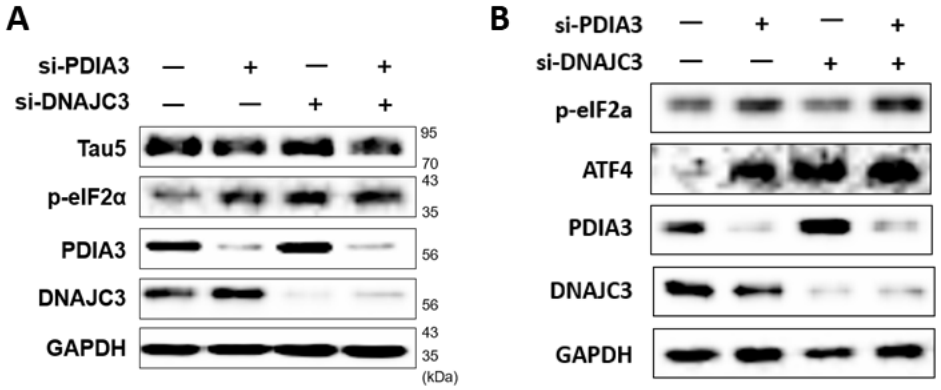

Figure S17. *PDIA3* and *DNAJC3* double knockdown effects on PERK signaling activation in BiFC-tau Venus HEK293 cells. BiFC-tau cells were transfected with si2-PDIA3 and/or si1-DNAJC3 for 48 h. PERK activation upon gene knockdown was confirmed by increased p-eIF2α (A) and enhanced ATF4 (B) levels in BiFC-tau cells.

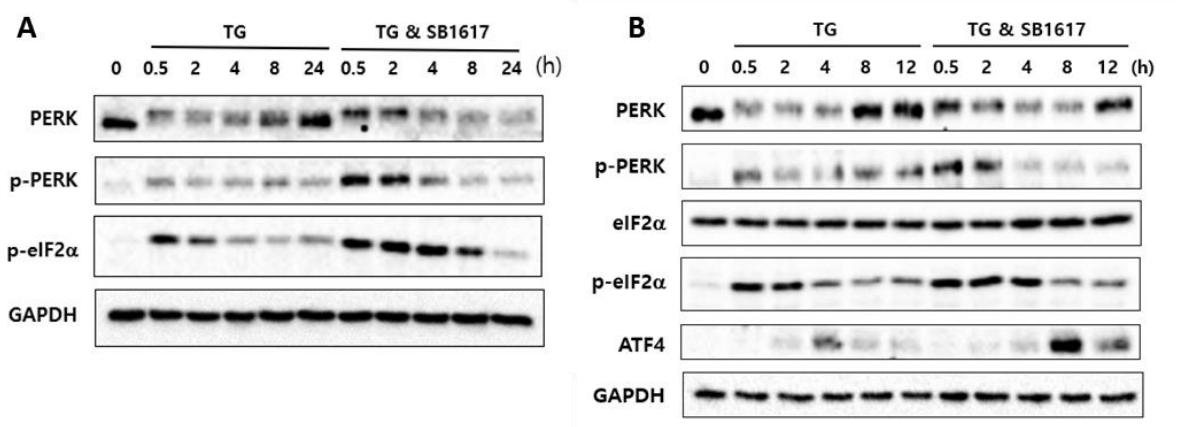

Figure S18. Investigation of the PERK signaling pathway by western blot analyses. PERK signaling pathway was investigated by western blot analyses upon treatment with thapsigargin (TG) with or without SB1617 up to 24 h. (A) PERK signaling activation by monitoring phospho-PERK and phospho-eIF2α up to 24 h. Human neuroblastoma SH-SY5Y cells were treated with 1 μM TG with or without 10 μM SB1617. (B) PERK activation (p-PERK, p-eIF2α, and ATF4) was promoted using a lower dosage of SB1617. SH-SY5Y cells were treated with 1 μM TG with or without 5 μM SB1617.

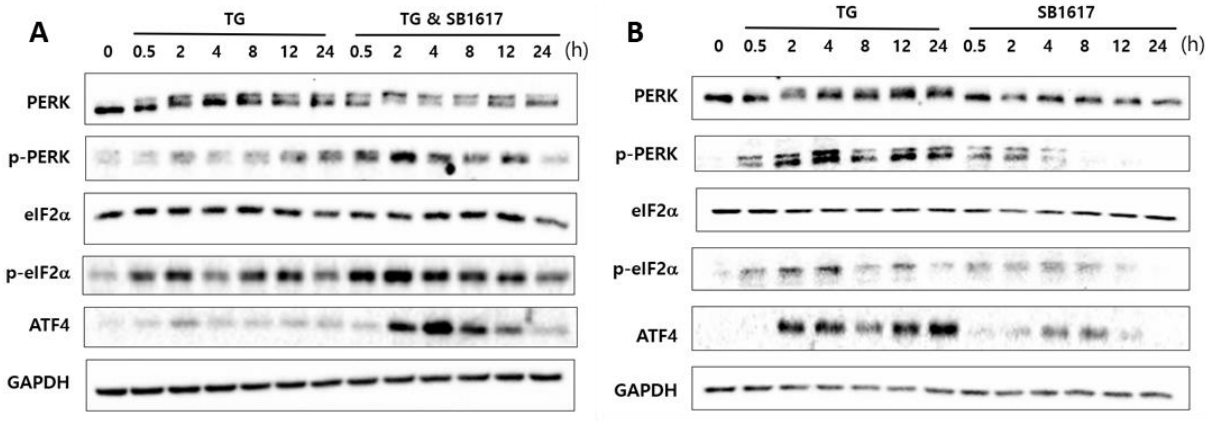

Figure S19. Conditional activation of the PERK signaling pathway by SB1617 treatment monitored using western blot analyses in BiFC-tau Venus HEK293 cells. (A) To mimic the ER stress condition, BiFC-tau cells were treated with 200 nM thapsigargin (TG) without or with 10 μM SB1617. (B) BiFC-tau cells were treated with 200 nM TG only or 10 μM SB1617 only.

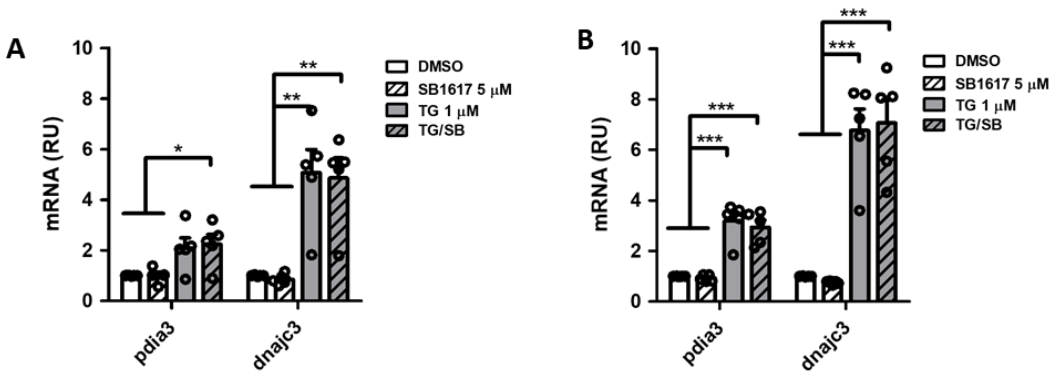

Figure S20. Upregulation of PDIA3 and DNAJC3 mRNA levels upon ER stress. mRNA levels of PDIA3 and DNAJC3 were assessed by RT-qPCR. SH-SY5Y human neuroblastoma cells were treated with 1 μM thapsigargin (TG) with or without 5 μM SB1617 for 4 h (A) and 8 h (B). All mRNA levels were normalized to GAPDH. Data are shown as the mean ± SEM. Multiple group comparisons were performed by one-way ANOVA with Bonferroni's multiple comparison analysis, * $P \leq 0.05$, ** $P \leq 0.01$, *** $P \leq 0.001$.

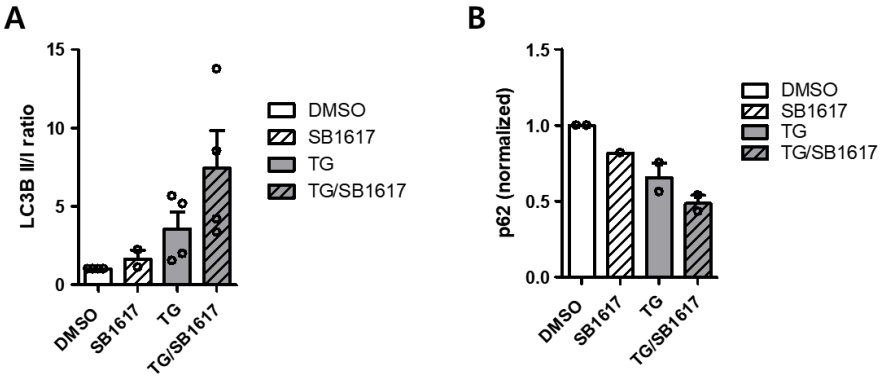

Figure S21. Quantification data of western blot analysis in Figure 3H for the ratio of LC3B-II to LC3B-I (A) and the level of p62 (B) upon treatment of 5 μM SB1617 in the absence and presence of 500 nM TG for 6–8 h in HEK293-BiFC-tau cells. Data are shown as the mean ± SEM.

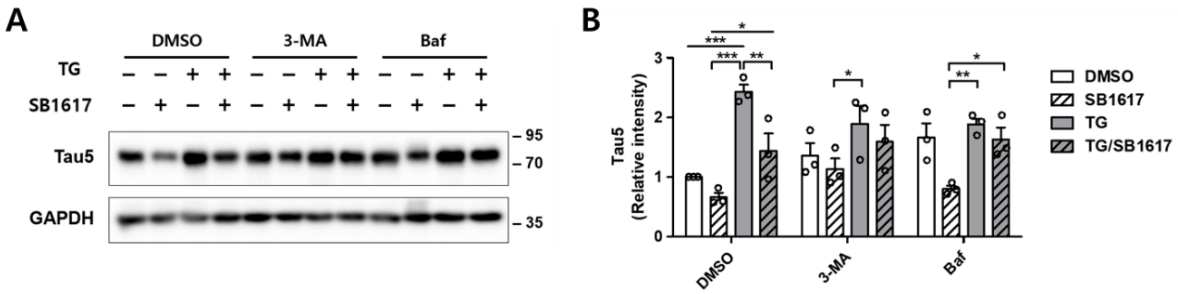

Figure S22. Representative data (A) and the quantitative data (B) of immunoblot analysis of total tau upon treatment for 18 h with SB1617 (5 μM) and TG (100 nM) in the absence and presence of the autophagy inhibitors, 3-methyladenine (3-MA, 5 mM) and bafilomycin A1 (Baf, 50 nM), in HEK293 BiFC-tau cells. Results are representative of at least three independent experiments. Data are shown as the mean ± SEM. Multiple group comparisons were performed by two-way ANOVA with Bonferroni's post hoc analysis, ns, $P > 0.05$*, $P \leq 0.05$, ** $P \leq 0.01$, *** $P \leq 0.001$.

A

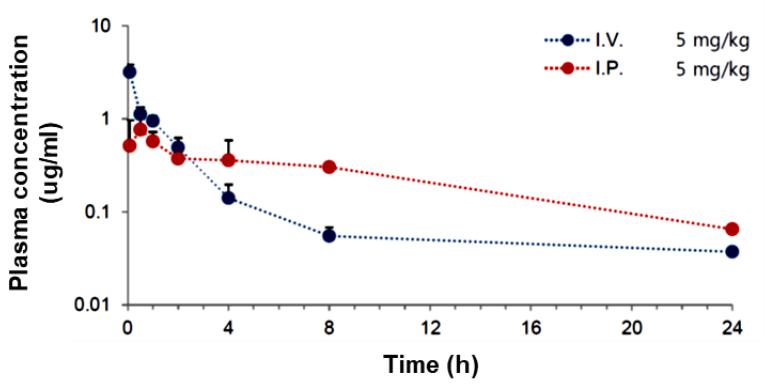

B

Parameters	I.V., 5 mg/kg	I.P., 5 mg/kg
T_{max} (h)	NA	1.67 ± 2.02
C_{max} (μg/mL)	NA	0.857 ± 0.339
$T_{1/2}$ (h)	5.51 ± 1.86	6.57 ± 0.0563
AUC_t (μg·h/mL)	4.19 ± 0.112	6.07 ± 2.81
AUC_∞ (μg·h/mL)	4.49 ± 0.15	5.65 ± 3.32
CL (L/h/kg)	1.12 ± 0.038	NA
V_{ss} (L/kg)	6.27 ± 0.928	NA

NA, not applicable

Figure S23. *In vivo* pharmacokinetic characterization of SB1617 using male ICR mice. (A) The concentration of SB1617 in plasma up to 24 h. Intraperitoneally (IP) injected data are shown in red dots and intravenously (IV) injected data are shown in blue dots. (B) Pharmacokinetic parameters. Data are shown as the mean ± SEM (male ICR mice, n = 3).

A

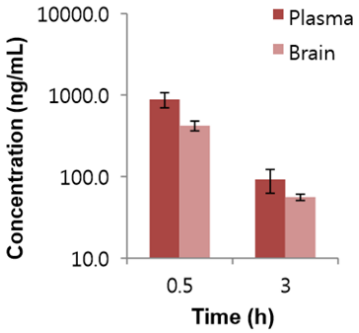

B

Time (h)	Concentration (ng/mL)		Brain/Plasma ratio
	Plasma	Brain tissue	
0.5	885 ± 187	421 ± 58.2	0.50 ± 0.14
3	92.4 ± 29.8	55.9 ± 5.00	0.66 ± 0.21

Figure S24. Evaluation of *in vivo* blood-brain barrier permeability of SB1617. SB1617 concentration in plasma and brain tissue at the indicated times. Male ICR mice were intraperitoneally injected with SB1617 as 5 mg/kg. Data are shown as the mean ± SEM (n = 3).

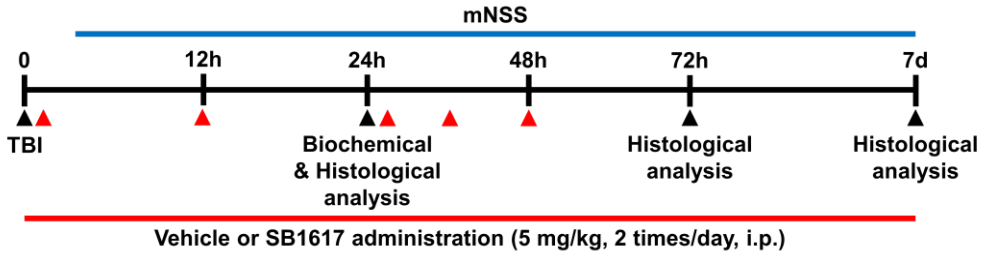

Figure S25. Timeline showing the *in vivo* experimental design with a TBI mouse model. Initial time points for vehicle/SB1617 injections are shown by red arrows. The first compound/vehicle injection is right after the TBI/sham surgery, and the second compound/vehicle injection is 12 h post-TBI/sham surgery for the investigation of 24 h vehicle/SB1617 treated condition (vehicle/SB1617 treated twice in total).

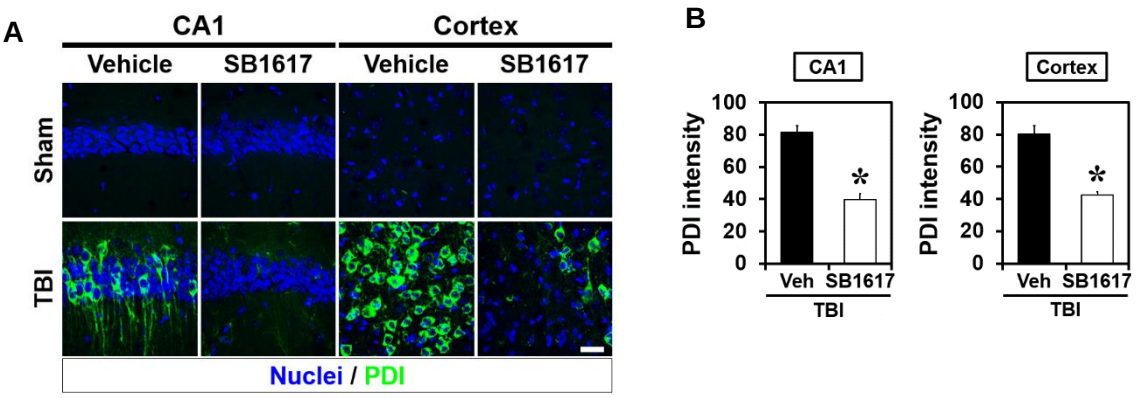

Figure S26. (A) Representative immunofluorescence images showing expression of the ER stress marker PDI in the ipsilateral hippocampal CA1 and cortex sections at 24 h after sham surgery or TBI. Scale bar, 20 μm. (B) Quantification of the expression of PDI. Data are represented as means ± SEM.; n = 3–6 from each group; * P < 0.05 versus vehicle-treated TBI group.

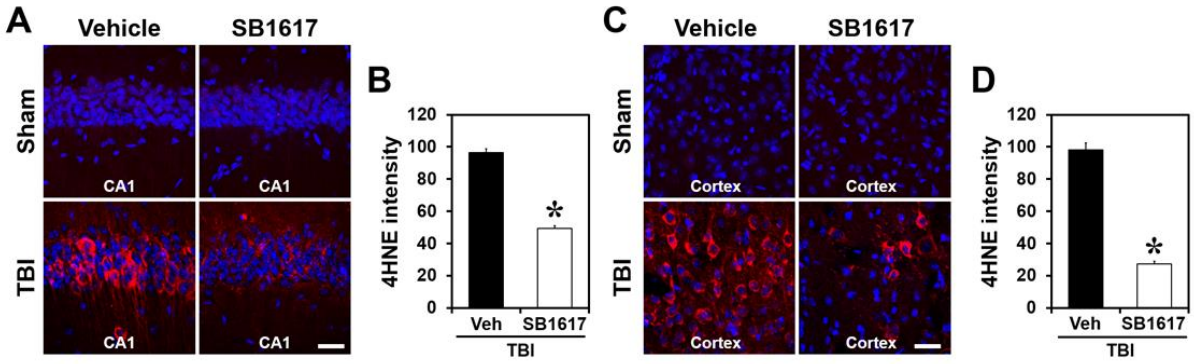

Figure S27. Representative immunofluorescence images showing expression of the oxidative stress marker 4HNE in the ipsilateral hippocampal CA1 (A) and cortex (C). Scale bar, 20 μm. Quantification of the intensity of 4HNE from ipsilateral hippocampal CA1 (B) and cortex (D). Data are mean ± SEM ; n = 3–6 from each group, * *P* < 0.05 versus vehicle-treated TBI group.

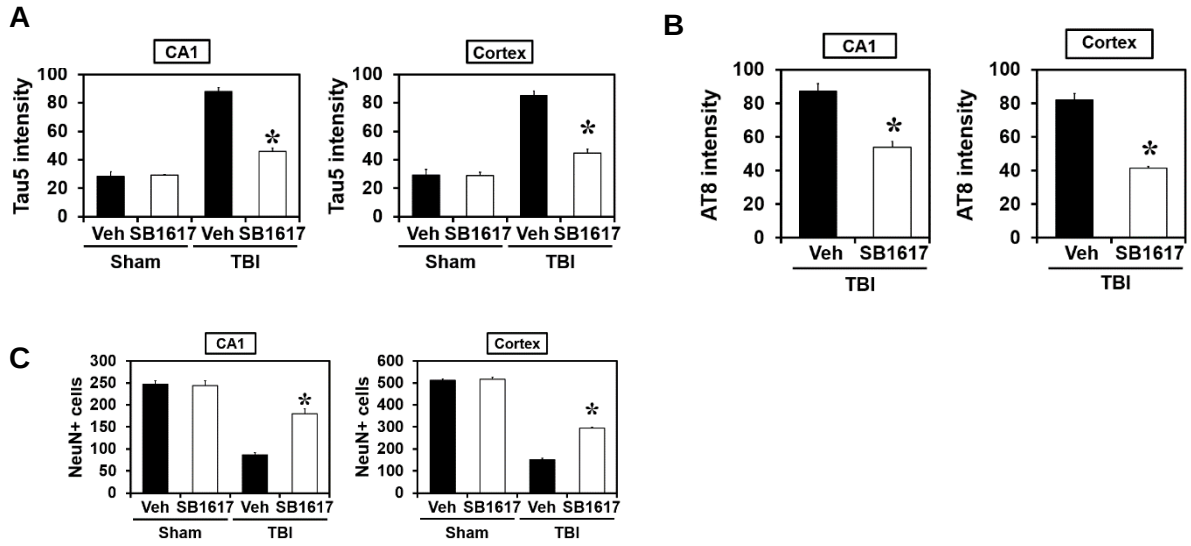

Figure S28. Quantitative data of Figures 5A–C. Ipsilateral hippocampal CA1 and cortex sections from vehicle- and SB1617-treated mice at 24 h (A, B) 72 h (C) after sham surgery or TBI were stained for total tau (A), phsopho-tau (B), and live neuronal cells (C) with anti-Tau5, anti-AT8, and NeuN, respectively. Data are represented as means ± SEM; n = 3–6 from each group; * $P < 0.05$ versus vehicle-treated group.

Supplementary Tables

Table S1. Description for the small molecule screening.

Category	Parameter	Description
Assay	Type of assay	Cell-based
	Target	Phenotype-based, HTS/HCS format
	Primary measurement	Fluorescence intensity per cell from BiFC-tau-Venus
	Key reagents	Thapsigargin
	Assay protocol	'Tau screening' section in methods
	Additional comments	The assay was adapted from ref [8].
Library	Library size	3,000 compounds
	Library composition	Small-molecules
	Source	In house synthesized library
	Additional comments	Details about parts of library design can be found in ref[9].
Screen	Format	384-well plates
	Concentration(s) tested	10 µM compound, 0.1 % DMSO
	Plate controls	In each plate, positive (thapsigargin and DMSO) and negative (DMSO), control active compound (thapsigargin and P52F08 as 70% inhibition for the BiFC-Venus fluorescence intensity, the compound is an unpublished molecule)
	Reagent/ compound dispensing system	Pin-tool 0.1 µL for screening compound treatment, multichannel pipette for thapsigargin treatment
	Detection instrument and software	INCell Analyzer 2000 (GE Healthcare), Developer software (GE Healthcare)
	Assay validation/QC	Z' score, 0.6 (Figure S1B)
	Normalization	DMSO control as 0 % and thapsigargin control as 100 %
Post-HTS analysis	Hit criteria	> 50 % inhibition, > 90 % viability, solubility
	Hit rate	4 %
	Additional assay(s)	Investigation of Tau and phospho-Tau by Western blot
	Confirmation of hit purity and structure	Compounds were resynthesized.

Table S2. Protein list obtained from the red spots of TS-FITGE images shown in fig. S4 by mass spectroscopy analyses. Column Etc. [a] Proteins selected for further target validation. [b] Proteins known to be non-specific binders to aliphatic chains *e.g.* linkers.[10]
[c] Proteins known to be non-specific binders from unpublished data.

Spot #	Match to	MW	Mascot Score	Quaries matched	Sequence Coverage (%)	Protein	Etc
1	HSP74_HUMAN	94240	347	20	30	Heat shock 70 kDa protein 4	*c*
2	C1TC_HUMAN	101495	721	82	38	C-1-tetrahydrofolate synthase, cytoplasmic	*a*
3	SIAS_HUMAN	40281	159	7	19	Sialic acid synthase	*b*
	ACAD8_HUMAN	45040	95	2	5	Acyl-CoA dehydrogenase family member 8, mitochondrial precursor	*c*
4	PGAM1_HUMAN	28786	151	10	37	Phosphoglycerate mutase 1	*b*
5	ECHM_HUMAN	31367	182	15	39	Enoyl-CoA hydratase, mitochondrial precursor	*c*
	PRDX6_HUMAN	25019	139	18	59	Peroxiredoxin-6	*a*
6	GSTP1_HUMAN	23341	305	23	56	Glutathione S-transferase P	*a*
7	NAMPT_HUMAN	55487	307	28	47	Nicotinamide phosphoribosyltransferase	*a*
	ATPA_HUMAN	59714	167	13	21	ATP synthase subunit alpha, mitochondrial precursor	*b*
8	TXND5_HUMAN	47599	472	34	43	Thioredoxin domain-containing protein 5 precursor	*c*
	ACTB_HUMAN	41710	395	25	38	Actin, cytoplasmic 1	*b*
	ATPB_HUMAN	56525	258	13	28	ATP synthase subunit beta, mitochondrial precursor	*1*
9	**PDIA3_HUMAN**	**56747**	**817**	**47**	**49**	**Protein disulfide-isomerase A3 precursor**	*a*
	VATB2_HUMAN	56465	177	14	31	Vacuolar ATP synthase subunit B, brain isoform	*c*
	ALBU_HUMAN	69321	155	9	9	Serum albumin precursor	*c*
10	**DNJC3_HUMAN**	**57544**	**67**	**8**	**13**	**DnaJ homolog subfamily C member3**	*a*
11	GSTO1_HUMAN	27548	171	19	48	Glutathione transferase omega-1	*c*

Table S3. Description of the Neurological severity score (NSS) for mice.

		Points	
Task	**Description**	**Success**	**Failure**
Exit circle	Ability and initiative to exit a circle of 30 cm diameter (time limit: 3 minutes)	o	1
Mono-/Hemiparesis	Paresis of upper and/or lower limb of the contralateral side	o	1
Straight walk	Alertness, initiative, and motor ability to walk straight, once the mouse is put on the floor	o	1
Startle reflex	Innate reflex; the mouse will bounce in response to a loud hand clap	o	1
Seeking behavior	Physiological behavior as a sign of "interest" in the environment	o	1
Beam balancing	Ability to balance on a beam of 7 mm width for at least 10 seconds	o	1
Round stick balancing	Ability to balance on a round stick of 5 mm diameter for at least 10 seconds	o	1
Beam walk: 3 cm	Ability to cross a 30 cm long beam of 3 cm width	o	1
Beam walk: 2 cm	Same task, increased difficulty on a 2 cm wide beam	o	1
Beam walk: I cm	Idem, increased difficulty on a 1 cm wide beam	o	1
Maximal score			10

*Mice are awarded one point for each failure to perform a task.

Table S4. DNA sequences of the primers used for Real-Time quantitative PCR.

Gene symbol	Primer sequence (5' → 3')	
	Forward	**Reverse**
ATF4	GTTCTCCAGCGACAAGGCTA	ATCCTCCTTGCTGTTGTTGG
ATG3	CCAACATGGCAATGGGCTAC	ACCGCCAGCATCAGTTTTGG
ATG5	AGTATCAGACACGATCATGG	TGCAAAGGCCTGACACTGGT
ATG12	GAGACCAGCCTGGTTAGCAA	CTGAACCCTCAGTGGCAAAC
NBR1	GGAAGCAGAAGAAGACCTGAGTG	CCAGAGTCTGTGAGGTCGTGAG
p62/SQSTM11	GTGGTAGGAACCCGCTACAA	GCGATCTTCCTCATCTGCTC
GABARAP	ACATTGCCTACAGTGACGAA	TTTCAGTCCCTTCCAACTAC
GABARAPL2	CGTGGAGTCCGCGAAGATTC	AGGCATGAGGACAATGCACA
GAPDH	ACCAGCCCCAGCAAGAGCACAAG	TTCAAGGGGTCTACATGGCAACTG
GSTP1	GACTACAACCTGCTGGACTTG	ATTGATGGGGAGGTTCACGTA
PRDX6	ACAATTGTGAAGAGCCCACAG	ACCAAAAACAAACACCACACG
C1TC	AAACCGAAGCCCATTGGTAAG	CCAGTCACCACCACGTATTTC
NAMPT	AGGGTTACAAGTTGCTGCCACC	CTCCACCAGAACCGAAGGCAAT
DNAJC3	AGATCGAGCAGAGGCCTATTT	TCTCGTTTCTGCGACTGTTTC
PDIA3	CTGAACCTATCCCAGAGAGCA	ATACTTGGGCTCCAGGTTCTT

Synthetic Procedures and Compound Characterization

General Information on Synthetic Protocols

NMR spectra were obtained on an Agilent 400-MR DD2 Magnetic Resonance System (400 MHz, Agilent, USA), Varian/Oxford As-500 (500 MHz, Varian Assoc., Palo Alto, USA), or Bruker Avance 600 MHz Cryo-NMR Spectrometer (600 MHz, Bruker, Germany). Chemical shift values were recorded as parts per million (δ), referenced to tetramethylsilane (TMS) as the internal standard, or to the residual solvent peak ($CDCl_3$, ^{1}H: 7.26, ^{13}C: 77.16, DMSO-d_6, ^{1}H: 2.50, ^{13}C: 39.52). Multiplicities were indicated as follows: s (singlet), d (doublet), t (triplet), q (quartet); m (multiplet); dd (doublet of doublet); dt (doublet of triplet); td (triplet of doublets); br s (broad singlet), br d (broad doublet) and so on. Coupling constants were reported in hertz (Hz). IR spectra were measured on a Thermo Scientific Nicolet 6700 FT-IR spectrometer. High-resolution mass spectra were analyzed at the Mass Spectrometry Laboratory of National Instrumentation Center for Environmental Management (NICEM) at Seoul National University on a LCQ LC/MS (Thermo) using the electrospray ionization (ESI) method or by Ultra High-Resolution ESI Q-TOF mass spectrometer (Bruker). Commercially available reagents were obtained from Sigma-Aldrich, TCI, Acros, or Alfa Aesar, and used without further purification unless noted otherwise. All solvents were obtained by passing them through activated alumina columns of solvent purification systems from Glass Contour. Analytical thin-layer chromatography (TLC) was performed using Merck Kiselgel 60 F_{254} plates, and the components were visualized by observation under UV light (254 and 365 nm) or by treating the plates with ninhydrin followed by thermal visualization. Flash column chromatography was performed on Merck Kieselgel 60 (230–400 mesh).

General procedure for the preparation of 1–9

The synthesis of the **1–9** was previously reported [see: Kim, J. *et al*. Diversity-Oriented Synthetic Strategy for Developing Chemical Modulator of Protein-Protein Interaction. *Nat. Commun.* **7**, 13196 (2016)].[11]

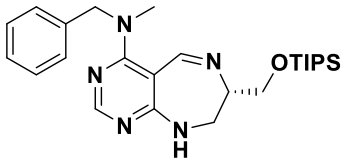

1

Compound 1. The synthesis and characterization of compound **1** were identical to the previous report.[11]

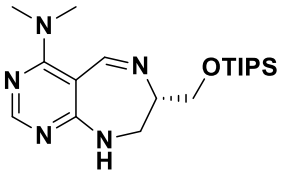

2

Compound 2. A light yellow solid; R_f = 0.15 (DCM/MeOH = 20:1); 62 % overall yield; ^{1}H NMR (400 MHz, $CDCl_3$) δ 8.04 (br d, *J* = 2.0 Hz, 1H), 7.98 (s, 1H), 6.68 (br s, 1H), 4.16 (dd, *J* = 9.8, 4.7 Hz, 1H), 3.83 (m, 2H), 3.64 (t, *J* = 10.0 Hz, 1H), 3.28 (ddd, *J* = 12.8, 6.9, 2.2 Hz, 1H), 3.09 (S, 6H), 1.10 (m, 21H); ^{13}C NMR (100 MHz, $CDCl_3$) δ 167.4, 162.2, 157.7, 157.1, 92.4, 65.2, 64.5, 47.4, 42.0, 18.1, 12.0; HRMS(ESI+): Calcd for $C_{19}H_{36}N_5OSi^+$ $[M+H]^+$ 378.2684, found 378.2682, Δppm –0.53; mp: 76–78 °C.

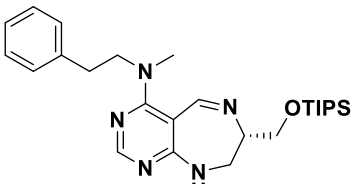

3

Compound 3. A yellow oil; R_f = 0.36 (DCM/MeOH = 20:1); 61 % overall yield; ^{1}H NMR (400 MHz, $CDCl_3$) δ 8.01 (s, 1H), 7.96 (s, 1H), 7.27 (m, 2H), 7.20 (m, 3H), 6.74 (br s, 1H), 4.18 (dd, *J* = 9.8, 4.3 Hz, 1H), 3.89 (m, 3H), 3.67 (t, *J* = 10.2 Hz, 1H), 3.60 (m, 1H), 3.30 (dd, *J* = 11.0, 7.4 Hz, 1H), 3.09 (s, 3H), 2.96 (m, 2H), 1.13 (m, 21H); ^{13}C NMR (100 MHz, $CDCl_3$) δ 167.1, 162.1, 157.8, 157.0, 139.0, 128.8, 128.6, 126.5, 92.7, 65.2, 64.4, 54.8, 47.5, 40.8, 34.1, 18.1, 12.0; HRMS(ESI+): Calcd for $C_{26}H_{42}N_5OSi^+$ $[M+H]^+$ 468.3153, found 468.3151, Δppm –0.43;

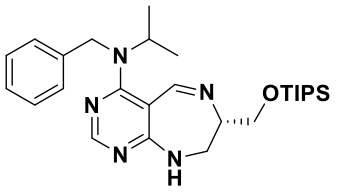

4

Compound 4. A yellow oil; R_f = 0.42 (DCM/MeOH = 20:1); 57 % overall yield; ^{1}H NMR (400 MHz, $CDCl_3$) δ 8.24 (d, *J* = 2.0 Hz, 1H), 8.00 (s, 1H), 7.27–7.15 (m, 5H), 6.40 (br s, 1H), 4.85 (d, *J* = 15.3 Hz, 1H), 4.38 (d, *J* = 15.3 Hz, 1H), 4.19 (dd, *J* = 9.6, 4.5 Hz, 1H), 4.04 (m, 1H), 3.78 (m, 2H), 3.65 (t, *J* = 9.8 Hz, 1H), 3.25 (ddd, *J* = 12.9, 7.0, 2.3 Hz, 1H), 1.37 (d, *J* = 6.3 Hz, 3H), 1.24 (d, *J* = 6.7 Hz, 3H), 1.12 (m, 21H); ^{13}C NMR (100 MHz, $CDCl_3$) δ 168.1, 162.3, 157.2, 157.1, 139.8, 128.3, 127.6, 126.7, 96.4, 65.2, 64.8, 56.7, 47.2, 45.9, 21.2, 20.7, 18.1, 12.0; HRMS(ESI+): Calcd for $C_{27}H_{44}N_5OSi^+$ $[M+H]^+$ 482.3310, found 482.3313, Δppm +0.62;

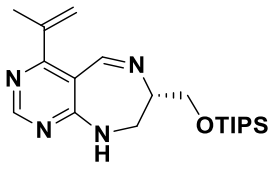

5

Compound 5. The synthesis and characterization of **5** were identical to the previous report.[11]

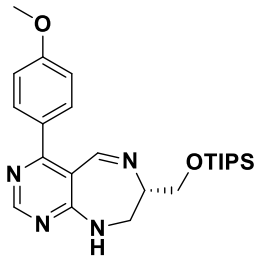

6

Compound 6. A yellow oil; R_f = 0.5 (DCM/MeOH = 20:1); 61% overall yield; ^{1}H NMR (500 MHz, $CDCl_3$) δ 8.52 (s, 1H), 8.27 (s, 1H), 7.58 (d, *J* = 8.3 Hz, 2H), 7.35 (br d, *J* = 5.4 Hz, 1H), 7.01 (d, *J* = 8.3 Hz, 2H), 4.32 (dd, *J* = 9.5, 4.6 Hz, 1H), 4.01 (dd, *J* = 12.7, 6.4 Hz, 1H), 3.95 (br s, 1H), 3.88 (s, 3H), 3.76 (t, *J* = 10.3 Hz, 1H), 3.28 (dd, *J* = 12.7, 7.3 Hz, 1H), 1.17 (m, 21H); ^{13}C NMR (100 MHz, $CDCl_3$) δ 168.9, 161.3, 161.1, 159.0, 158.1, 131.9, 129.7, 113.9, 107.2, 64.94, 64.92, 55.5, 47.9, 18.08, 18.07, 12.0; HRMS(ESI+): Calcd for $C_{24}H_{37}N_4O_2Si^+$ $[M+H]^+$ 441.2680, found 441.2679, Δppm –0.22.

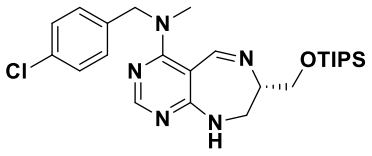

7

Compound 7. A light yellow oil; R_f = 0.39 (DCM/MeOH = 20:1); 73 % overall yield; ^{1}H NMR (400 MHz, $CDCl_3$) δ 8.15 (s, 1H), 8.05 (s, 1H), 7.30 (d, *J* = 8.0 Hz, 2H), 7.23 (d, *J* = 8.0 Hz, 2H), 6.86 (br s, 1H), 4.75, 4.68 (ABq, J_{AB} = 15.6 Hz, 2H), 4.18 (dd, *J* = 9.8, 4.3 Hz, 1H), 3.87 (m, 2H), 3.66 (t, *J* = 10.0 Hz, 1H), 3.33 (dd, *J* = 11.0, 7.4 Hz, 1H), 3.02 (s, 3H), 1.12 (m, 21H); ^{13}C NMR (100 MHz, $CDCl_3$) δ 167.3, 162.5, 157.2, 157.1, 136.0, 133.3, 129.2, 128.9, 92.8, 65.2, 64.6, 55.8, 47.3, 40.4, 18.1, 12.0; HRMS(ESI+): Calcd for $C_{25}H_{39}ClN_5OSi^+$ $[M+H]^+$ 488.2607, found 488.2608, Δppm +0.20.

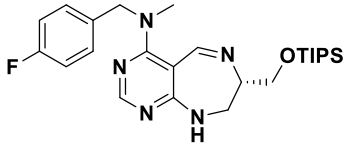

8

Compound 8. A yellow oil; R_f = 0.35 (DCM/MeOH = 20:1); 76% overall yield; ^{1}H NMR (500 MHz, $CDCl_3$) δ 8.12 (d, *J* = 2.4 Hz, 1H), 8.03 (s, 1H), 7.23 (m, 2H), 6.99 (m, 2H), 6.86 (d, *J* = 2.9 Hz, 1H), 4.73, 4.66 (ABq, J_{AB} = 12.2 Hz, 2H), 4.16 (dd, *J* = 9.8, 4.9 Hz, 1H), 3.86 (m, 2H), 3.64 (t, *J* = 10.0 Hz, 1H), 3.31 (ddd, *J* = 13.0, 7.1, 2.9 Hz, 1H), 2.99 (s, 3H), 1.09 (m, 21H); ^{13}C NMR (100 MHz, $CDCl_3$) δ 167.4, 162.5, 162.3 (d, $^1J_{C,F}$ = 244.4 Hz), 157.19, 157.17, 133.1 (d, $^4J_{C,F}$ = 3.0 Hz), 129.5 (d, $^3J_{C,F}$ = 7.6 Hz), 115.6 (d, $^2J_{C,F}$ = 21.2 Hz), 92.8, 65.2, 64.6, 55.7, 47.3, 40.2, 18.1, 12.0; HRMS(ESI+): Calcd for $C_{25}H_{39}FN_5OSi^+$ $[M+H]^+$ 472.2902, found 472.2904, Δppm +0.42.

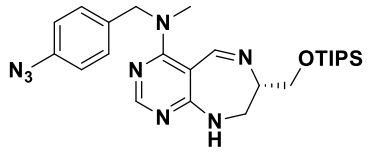

9a

Compound 9a. A yellow oil; R_f = 0.35 (DCM/MeOH = 20:1); 67 % overall yield; ^{1}H NMR (400 MHz, $CDCl_3$) δ 8.14 (s, 1H), 8.05 (s, 1H), 7.27 (d, *J* = 8.2 Hz, 2H), 6.99 (d, *J* = 8.2 Hz, 2H), 6.80 (br s, 1H), 4.76, 4.68 (ABq, J_{AB} = 15.4 Hz, 2H), 4.18 (dd, *J* = 9.8, 4.3 Hz, 1H), 3.87 (m, 2H), 3.66 (t, *J* = 10.0 Hz, 1H), 3.33 (m, 1H), 3.02 (s, 3H), 1.16 (m, 21H); ^{13}C NMR (100 MHz, $CDCl_3$) δ 167.3, 162.4, 157.2, 157.1, 139.3, 134.2, 129.3, 119.3, 92.8, 65.1, 64.5, 55.9, 47.3, 40.2, 18.1, 12.0; HRMS(ESI+): Calcd for $C_{25}H_{39}N_8OSi^+$ $[M+H]^+$ 495.3011, found 495.3011.

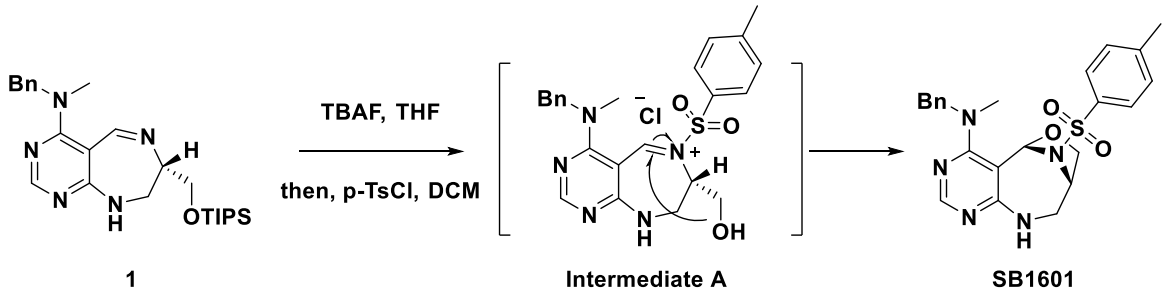

Synthetic procedure for the preparation of 1

To a solution of **1** (90.0 mg, 0.198 mmol) in tetrahydrofuran (THF, 4 mL) was added *tetra*-n-butylammonium fluoride solution (TBAF, 1.0 $_M$ solution in THF, 0.257 mL, 0.257 mmol) and the mixture was stirred at room temperature (r.t.). After completion of the reaction as indicated by TLC, the reaction mixture was quenched with saturated $NaHCO_3$(aq). The resultant was extracted twice with DCM, dried with anhydrous Na_2SO_4(s), filtered, and concentrated *in vacuo*. To a solution of the crude product in dichloromethane (DCM, 4 mL) was added *p*-toluenesulfonyl chloride (*p*-TsCl, 49.1 mg, 0.257 mmol) and then, the mixture was stirred at r.t. After completion of the reaction as indicated by TLC, solvent was removed under reduced pressure and the residue was purified by silica-gel flash column chromatography to obtain desired product **SB1601** (59.9 mg, 67% overall yield) as a white solid. R_f = 0.39 (EtOAc); ^{1}H NMR (500 MHz, $CDCl_3$) δ 8.12 (s, 1H), 7.44–7.32 (m, 7H), 7.18 (d, J = 7.8 Hz, 2H), 6.62 (s, 1H), 5.71 (br d, J = 4.9 Hz, 1H), 4.73, 4.69 (ABq, J_{AB} = 16.5 Hz, 2H), 4.49 (br s, 1H), 3.75 (d, J = 6.8 Hz, 1H), 3.56 (d, J = 13.2 Hz, 1H), 3.40 (dt, J = 13.2, 4.9 Hz, 1H), 3.00 (s, 3H), 2.95 (t, J = 6.8 Hz, 1H), 2.39 (s, 3H); ^{13}C NMR (100 MHz, $CDCl_3$) δ 166.3. 163.5, 156.0, 144.7, 138.2, 134.9, 130.0, 128.8, 127.8, 127.7, 127.3, 103.5, 87.7, 66.8, 58.6, 56.4, 48.8, 40.0, 21.7; IR (neat) ν_{max}: 3249, 1737, 1559, 1336, 1166, 678 cm^{-1}; HRMS(ESI+): Calcd for $C_{23}H_{26}N_5O_3S^+$ $[M+H]^+$ 452.1751, found 452.1753, Δppm +0.44; mp: 150–152 °C.

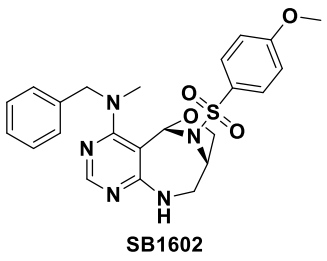

SB1602. A white solid; R_f = 0.30 (EtOAc); 65.7 mg, 71 % overall yield; ^{1}H NMR (500 MHz, $CDCl_3$) δ 8.11 (s, 1H), 7.43–7.37 (m, 6H), 7.32 (m, 1H), 6.83 (m, 2H), 6.61 (s, 1H), 5.93(br d, J = 5.4 Hz, 1H), 4.73, 4.67 (ABq, J_{AB} = 16.3 Hz, 2H), 4.46 (br t, J = 4.9 Hz, 1H), 3.82 (s, 3H),

3.75 (dd, *J* = 7.3, 2.0 Hz, 1H), 3.55 (d, *J* = 13.2 Hz, 1H), 3.39 (dt, *J* = 13.3, 5.1 Hz, 1H), 2.99 (s, 3H), 2.96 (t, *J* = 7.1 Hz, 1H); ^{13}C NMR (100 MHz, $CDCl_3$) δ 166.2, 163.6, 163.5, 155.9, 138.2, 129.9, 129.3, 128.7, 127.6, 127.2, 114.5, 103.3, 87.8, 66.8, 58.6, 56.3, 55.7, 48.7, 40.0; IR (neat) ν_{max}: 3388, 2952, 1739, 1572, 1533, 1357, 1159, 673 cm^{-1}; HRMS(ESI+): Calcd for $C_{23}H_{26}N_5O_4S^+$ $[M+H]^+$ 468.1700, found 468.1703, Δppm +0.64; mp: 121–123 °C. The product was synthesized according to the synthetic procedure for the preparation of **SB1601** from **1** and 4-methoxybenzenesulfonyl chloride.

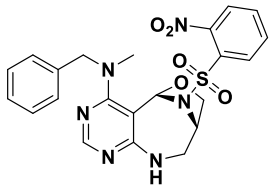

SB1603

SB1603. A yellow solid; R_f = 0.30 (EtOAc); 55.4 mg, 58 % overall yield; ^{1}H NMR (400 MHz, $CDCl_3$) δ 8.09 (s, 1H), 7.62 (m, 1H), 7.52 (d, *J* = 8.2 Hz, 2H), 7.45 (m, 1H), 7.37 (m, 2H), 7.31 (m, 3H), 6.74 (s, 1H), 6.06 (br s, 1H), 4.88 (br s, 1H), 4.60 (s, 2H), 3.99 (d, *J* = 7.4 Hz, 1H), 3.58–3.45 (m, 3H), 2.91 (s, 3H); ^{13}C NMR (100 MHz, $CDCl_3$) δ 166.4, 163.9, 156.1, 148.2, 137.9, 134.5, 132.0, 131.7, 130.7, 128.7, 127.8, 127.4, 124.2, 102.0, 87.9, 68.3, 58.1, 56.7, 48.1, 40.0; IR (neat) ν_{max}: 2912, 1540, 1353, 1169, 738, 699 cm^{-1}; HRMS(ESI+): Calcd for $C_{22}H_{23}N_6O_5S^+$ $[M+H]^+$ 483.1445, found 483.1443, Δppm –0.41; mp: 80–82 °C. The product was synthesized according to the synthetic procedure for the preparation of **SB1601** from **1** and 2-nitrobenzenesulfonyl chloride.

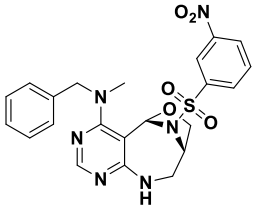

SB1604

SB1604. The synthesis, characterization and X-ray crystallographic analysis (CCDC number 1500586) of **SB1604** was previously reported.[11]

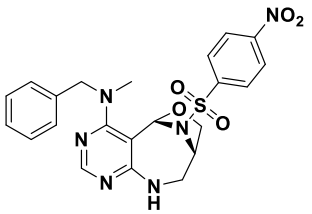

SB1605

SB1605. a pale yellow solid; R_f = 0.3 (EtOAc); 53.5mg, 59% yield; ^{1}H NMR (400 MHz, $CDCl_3$) δ 8.16–8.14 (m, 3H), 7.51–7.40 (m, 7H), 6.54 (s, 1H), 5.65 (d, *J* = 3.9 Hz, 1H), 4.71 (s, 2H), 4.53 (br s, 1H), 3.82 (dd, *J* = 7.4, 2.0 Hz, 1H), 3.64 (d, *J* = 13.3 Hz, 1H), 3.45 (m, 1H), 3.05–3.01 (m, 4H); ^{13}C NMR (100 MHz, $CDCl_3$) δ 166.4, 163.3, 156.2, 150.5, 143.6, 138.2, 129.1, 129.0, 127.5, 127.4, 124.5, 102.5, 87.5, 66.8, 58.9, 56.6, 48.6, 39.5; IR (neat) ν_{max}: 2970, 1739, 1558, 1530, 1400, 1351, 1169, 738 cm^{-1}; HRMS(ESI+): Calcd for $C_{22}H_{23}N_6O_5S^+$ $[M+H]^+$ 483.1445, found 483.1439, Δppm –1.24; mp: 97–99 °C. The product was synthesized according to the synthetic procedure for the preparation of **SB1601** from **1** and 4-nitrobenzenesulfonyl chloride.

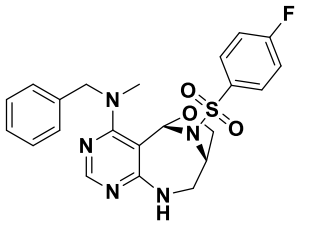

SB1606

SB1606. A white solid; R_f = 0.4 (EtOAc); 56.8 mg, 63 % overall yield; ^{1}H NMR (500 MHz, $CDCl_3$) δ 8.12 (s, 1H), 7.45–7.39 (m, 6H), 7.34 (m, 1H), 7.03 (m, 2H), 6.57 (s, 1H), 5.97 (br s, 1H), 4.72, 4.69 (ABq, J_{AB} = 16.5 Hz, 2H), 4.47 (br s, 1H), 3.77 (dd, *J* = 7.6, 2.2 Hz, 1H), 3.58 (d, *J* = 13.2 Hz, 1H), 3.40 (dt, *J* = 13.2, 4.9 Hz, 1H), 2.99 (s, 3H), 2.97 (d, *J* = 7.5 Hz, 1H); ^{13}C NMR (100 MHz, $CDCl_3$) δ 166.3, 165.6 (d, $^1J_{C,F}$ = 255.1 Hz), 163.4, 156.0, 138.2, 133.9 (d, $^4J_{C,F}$ = 3.0 Hz), 130.5 (d, $^3J_{C,F}$ = 9.9 Hz), 128.8, 127.5, 127.3, 116.7 (d, $^2J_{C,F}$ = 22.0 Hz), 103.0, 87.6, 66.7, 58.7, 56.4, 48.7, 39.7; IR (neat) ν_{max}: 3245, 2921, 1571, 1351, 1169, 1155, 679 cm^{-1}; HRMS(ESI+): Calcd for $C_{22}H_{23}FN_5O_3S^+$ $[M+H]^+$ 456.1500, found 456.1501, Δppm +0.22; mp: 105–107 °C. The product was synthesized according to the synthetic procedure for the preparation of **SB1601** from **1** and 4-fluorobenzenesulfonyl chloride.

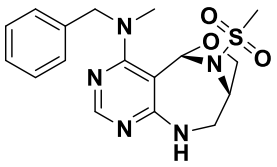

SB1607

SB1607. A white solid; R_f = 0.25 (EtOAc); 55.8 mg, 75 % overall yield; ^{1}H NMR (400 MHz, $CDCl_3$) δ 8.14 (s, 1H), 7.37–7.26 (m, 5H), 6.58 (s, 1H), 5.92 (br d, *J* = 4.3 Hz, 1H), 4.73 (d, *J* = 16.0 Hz, 1H), 4.64 (br s, 1H), 4.55 (d, *J* = 16.0 Hz, 1H), 4.10 (dd, *J* = 7.6, 1.8 Hz, 1H), 3.92 (t, *J* = 7.4 Hz, 1H), 3.60–3.47 (m, 2H), 2.96 (s, 3H), 2.73 (s, 3H); ^{13}C NMR (100 MHz, $CDCl_3$) δ 166.6, 163.5, 156.1, 138.0, 128.7, 127.6, 127.3, 102.5, 87.3, 67.1, 58.2, 56.6, 48.7, 40.4, 38.5; IR (neat) ν_{max}: 2912, 2109, 1571, 1538, 1350, 1168, 738 cm^{-1}; HRMS(ESI+): Calcd for $C_{17}H_{22}N_5O_3S^+$ $[M+H]^+$ 376.1438, found 376.1437, Δppm –0.27; mp: 136–138 ^{o}C. The product was synthesized according to the synthetic procedure for the preparation of **SB1601** from **1** and methanesulfonyl chloride.

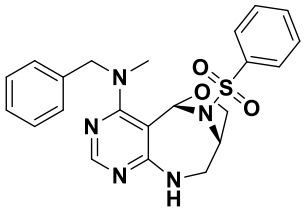

SB1608

SB1608. A white solid; R_f = 0.38 (EtOAc); 67.6 mg, 78% overall yield; ^{1}H NMR (500 MHz, $CDCl_3$) δ 8.12 (s, 1H), 7.56 (m, 1H), 7.56 (m, 2H), 7.44–7.37 (m, 6H), 7.33 (m, 1H), 6.63 (s, 1H), 5.95 (br d, *J* = 4.9 Hz, 1H), 4.73, 4.69 (ABq, J_{AB} = 16.3 Hz, 2H), 4.50 (br t, *J* = 4.9 Hz, 1H), 3.75 (dd, *J* = 7.3, 1.5 Hz, 1H), 3.56 (d, *J* = 12.7 Hz, 1H), 3.40 (dt, *J* = 13.2, 5.0 Hz, 1H), 3.00 (s, 3H), 2.93 (t, *J* = 6.8 Hz, 1H); ^{13}C NMR (100 MHz, $CDCl_3$) δ 166.3, 163.5, 155.9, 138.2, 137.9, 133.6, 129.4, 128.8, 127.7, 127.6, 127.2, 103.2, 87.7, 66.8, 58.6, 56.3, 48.7, 40.0; IR (neat) ν_{max}: 3380, 1739, 1536, 1352, 1170, 974, 723, 696 cm^{-1}; HRMS(ESI+): Calcd for $C_{22}H_{24}N_5O_3S^+$ $[M+H]^+$ 438.1594, found 438.1595, Δppm +0.23; mp: 120–122 ^{o}C. The product was synthesized according to the synthetic procedure for the preparation of **SB1601** from **1** and benzenesulfonyl chloride.

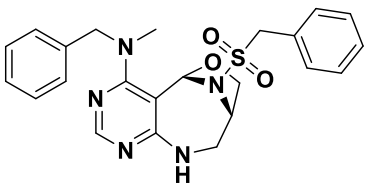

SB1609

SB1609. A white solid; R_f = 0.32 (EtOAc); 54.5 mg, 61 % overall yield; ^{1}H NMR (400 MHz, $CDCl_3$) δ 8.11 (s, 1H), 7.39–7.35 (m, 2H), 7.30–7.21 (m, 8H), 6.60 (s, 1H), 5.76 (br s, 1H), 4.66, 4.50 (ABq, J_{AB} = 15.6 Hz, 2H), 4.32 (br s, 1H), 4.09 (s, 2H), 3.97 (d, *J* = 7.4 Hz, 1H), 3.72 (t, *J* = 6.8 Hz, 1H), 3.28 (m, 2H), 2.81 (s, 3H); ^{13}C NMR (100 MHz, $CDCl_3$) δ 166.4, 163.6, 156.0, 138.0, 131.0, 129.1, 128.8, 128.7, 127.9, 127.7, 127.3, 102.2, 87.0, 68.0, 59.4, 57.7, 57.2, 48.1, 40.1; IR (neat) ν_{max}: 2970, 1741, 1558, 1403, 1349, 1161, 1049, 969, 696 cm^{-1}; HRMS(ESI+): Calcd for $C_{23}H_{26}N_5O_3S^+$ $[M+H]^+$ 452.1751, found 452.1747, Δppm –0.88; mp: 78–80 °C. The product was synthesized according to the synthetic procedure for the preparation of **SB1601** from **1** and benzylsulfonyl chloride.

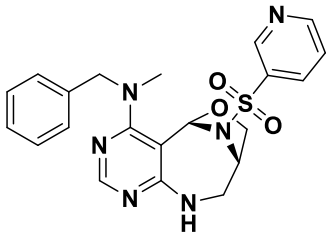

SB1610

SB1610. A white solid; R_f = 0.15 (EtOAc); 53.8 mg, 62 % overall yield; ^{1}H NMR (600 MHz, DMSO-d_6, 77 °C) δ 8.93 (s, 1H), 8.86 (d, *J* = 4.0 Hz, 1H), 8.05 (m, 2H), 7.56 (dd, *J* = 7.3, 5.1 Hz, 1H), 7.38 (m, 2H), 7.30 (m, 3H), 6.97 (br s, 1H), 6.66 (s, 1H), 4.80 (br s, 1H), 4.66 (d, *J* = 15.6 Hz, 1H), 4.66 (d, *J* = 15.6 Hz, 1H), 3.71 (br d, *J* = 6.6 Hz, 1H), 3.52 (m ,1H), 3.33 (d, *J* = 13.9 Hz, 1H), 3.04 (br s, 1H), 2.90 (s, 3H); ^{13}C NMR (150 MHz, DMSO-d_6, 77 °C) δ 165.5, 162.9, 155.3, 153.8, 147.2, 137.9, 134.9, 134.2, 128.0, 127.1, 126.6, 124.0, 101.7, 86.7, 66.4, 57.0, 55.6, 47.6, 39.8; IR (neat) ν_{max}: 3313, 1732, 1555, 1353, 1171, 980, 957, 690 cm^{-1}; HRMS(ESI+): Calcd for $C_{21}H_{23}N_6O_3S^+$ $[M+H]^+$ 439.1547, found 439.1553; Δppm +1.37, mp: 185–187 °C. The product was synthesized according to the synthetic procedure for the preparation of **SB1601** from **1** and pyridine-3-sulfonyl chloride.

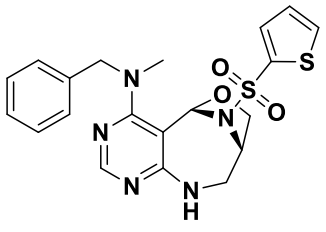

SB1611

SB1611. A white solid; R_f = 0.33 (EtOAc); 51.8 mg, 59 % overall yield; ^{1}H NMR (500 MHz, DMSO-d_6) δ 8.10 (dd, *J* = 4.9, 1.5 Hz, 1H), 8.03 (s, 1H), 7.57 (dd, *J* = 3.7, 1.2 Hz, 1H), 7.39–7.36 (m, 2H), 7.30–7.28 (m, 3H), 7.25 (d, *J* = 4.9 Hz, 1H), 7.22 (dd, *J* = 4.9, 3.9 Hz, 1H), 6.60

(s, 1H), 4.75 (br s, 1H), 4.66 (d, *J* = 15.7 Hz, 1H), 4.49 (d, *J* = 15.7 Hz, 1H), 3.63 (dd, *J* = 7.3, 1.5 Hz, 1H), 3.52 (dt, *J* = 13.9, 5.0 Hz, 1H), 3.28 (d, *J* = 13.2 Hz, 1H), 2.93 (t, *J* = 7.1 Hz, 1H), 2.86 (s, 3H); ^{13}C NMR (100 MHz, DMSO-d_6) δ 165.6, 163.3, 155.7, 138.1, 136.9, 135.5, 134.1, 128.5, 127.5, 127.0, 102.0, 87.1, 66.6, 57.4, 56.1, 47.9, 40.2; IR (neat) ν_{max}: 3241, 1739, 1577, 1542, 1355, 1166, 1026, 970, 674 cm^{-1}; HRMS(ESI+): Calcd for $C_{20}H_{22}N_5O_3S_2^+$ $[M+H]^+$ 444.1159, found 444.1159; mp: 112–114 °C. The product was synthesized according to the synthetic procedure for the preparation of **SB1601** from **1** and 2-thiophenesulfonyl chloride.

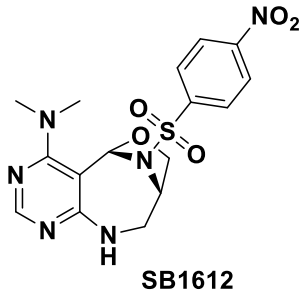

SB1612

SB1612. A yellow solid; R_f = 0.27 (EtOAc); 41.8 mg, 52 % overall yield; ^{1}H NMR (400 MHz, $CDCl_3$) δ 8.37 (d, *J* = 8.6 Hz, 2H), 8.12 (d, *J* = 9.0 Hz, 2H), 8.06 (s, 1H), 6.69 (s, 1H), 5.93 (br s, 1H), 4.54 (br s, 1H), 3.85 (dd, *J* = 7.6, 1.4 Hz, 1H), 3.46 (m, 2H), 3.07 (s, 6H), 3.01 (t, *J* = 7.0 Hz, 1H); ^{13}C NMR (100 MHz, $CDCl_3$) δ 166.8, 163.4, 156.1, 150.7, 144.2, 129.3, 124.6, 102.1, 88.3, 67.1, 56.5, 48.5, 43.2; IR (neat) ν_{max}: 3409, 2924, 1579, 1524, 1351, 1313, 1171, 738, 685 cm^{-1}; HRMS(ESI+): Calcd for $C_{16}H_{19}N_6O_5S^+$ $[M+H]^+$ 407.1132, found 407.1130, Δppm –0.49; mp: 118–120 °C. The product was synthesized according to the synthetic procedure for the preparation of **SB1601** from **2** and 4-nitrobenzenesulfonyl chloride.

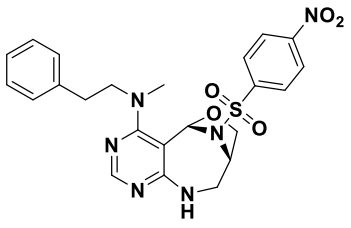

SB1613

SB1613. A pale yellow solid; R_f = 0.45 (EtOAc); 61.0 mg, 62 % overall yield; ^{1}H NMR (400 MHz, $CDCl_3$) δ 8.33 (d, *J* = 8.6 Hz, 2H), 8.08 (s, 1H), 7.99 (d, *J* = 8.6 Hz, 2H), 7.30–7.21 (m, 5H), 6.55 (s, 1H), 6.08 (br s, 1H), 4.54 (br s, 1H), 3.97 (m, 1H), 3.84 (d, *J* = 7.0 Hz, 1H), 3.46 (m, 3H), 3.09 (s, 3H), 3.00 (m, 2H), 2.89 (m, 1H); ^{13}C NMR (100 MHz, $CDCl_3$) δ 166.5, 163.5, 156.0, 150.6, 144.1, 139.6, 129.2, 128.9, 128.5, 126.2, 124.5, 102.6, 88.1, 67.0, 56.5, 54.5, 48.4, 42.5, 33.8; IR (neat) ν_{max}: 3411, 1739, 1580, 1524, 1354, 1169, 738 cm^{-1}; HRMS(ESI+): Calcd for $C_{23}H_{25}N_6O_5S^+$ $[M+H]^+$ 497.1602, found 497.1603, Δppm +0.20; mp: 108–110 °C. The product was synthesized according to the synthetic procedure for the preparation of **SB1601** from **3** and 4-nitrobenzenesulfonyl chloride.

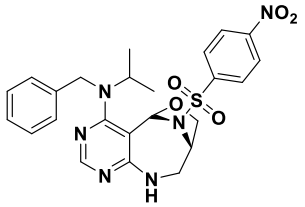

SB1614

SB1614. A light yellow solid; R_f = 0.5 (EtOAc); 51.6 mg, 51% overall yield; ^{1}H NMR (400 MHz, $CDCl_3$) δ 8.28 (d, *J* = 8.2 Hz, 2H), 8.05 (s, 1H), 7.92 (d, *J* = 7.8 Hz, 2H), 7.37 (d, *J* = 7.4 Hz, 2H), 7.28 (m, 2H), 7.18 (m, 1H), 6.85 (s, 1H), 5.82 (br s, 1H), 4.59 (m, 2H), 4.49 (d, *J* = 14.8 Hz, 1H), 3.96 (m, 1H), 3.85 (d, *J* = 7.8 Hz, 1H), 3.55 (d, *J* = 13.3 Hz, 1H), 3.38 (m, 1H), 3.27 (t, *J* = 7.2 Hz, 1H), 1.34 (d, *J* = 6.3 Hz, 3H), 1.29 (d, *J* = 6.3 Hz, 3H); ^{13}C NMR (100 MHz, $CDCl_3$) δ 167.0, 163.4, 155.9, 150.5, 144.2, 140.3, 128.9, 128.3, 127.9, 126.6, 124.6, 106.9, 87.5, 67.2, 56.7, 56.6, 48.3, 46.3, 20.7, 20.0; IR (neat) ν_{max}: 2970, 1738, 1568, 1531, 1348, 1169, 1061, 737 cm^{-1}; HRMS(ESI+): Calcd for $C_{24}H_{27}N_6O_5S^+$ $[M+H]^+$ 511.1758, found 511.1761, Δppm +0.59; mp: 85–87 °C. The product was synthesized according to the synthetic procedure for the preparation of **SB1601** from **4** and 4-nitrobenzenesulfonyl chloride.

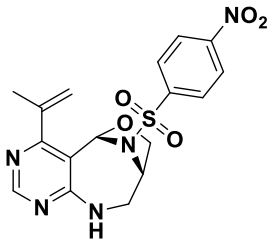

SB1615

SB1615. A pale yellow solid; R_f = 0.35 (EtOAc); 44.7 mg, 56 % overall yield; ^{1}H NMR (400 MHz, $CDCl_3$) δ 8.46 (s, 1H), 8.41 (d, *J* = 8.6 Hz, 2H), 8.09 (d, *J* = 9.0 Hz, 2H), 6.85 (s, 1H), 5.74 (br d, *J* = 3.9 Hz, 1H), 5.56 (s, 1H), 5.17 (s, 1H), 4.63 (br s, 1H), 3.91 (dd, *J* = 7.6, 1.8 Hz, 1H), 3.66 (d, *J* = 12.5 Hz, 1H), 3.50 (m, 1H), 3.25 (t, *J* = 7.2 Hz, 1H), 2.17 (s, 3H); ^{13}C NMR (100 MHz, $CDCl_3$) δ 167.4, 162.8, 157.0, 150.8, 143.8, 142.1, 129.1, 124.9, 119.5, 114.5, 87.9, 67.0, 56.2, 48.9, 22.9; IR (neat) ν_{max}: 3290, 2977, 1740, 1557, 1529, 1346, 1170, 907, 737 cm^{-1}; HRMS(ESI+): Calcd for $C_{17}H_{18}N_5O_5S^+$ $[M+H]^+$ 404.1023, found 404.1023; mp: 200–202 °C. The product was synthesized according to the synthetic procedure for the preparation of **SB1601** from **5** and 4-nitrobenzenesulfonyl chloride.

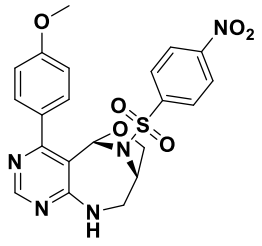

SB1616

SB1616. A white solid; R_f = 0.35 (EtOAc); 41.8 mg, 45 % overall yiel d; ^{1}H NMR (500 MHz, DMSO-d_6) δ 8.41 (m, 3H), 8.03 (d, J = 8.3 Hz, 2H), 7.65 (br d, J = 4.4 Hz, 1H), 7.52 (d, J = 8.3 Hz, 2H), 7.09 (d, J = 8.3 Hz, 2H), 6.47 (s, 1H), 4.89 (br s, 1H), 3.87 (s, 3H), 3.70 (d, J = 7.3 Hz, 1H), 3.55 (m, 1H), 3.39 (d, J = 14.0 Hz, 1H), 3.08 (t, J = 7.3 Hz, 1H); ^{13}C NMR (100 MHz, DMSO-d_6) δ 163.3, 162.5, 160.2, 156.6, 150.6, 142.5, 131.2, 129.6, 129.1, 125.1, 113.7, 113.5, 87.5, 66.9, 55.7, 55.3, 48.1; IR (neat) ν_{max}: 3244, 3109, 3005, 1739, 1570, 1528, 1352, 1168, 740 cm^{-1}; HRMS(ESI+): Calcd for $C_{21}H_{20}N_5O_6S^+$ $[M+H]^+$ 470.1129, found 470.1127, Δppm –0.43; mp: 250–252 ^{o}C. The product was synthesized according to the synthetic procedure for the preparation of **SB1601** from **6** and 4-nitrobenzenesulfonyl chloride.

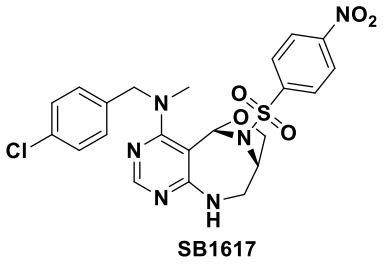

SB1617

SB1617. (58.3 mg, 57% overall yield) as a light yellow solid. R_f = 0.40 (EtOAc); ^{1}H NMR (400 MHz, $CDCl_3$) δ 8.24 (d, J = 8.6 Hz, 2H), 8.13 (s, 1H), 7.63 (d, J = 8.6 Hz, 2H), 7.42, 7.35 (ABq, J_{AB} = 8.2 Hz, 4H), 6.56 (s, 1H), 5.73 (d, J = 3.9 Hz, 1H), 4.67, 4.62 (ABq, J_{AB} = 17.0 Hz, 2H), 4.54 (br s, 1H), 3.84 (d, J = 7.4 Hz, 1H), 3.61 (d, J = 13.3 Hz, 1H), 3.45 (dt, J = 13.3, 4.7 Hz, 1H), 3.07 (t, J = 7.0 Hz, 1H), 2.99 (s, 3H); ^{13}C NMR (100 MHz, $CDCl_3$) δ 166.4, 163.4, 156.3, 150.6, 143.7, 136.8, 133.2, 129.1, 129.03, 128.95, 124.6, 102.8, 87.5, 67.0, 58.0, 56.5, 48.6, 40.1; IR (neat) ν_{max}: 3248, 3016, 1739, 1565, 1529, 1350, 1169, 738 cm^{-1}; HRMS(ESI+): Calcd for $C_{22}H_{22}ClN_6O_5S^+$ $[M+H]^+$ 517.1055, found 517.1053, Δppm –0.39; mp: 110–112 ^{o}C. The product was synthesized according to the synthetic procedure for the preparation of **SB1601** from **7** and 4-nitrobenzenesulfonyl chloride.

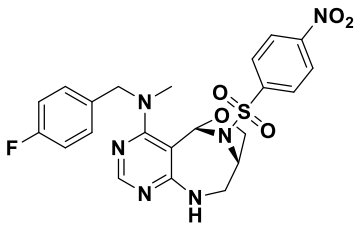

SB1618

SB1618. A light yellow solid; R_f = 0.39 (EtOAc); 54.5 mg, 55 % overall yield; ^{1}H NMR (500 MHz, $CDCl_3$) δ 8.24 (d, *J* = 8.8 Hz, 2H), 8.12 (s, 1H), 7.69 (d, *J* = 8.8 Hz, 2H), 7.36 (dd, *J* = 8.1, 5.6 Hz, 2H), 7.12 (t, *J* = 8.6 Hz, 2H), 6.61 (s, 1H), 5.76 (br d, *J* = 4.4 Hz, 1H), 4.64 (s, 2H), 4.54 (br s, 1H), 3.84 (dd, *J* = 7.8, 1.5 Hz, 1H), 3.59 (d, *J* = 13.2 Hz, 1H), 3.45 (dt, *J* = 13.7, 4.9 Hz, 1H), 3.07 (t, *J* = 7.1 Hz, 1H), 2.98 (s, 3H); ^{13}C NMR (100 MHz, $CDCl_3$) δ 166.4, 163.4, 162.3 (d, $^1J_{C,F}$ = 244.4 Hz), 156.3, 150.6, 143.8, 133.8 (d, $^4J_{C,F}$ = 3.8 Hz), 129.3 (d, $^3J_{C,F}$ = 7.6 Hz), 129.0, 124.5, 115.7 (d, $^2J_{C,F}$ = 21.3 Hz), 102.8, 87.6, 67.0, 57.9, 56.5, 48.6, 40.0; IR (neat) ν_{max}: 3246, 3018, 1739, 1567, 1533, 1498, 1349, 1170, 739 cm^{-1}; HRMS(ESI+): Calcd for $C_{22}H_{22}FN_6O_5S^+$ $[M+H]^+$ 501.1351, found 501.1353, Δppm +0.40; mp: 102–104 °C. The product was synthesized according to the synthetic procedure for the preparation of **SB1601** from **8** and 4-nitrobenzenesulfonyl chloride.

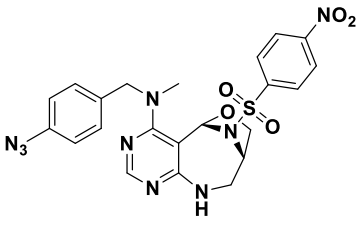

SB1619

SB1619. A pale yellow solid; R_f = 0.40 (EtOAc); 61.2 mg, 59 % overall yield; ^{1}H NMR (400 MHz, $CDCl_3$) δ 8.24 (d, *J* = 8.6 Hz, 2H), 8.11 (s, 1H), 7.72 (d, *J* = 8.6 Hz, 2H), 7.37 (d, *J* = 8.2 Hz, 2H), 7.09 (d, *J* = 8.2 Hz, 2H), 6.61 (s, 1H), 5.86 (br d, *J* = 4.3 Hz, 1H), 4.64 (s, 2H), 4.54 (br s, 1H), 3.84 (d, *J* = 7.8 Hz, 1H), 3.59 (d, *J* = 13.2 Hz, 1H), 3.45 (dt, *J* = 13.4, 4.8 Hz, 1H), 3.08 (t, *J* = 7.0 Hz, 1H), 2.98 (s, 3H); ^{13}C NMR (100 MHz, $CDCl_3$) δ 166.4, 163.5, 156.2, 150.6, 143.8, 139.3, 134.9, 129.2, 129.0, 124.5, 119.4, 102.8, 87.6, 67.0, 58.0, 56.5, 48.6, 40.1; IR (neat) ν_{max}: 2900, 2109, 1572, 1530, 1349, 1168, 738 cm^{-1}; HRMS(ESI+): Calcd for $C_{22}H_{22}N_9O_5S^+$ $[M+H]^+$ 524.1459, found 524.1460, Δppm +0.19; mp: 88–90 °C. The product was synthesized according to the synthetic procedure for the preparation of **SB1601** from **9a** and 4-nitrobenzenesulfonyl chloride.

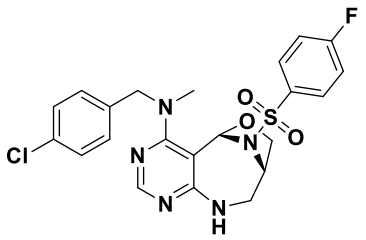

SB1620

SB1620. A white solid; R_f = 0.40 (EtOAc); 57.2 mg, 59 % overall yield; ^{1}H NMR (400 MHz, $CDCl_3$) δ 8.11 (s, 1H), 7.50 (dd, *J* = 8.6, 4.7 Hz, 2H), 7.39, 7.33 (ABq, J_{AB} = 8.4 Hz, 4H), 7.10 (t, *J* = 8.4 Hz, 2H), 6.56 (s, 1H), 5.92 (br d, *J* = 4.7 Hz, 1H), 4.65 (s, 2H), 4.48 (br s, 1H), 3.78 (d, *J* = 7.4 Hz, 1H), 3.56 (d, *J* = 13.2 Hz, 1H), 3.41 (dt, *J* = 13.5, 4.8 Hz, 1H), 2.99 (m, 4H); ^{13}C NMR (100 MHz, $CDCl_3$) δ 166.2, 165.7 (d, $^1J_{C,F}$ = 255.8 Hz), 163.5, 156.1, 136.8, 133.9 (d, $^4J_{C,F}$ = 3.0 Hz), 133.0, 130.5 (d, $^3J_{C,F}$ = 9.9 Hz), 129.1, 129.0, 116.8 (d, $^2J_{C,F}$ = 22.8 Hz), 103.3, 87.6, 66.8, 57.9, 56.3, 48.7, 40.2; IR (neat) ν_{max}: 3015, 1739, 1570, 1491, 1351, 1231, 1171, 1157, 678 cm^{-1}; HRMS(ESI+): Calcd for $C_{22}H_{22}ClFN_5O_3S^+$ $[M+H]^+$ 490.1110, found 490.1112, Δppm +0.41; mp: 150–152 °C. The product was synthesized according to the synthetic procedure for the preparation of **SB1601** from **7** and 4-fluorobenzenesulfonyl chloride.

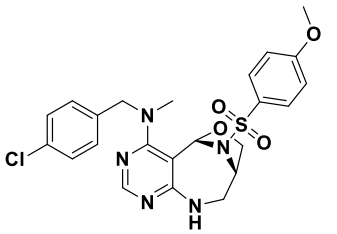

SB1621

SB1621. A white solid; R_f = 0.35 (EtOAc); 61.6 mg, 62 % overall yield; ^{1}H NMR (400 MHz, $CDCl_3$) δ 8.10 (s, 1H), 7.45 (d, *J* = 8.6 Hz, 2H), 7.37, 7.32 (ABq, J_{AB} = 8.2 Hz, 4H), 6.88 (d, *J* = 8.6 Hz, 2H), 6.57 (s, 1H), 5.85 (br s, 1H), 4.65 (s, 2H), 4.47 (br s, 1H), 3.85 (s, 3H), 3.75 (d, *J* = 7.4 Hz, 1H), 3.54 (d, *J* = 13.3 Hz, 1H), 3.40 (dt, *J* = 13.2, 4.9 Hz, 1H), 2.99 (m, 4H); ^{13}C NMR (100 MHz, $CDCl_3$) δ 166.1, 163.7, 163.5, 156.0, 136.9, 132.9, 129.9, 129.3, 129.2, 128.9, 114.6, 103.7, 87.7 (C11, d, *J* = 2.3 Hz), 66.9, 57.9, 56.3, 55.8 (C25, d, *J* = 2.3 Hz), 48.8, 40.3; IR (neat) ν_{max}: 2970, 1739, 1574, 1496, 1349, 1161, 680 cm^{-1}; HRMS(ESI+): Calcd for $C_{23}H_{25}ClN_5O_4S^+$ $[M+H]^+$ 502.1310, found 502.1310; mp: 156–158 °C. The product was synthesized according to the synthetic procedure for the preparation of **SB1601** from **7** and 4-methoxybenzenesulfonyl chloride.

Synthetic procedure for the preparation of SB1622

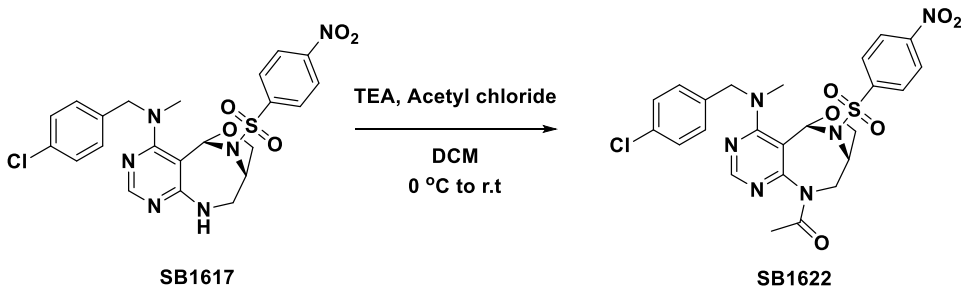

To a solution of **SB1617** (58.3 mg, 0.113 mmol) in DCM (5 mL) were sequentially added Et_3N (0.032 mL, 0.226 mmol) and acetyl chloride (0.010 mL, 0.147 mmol) at 0 °C. The resulting mixture was left to stir and allowed to warm to r.t. After completion of the reaction as indicated by TLC, the resultant was quenched with saturated $NaHCO_3$(aq) and extracted twice with DCM. The combined organic layer was dried over anhydrous Na_2SO_4(s) and the filtrate was condensed under reduced pressure, followed by silica-gel flash column chromatography to afford the desired product **SB1622** (51.2 mg, 81% yield) as a white solid.

SB1622. R_f = 0.2 (Hexane/EtOAc = 1:1); ^{1}H NMR (400 MHz, $CDCl_3$) δ 8.50 (s, 1H), 8.24 (d, J = 9.0 Hz, 2H), 7.59 (d, J = 9.0 Hz, 2H), 7.45, 7.39 (ABq, J_{AB} = 8.2 Hz, 4H), 6.47 (s, 1H), 4.81–4.65 (m, 3H), 4.45 (br s, 1H), 3.80 (d, J = 8.2 Hz, 1H), 3.38 (br s, 1H), 3.14 (s, 3H), 2.96 (dd, J = 7.8, 5.5 Hz, 1H), 2.06 (s, 3H); ^{13}C NMR (100 MHz, $CDCl_3$) δ 171.1, 165.8, 161.0, 156.1, 150.6, 144.0, 135.7, 133.7, 129.3, 128.9, 128.6, 124.8, 86.3, 69.1, 58.2, 57.6, 46.1, 40.2, 23.6; IR (neat) ν_{max}: 2970, 1739, 1674, 1559, 1530, 1350, 1229, 1169, 738 cm^{-1}; HRMS(ESI+): Calcd for $C_{24}H_{24}ClN_6O_6S^+$ $[M+H]^+$ 559.1161, found 559.1175, Δppm +2.50, mp: 105–107 °C.

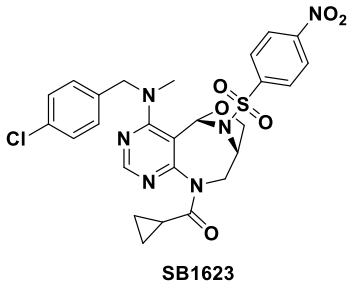

SB1623. A light yellow solid; R_f = 0.35 (Hexane/EtOAc = 1:1); 56.2 mg, 85 % yield; ^{1}H NMR (400 MHz, $CDCl_3$) δ 8.53 (s, 1H), 8.23 (d, J = 8.6 Hz, 2H), 7.59 (d, J = 9.0 Hz, 2H), 7.45, 7.40 (ABq, J_{AB} = 8.2 Hz, 4H), 6.51 (s, 1H), 4.74 (m, 3H), 4.45 (br s, 1H), 3.75 (d, J = 7.8 Hz, 1H), 3.40 (br d, J = 8.6 Hz, 1H), 3.14 (s, 3H), 2.94 (m ,1 H), 1.63 (m, 1H), 1.05 (m, 2H), 0.81 (m, 1H), 0.70 (m, 1H); ^{13}C NMR (100 MHz, $CDCl_3$) δ 174.8, 165.9, 161.0, 156.1 (C2, d, J = 3.8 Hz), 150.6, 144.0, 135.7, 133.7, 129.3, 128.9, 128.7, 124.8, 86.4, 69.0, 58.2, 57.6, 46.5, 40.2

(C25, d, J = 3.7 Hz), 14.0; IR (neat) ν_{max}: 2970, 1739, 1665, 1558, 1530, 1398, 1350, 1168, 738 cm^{-1}; HRMS(ESI+): Calcd for $C_{26}H_{26}ClN_6O_6S^+$ $[M+H]^+$ 585.1318, Δppm +1.03; found 585.1324; mp: 124–126 ºC. The product was synthesized according to the synthetic procedure for the preparation of **SB1622** from **SB1617** and cyclopropanecarbonyl chloride.

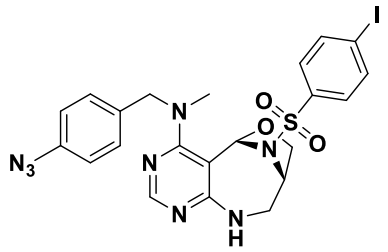

9b

Compound 9b. A pale yellow solid; R_f = 0.45 (EtOAc); 73.0 mg, 61 % overall yield; ^{1}H NMR (500 MHz, $CDCl_3$) δ 8.12 (s, 1H), 7.79 (d, J = 8.3 Hz, 2H), 7.36 (d, J = 8.3 Hz, 2H), 7.28 (d, J = 8.3 Hz, 2H), 7.07 (d, J = 8.3 Hz, 2H), 6.62 (s, 1H), 5.90 (br d, J = 3.9 Hz, 1H), 4.66, 4.62 (ABq, J_{AB} = 16.8 Hz, 2H), 4.49 (br s, 1H), 3.81 (d, J = 6.8 Hz, 1H), 3.56 (d, J = 13.0 Hz, 1H), 3.43 (dt, J = 13.6, 5.0 Hz, 1H), 3.06 (t, J = 6.8 Hz, 1H), 2.97 (s, 3H); ^{13}C NMR (100 MHz, $CDCl_3$) δ 166.3, 163.5, 156.2, 139.2, 138.7, 137.7, 135.0, 129.2, 129.0, 119.4, 103.4, 101.6, 87.7, 66.9, 58.0, 56.4, 48.7, 40.3; IR (neat) ν_{max}: 2969, 2107, 1736, 1567, 1351, 1166, 733 cm^{-1}; HRMS(ESI+): Calcd for $C_{22}H_{22}IN_8O_3S^+$ $[M+H]^+$ 605.0575, found 605.0577, Δppm +0.33; mp: 98–100 ^{o}C. The product was synthesized according to the synthetic procedure for the preparation of **SB1601** from **9a** and 4-iodobenzenesulfonyl chloride.

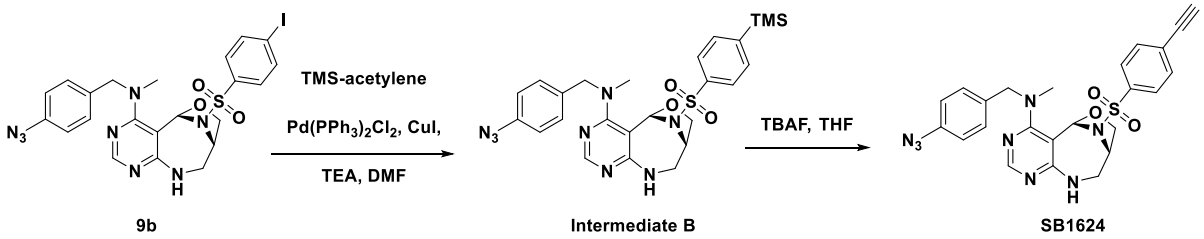

Synthetic procedure for the preparation of SB1624

To a solution of **9b** (73.0 mg, 0.121 mmol) in dimethylformamide (DMF, 6 mL) were added trimethylsilylacetylene (0.033 mL, 0.242 mmol), $Pd(PPh_3)_2Cl_2$ (8.50 mg, 0.012 mmol, 10 mol %), copper(I) iodide (CuI, 11.6 mg, 0.061 mmol) and triethylamine (TEA, 0.051 mL, 0.363 mmol). Then the resulting mixture was left to stir at r.t. After completion of the reaction indicated by TLC, the resultant was quenched with saturated NH_4Cl(aq) and extracted twice with ethyl acetate. The combined organic layer was dried over anhydrous Na_2SO_4 and filtered. The filtrate was condensed under reduced pressure, followed by silica-gel flash column chromatography to afford intermediate **B** (54.0 mg, 81% yield). To a solution of intermediate **B** (54.0 mg, 0.098 mmol) in THF (2 mL) was added TBAF (1.0 $_M$ solution in THF, 0.127 mL, 0.127 mmol). The reaction mixture was then left to stir at r.t. After completion of the reaction as indicated by TLC, the solvent was removed under reduced pressure and the residue was purified through the silica-gel flash column chromatography to obtain product **SB1624** (25.1 mg, 51% yield, 41% overall yield) as a light yellow solid. R_f = 0.45 (EtOAc); ^{1}H NMR (400 MHz, $CDCl_3$) δ 8.14 (s, 1H), 7.53 (s, 4H), 7.37 (d, *J* = 8.0 Hz, 2H), 7.08 (d, *J* = 8.0 Hz, 2H), 6.63 (s, 1H), 5.57 (br s, 1H), 4.66 (s, 2H), 4.49 (br s, 1H), 3.81 (d, *J* = 8.0 Hz, 1H), 3.57 (d, *J* = 12.0 Hz, 1H), 3.43 (m, 1H), 3.31 (s, 1H), 3.02 (m, 4H); ^{13}C NMR (100 MHz, $CDCl_3$) δ 166.3, 163.3, 155.9, 139.2, 137.9, 135.0, 133.0, 129.3, 128.0, 127.7, 119.4, 103.4, 87.7, 81.80, 81.78, 66.9, 58.0, 56.4, 48.8, 40.3; IR (neat) ν_{max}: 3373, 3215, 2955, 2102, 1737, 1574, 1353, 1166, 973 cm^{-1}; HRMS(ESI+): Calcd for $C_{24}H_{23}N_8O_3S^+$ $[M+H]^+$ 503.1608, found 503.1607, Δppm –0.20; mp: 139–141 ^{o}C.

^{1}H and ^{13}C NMR Spectra

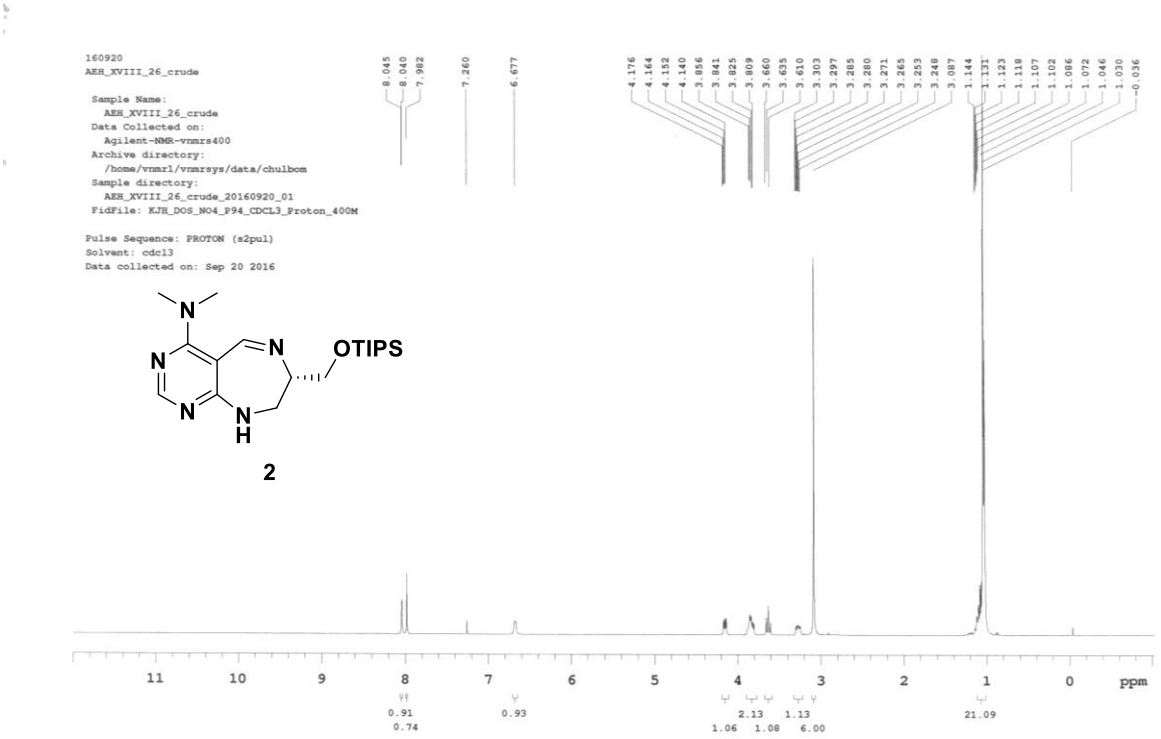

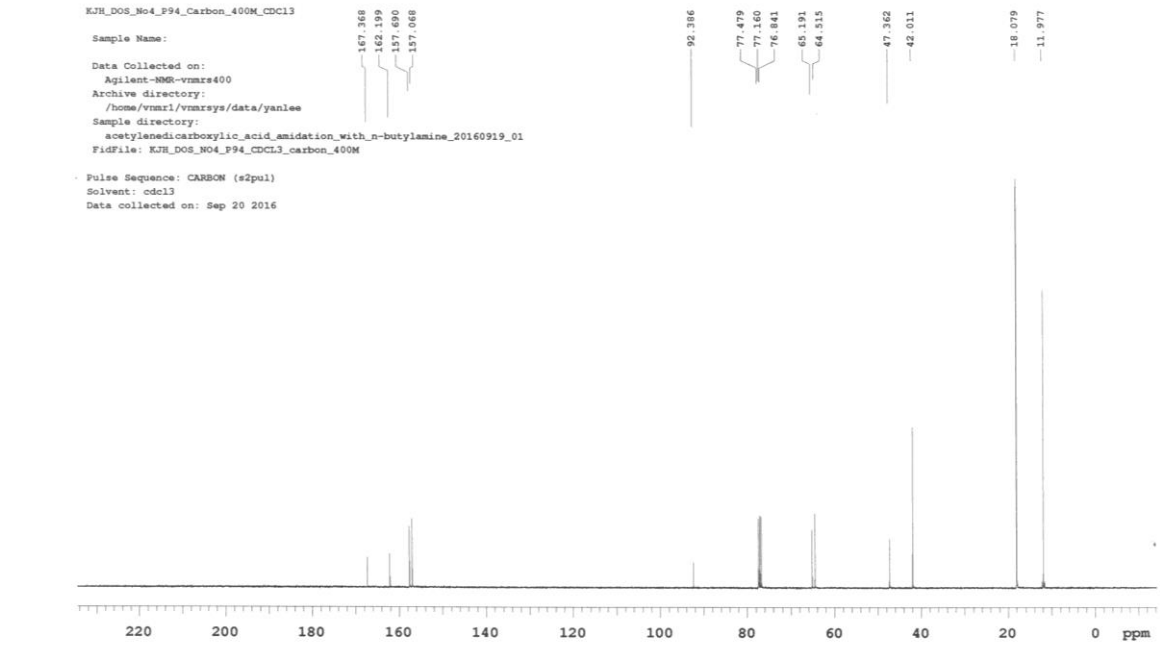

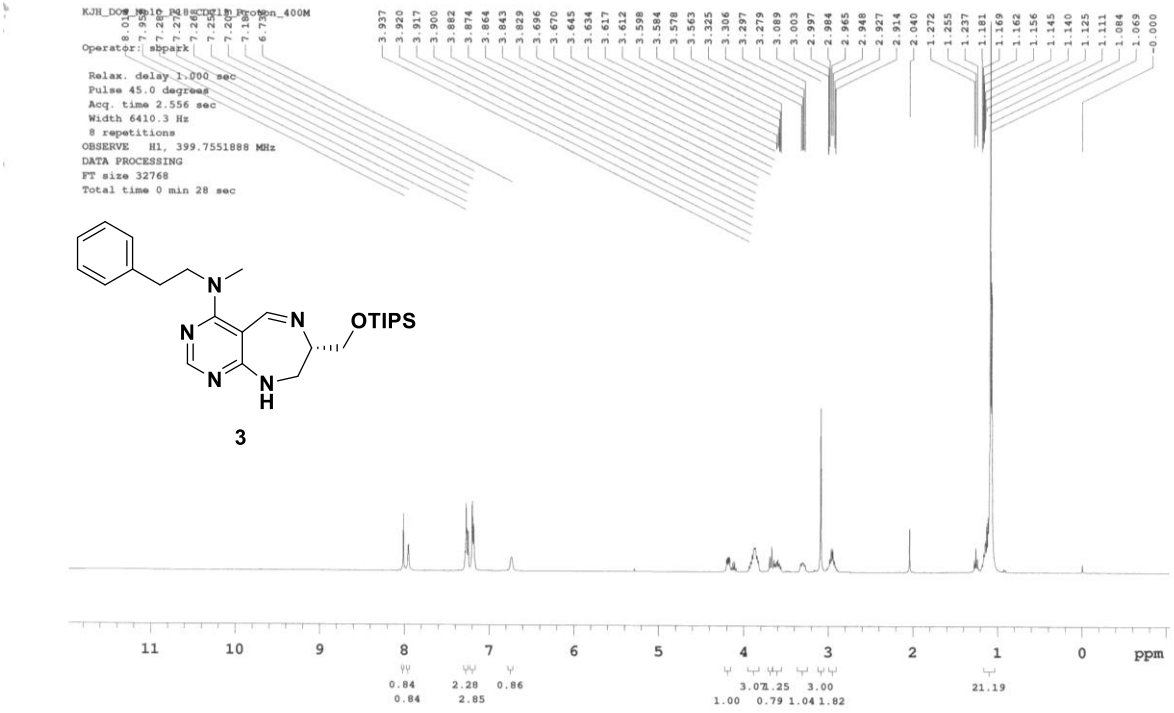
Operator: sbpark
Relax. delay 1.000 sec
Pulse 45.0 degrees
Acq. time 2.556 sec
Width 6410.3 Hz
8 repetitions
OBSERVE H1, 399.7551888 MHz
DATA PROCESSING
FT size 32768
Total time 0 min 28 sec
OTIPS
3
ppm

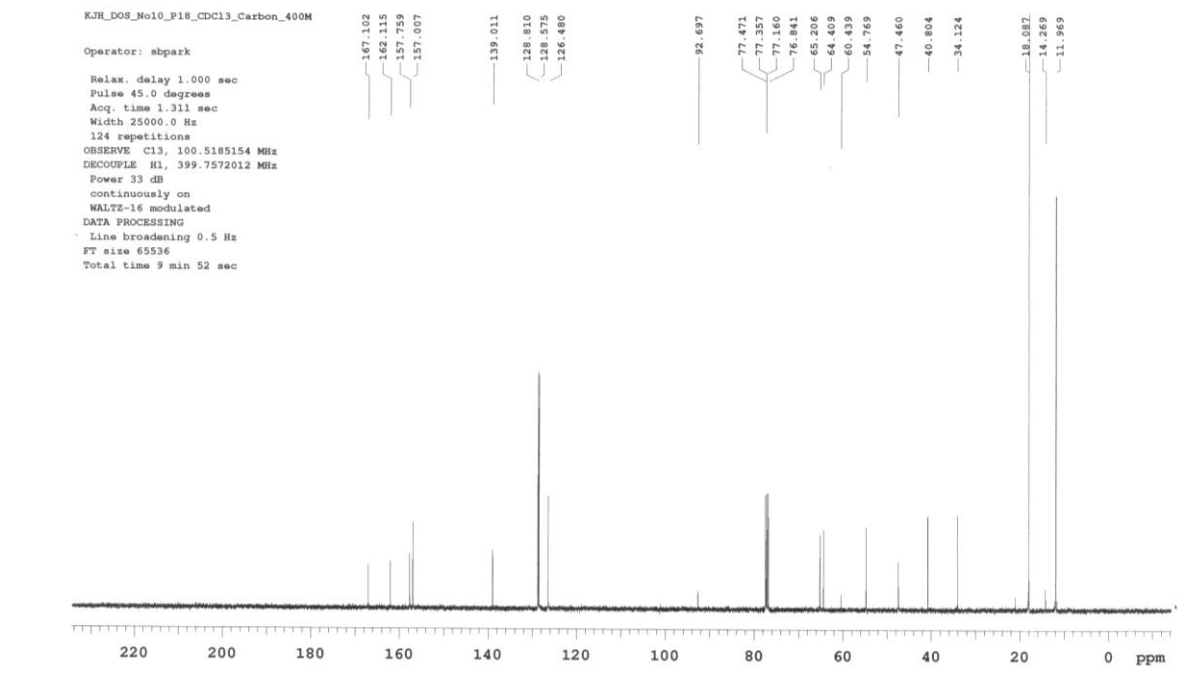
KJH_DOS_No10_P18_CDCl3_Carbon_400M
Operator: sbpark
Relax. delay 1.000 sec
Pulse 45.0 degrees
Acq. time 1.311 sec
Width 25000.0 Hz
124 repetitions
OBSERVE C13, 100.5185154 MHz
DECOUPLE H1, 399.7572012 MHz
Power 33 dB
continuously on
WALTZ-16 modulated
DATA PROCESSING
Line broadening 0.5 Hz
FT size 65536
Total time 9 min 52 sec
ppm

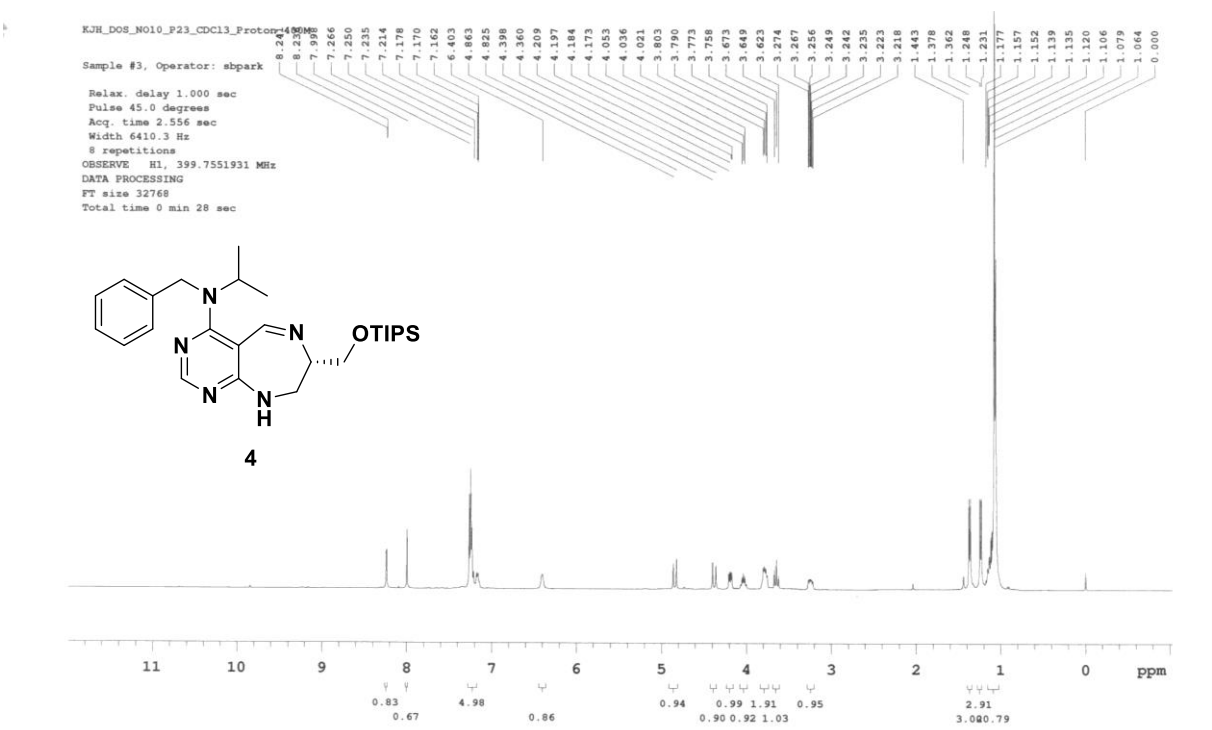
KJH_DOS_N010_P23_CDCl3_Proton_400M
Sample #3, Operator: sbpark
Relax. delay 1.000 sec
Pulse 45.0 degrees
Acq. time 2.556 sec
Width 6410.3 Hz
8 repetitions
OBSERVE H1, 399.7551931 MHz
DATA PROCESSING
FT size 32768
Total time 0 min 28 sec
OTIPS
4
ppm

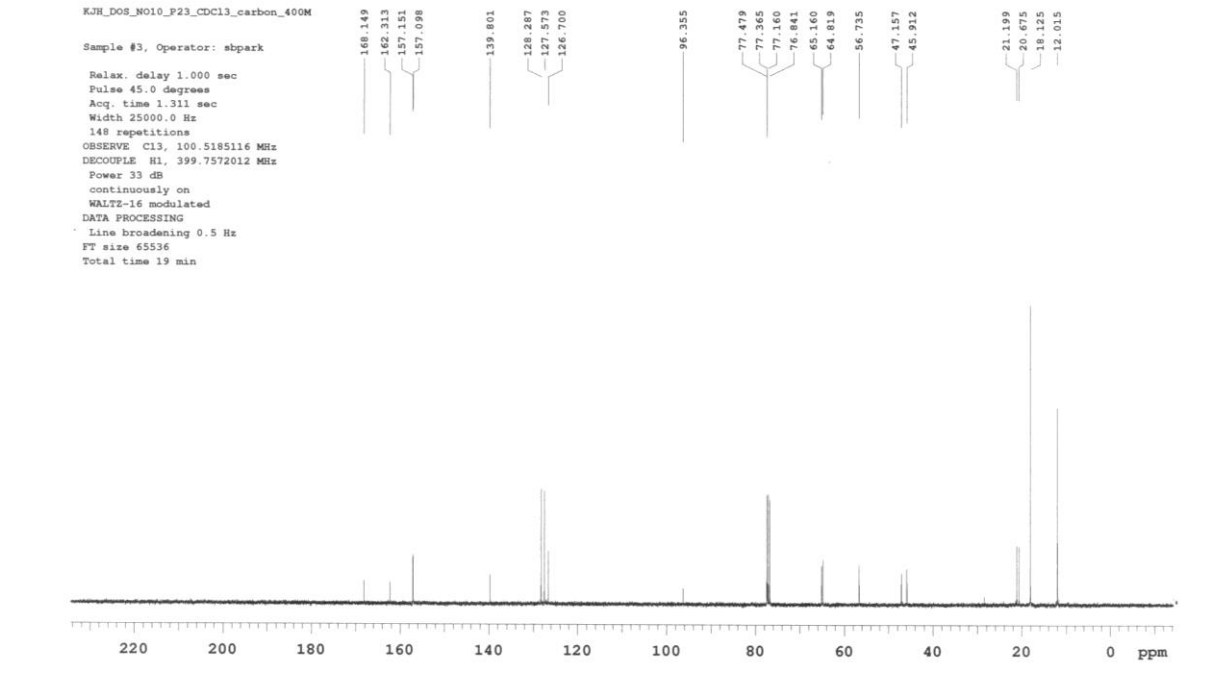
KJH_DOS_N010_P23_CDCl3_carbon_400M
Sample #3, Operator: sbpark
Relax. delay 1.000 sec
Pulse 45.0 degrees
Acq. time 1.311 sec
Width 25000.0 Hz
148 repetitions
OBSERVE C13, 100.5185116 MHz
DECOUPLE H1, 399.7572012 MHz
Power 33 dB
continuously on
WALTZ-16 modulated
DATA PROCESSING
Line broadening 0.5 Hz
FT size 65536
Total time 19 min
ppm

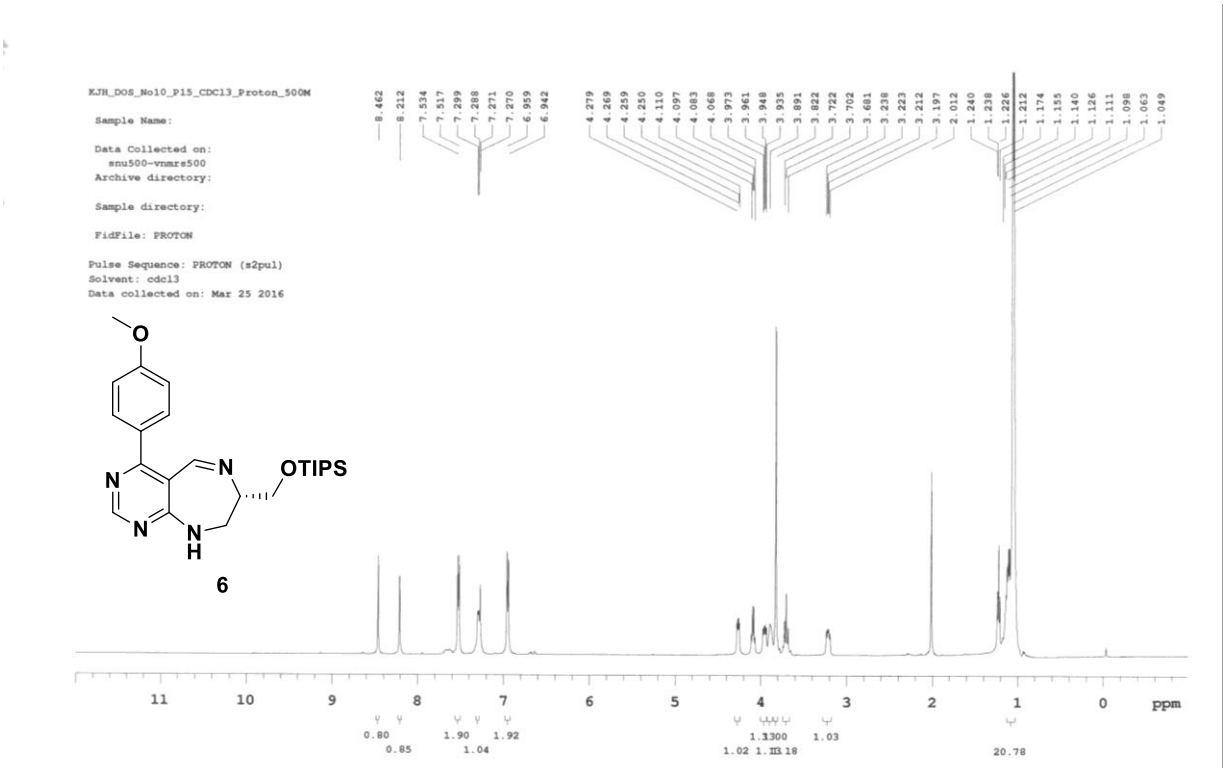
KJH_DOS_No10_P15_CDC13_Proton_500M
Sample Name:
Data Collected on:
snu500-vnmrs500
Archive directory:
Sample directory:
FidFile: PROTON
Pulse Sequence: PROTON (s2pul)
Solvent: cdcl3
Data collected on: Mar 25 2016
O
N
N
N
N
H
OTIPS
6
ppm

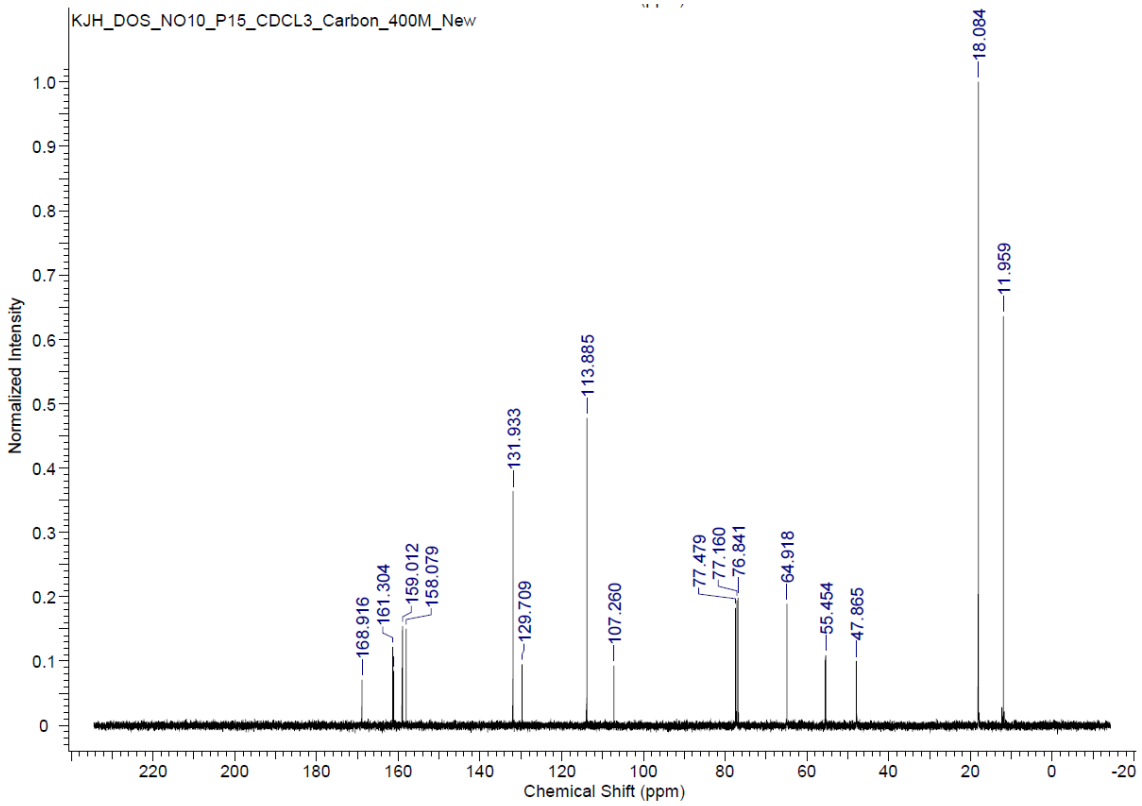
KJH_DOS_NO10_P15_CDCL3_Carbon_400M_New
Normalized Intensity
Chemical Shift (ppm)
18.084
11.959
113.885
131.933
168.916
161.304
159.012
158.079
129.709
107.260
77.479
77.160
76.841
64.918
55.454
47.865

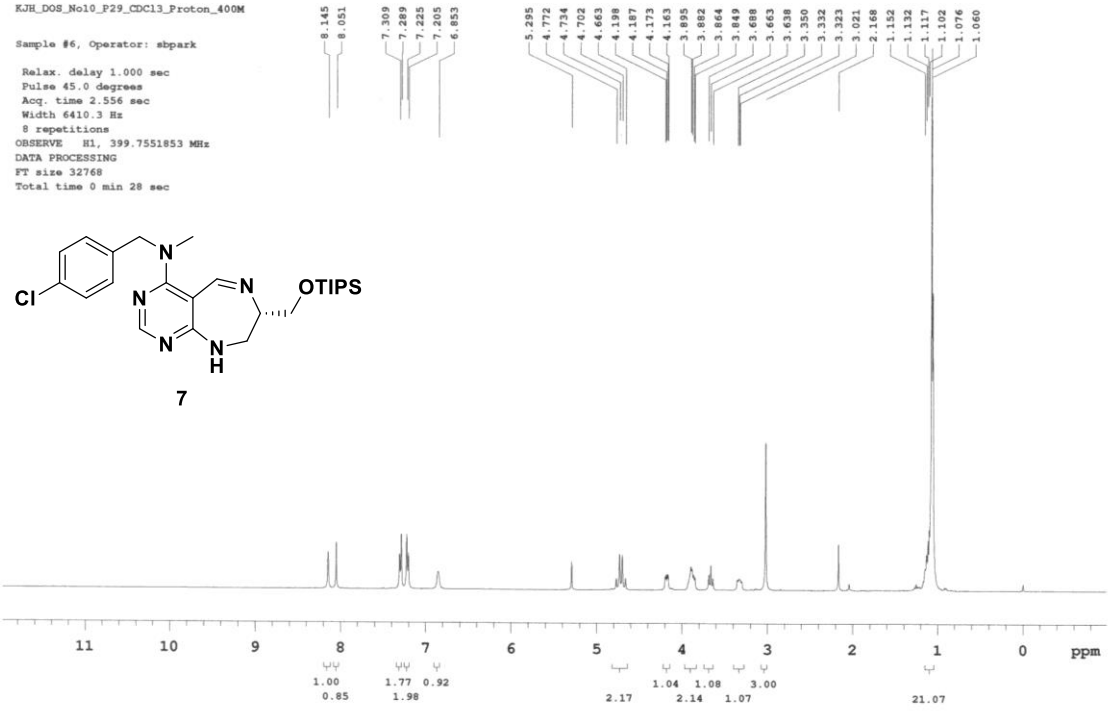
KJH_DOS_No10_P29_CDCl3_Proton_400M
Sample #6, Operator: sbpark
Relax. delay 1.000 sec
Pulse 45.0 degrees
Acq. time 2.556 sec
Width 6410.3 Hz
8 repetitions
OBSERVE H1, 399.7551853 MHz
DATA PROCESSING
FT size 32768
Total time 0 min 28 sec
8.145
8.051
7.309
7.289
7.225
7.205
6.853
5.295
4.772
4.734
4.702
4.663
4.198
4.187
4.173
4.163
3.895
3.882
3.864
3.849
3.688
3.663
3.638
3.350
3.332
3.323
3.021
2.168
1.152
1.132
1.117
1.102
1.076
1.060
Cl
N
N
N
N
H
OTIPS
7
11
10
9
8
7
6
5
4
3
2
1
0
ppm
1.00
0.85
1.77
1.98
0.92
2.17
1.04
2.14
1.08
1.07
3.00
21.07

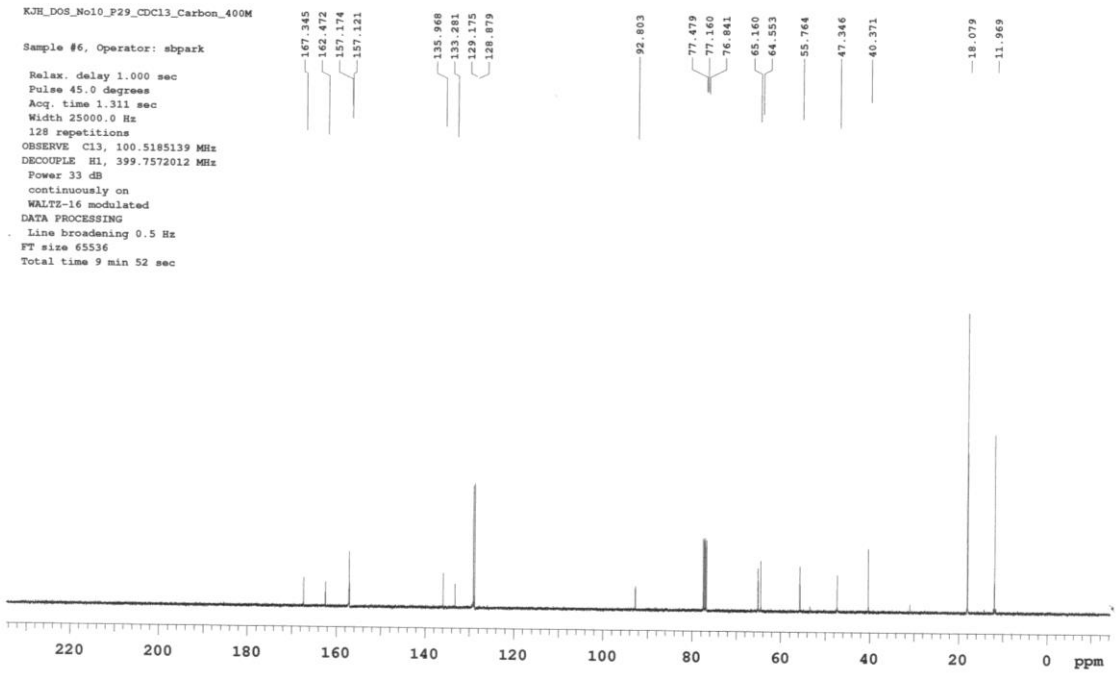
KJH_DOS_No10_P29_CDCl3_Carbon_400M
Sample #6, Operator: sbpark
Relax. delay 1.000 sec
Pulse 45.0 degrees
Acq. time 1.311 sec
Width 25000.0 Hz
128 repetitions
OBSERVE C13, 100.5185139 MHz
DECOUPLE H1, 399.7572012 MHz
Power 33 dB
continuously on
WALTZ-16 modulated
DATA PROCESSING
Line broadening 0.5 Hz
FT size 65536
Total time 9 min 52 sec
167.345
162.472
157.174
157.121
135.968
133.281
129.175
128.879
92.803
77.479
77.160
76.841
65.160
64.553
55.764
47.346
40.371
18.079
11.969
220
200
180
160
140
120
100
80
60
40
20
0
ppm

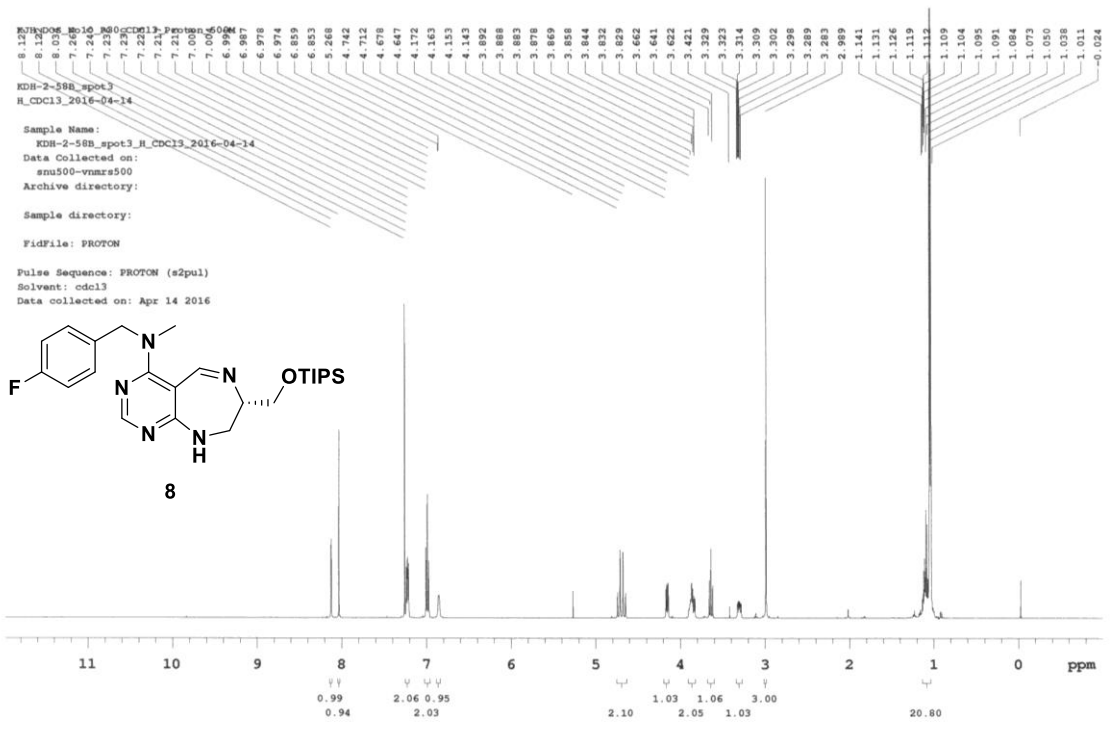
KDH-2-58B_spot3
H_CDCl3_2016-04-14
Sample Name:
KDH-2-58B_spot3_H_CDCl3_2016-04-14
Data Collected on:
snu500-vnmrs500
Archive directory:
Sample directory:
FidFile: PROTON
Pulse Sequence: PROTON (s2pul)
Solvent: cdcl3
Data collected on: Apr 14 2016
F
N
N
N
N
H
N
OTIPS
8
ppm

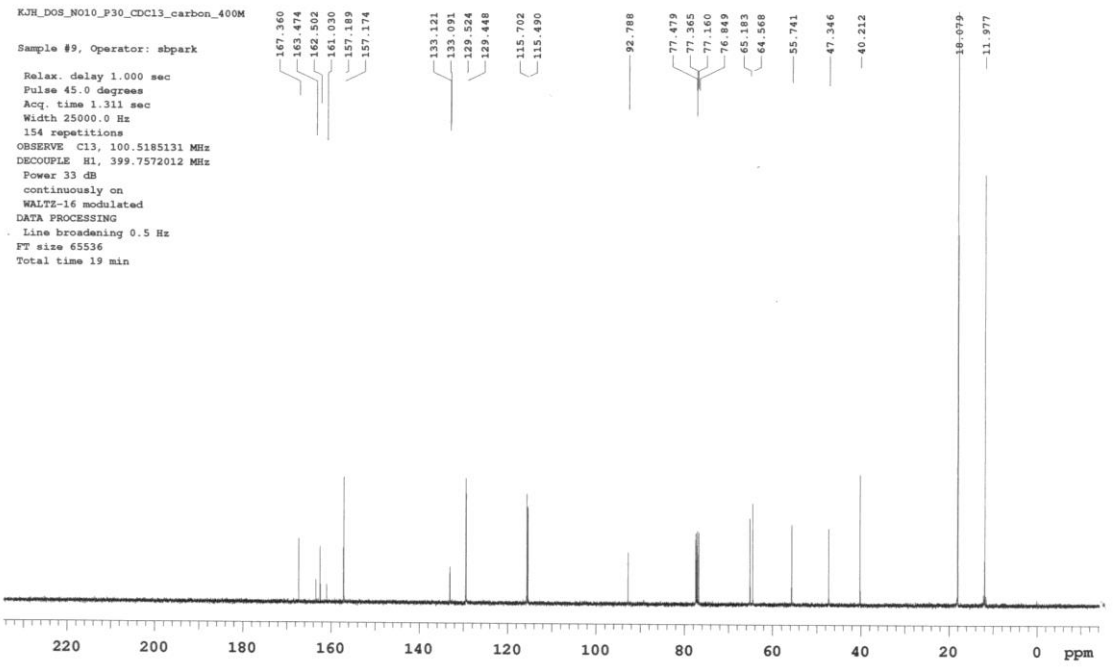
KJH_DOS_NO10_P30_CDCl3_carbon_400M
Sample #9, Operator: sbpark
Relax. delay 1.000 sec
Pulse 45.0 degrees
Acq. time 1.311 sec
Width 25000.0 Hz
154 repetitions
OBSERVE C13, 100.5185131 MHz
DECOUPLE H1, 399.7572012 MHz
Power 33 dB
continuously on
WALTZ-16 modulated
DATA PROCESSING
Line broadening 0.5 Hz
FT size 65536
Total time 19 min
ppm

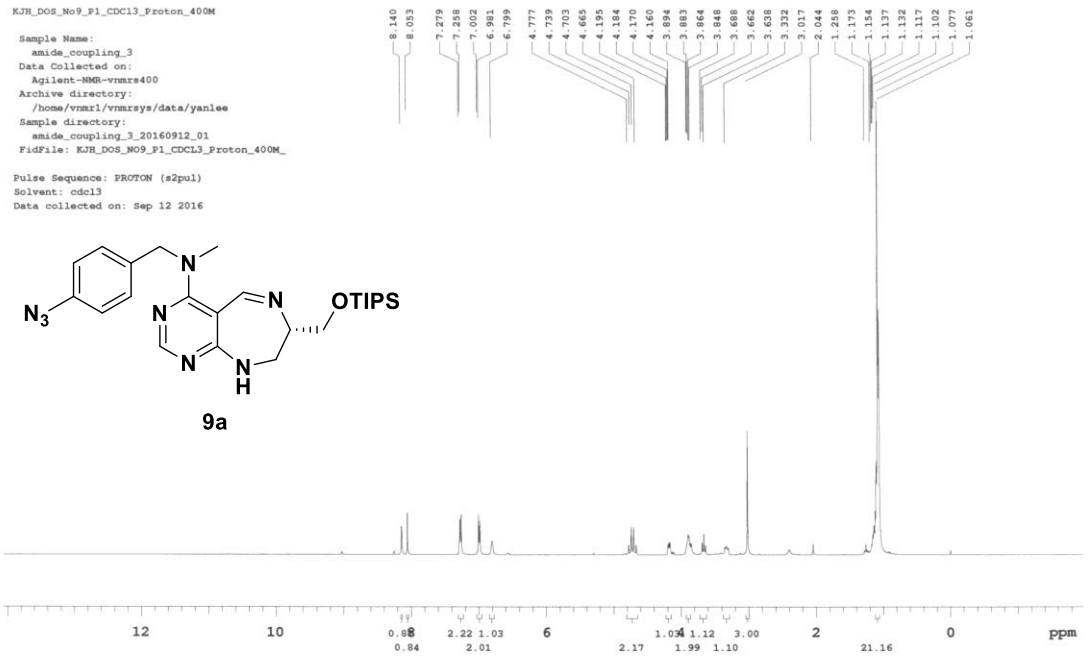
KJH_DOS_No9_P1_CDCl3_Proton_400M
Sample Name:
amide_coupling_3
Data Collected on:
Agilent-NMR-vnmrs400
Archive directory:
/home/vnmrl/vnmrsys/data/yanlee
Sample directory:
amide_coupling_3_20160912_01
FidFile: KJH_DOS_NO9_P1_CDCL3_Proton_400M_
Pulse Sequence: PROTON (s2pul)
Solvent: cdcl3
Data collected on: Sep 12 2016
8.140
8.053
7.279
7.258
7.002
6.981
6.799
4.777
4.739
4.703
4.665
4.195
4.184
4.170
4.160
3.894
3.883
3.864
3.848
3.688
3.662
3.638
3.332
3.017
2.044
1.258
1.173
1.154
1.137
1.132
1.117
1.102
1.077
1.061
N3
N
N
N
N
H
OTIPS
9a
12
10
8
6
2
0
ppm
0.84
2.01
2.17
1.99
1.10
21.16

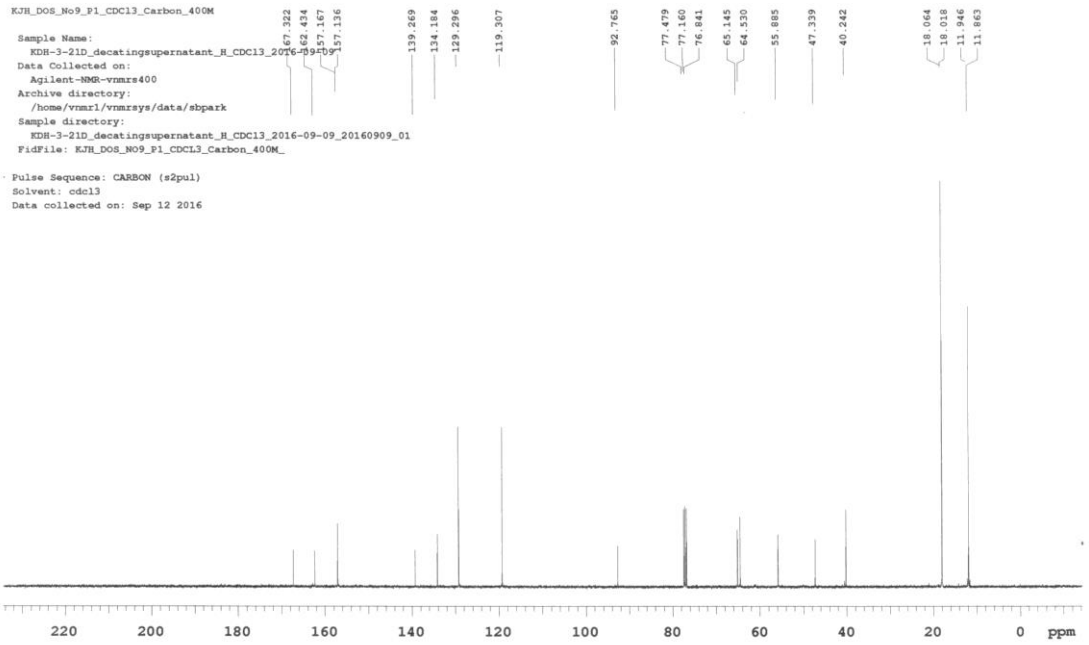
KJH_DOS_No9_P1_CDCl3_Carbon_400M
Sample Name:
KDH-3-21D_decatingsupernatant_H_CDCl3_2016-09-09
Data Collected on:
Agilent-NMR-vnmrs400
Archive directory:
/home/vnmrl/vnmrsys/data/sbpark
Sample directory:
KDH-3-21D_decatingsupernatant_H_CDCl3_2016-09-09_20160909_01
FidFile: KJH_DOS_NO9_P1_CDCL3_Carbon_400M_
Pulse Sequence: CARBON (s2pul)
Solvent: cdcl3
Data collected on: Sep 12 2016
167.322
162.434
157.167
157.136
139.269
134.184
129.296
119.307
92.765
77.479
77.160
76.841
65.145
64.530
55.885
47.339
40.242
18.064
18.018
11.946
11.863
220
200
180
160
140
120
100
80
60
40
20
0
ppm

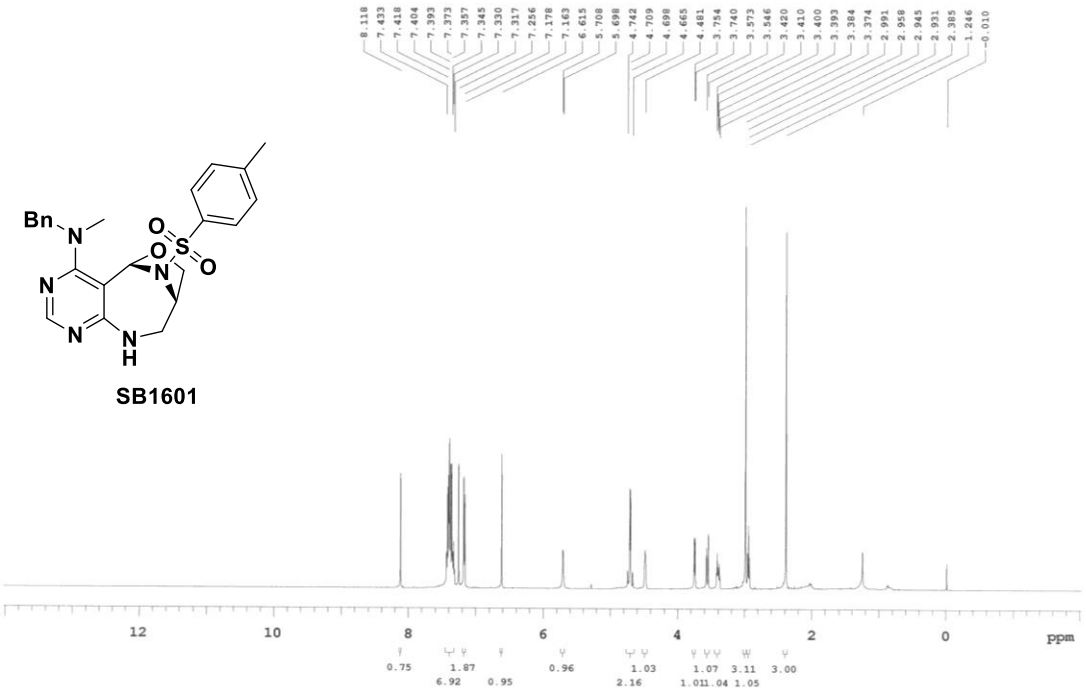
8.118
7.433
7.418
7.404
7.393
7.373
7.357
7.345
7.330
7.317
7.256
7.178
7.163
6.615
5.708
5.698
4.742
4.709
4.698
4.665
4.481
3.754
3.740
3.573
3.546
3.420
3.410
3.400
3.393
3.384
3.374
2.991
2.958
2.945
2.931
2.385
1.246
0.010
Bn
N
O
S
O
O
N
N
N
N
H
SB1601
12
10
8
6
4
2
0
ppm
0.75
1.87
6.92
0.95
0.96
1.03
2.16
1.07
1.01
3.11
1.04
1.05
3.00

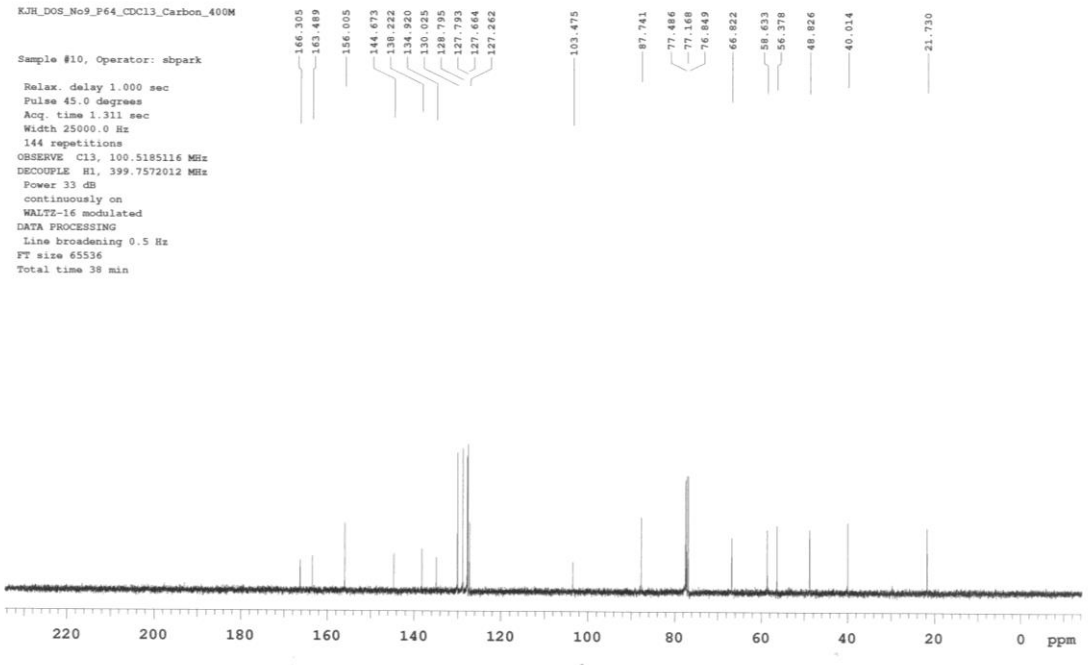
KJH_DOS_No9_P64_CDCl3_Carbon_400M
Sample #10, Operator: sbpark
Relax. delay 1.000 sec
Pulse 45.0 degrees
Acq. time 1.311 sec
Width 25000.0 Hz
144 repetitions
OBSERVE C13, 100.5185116 MHz
DECOUPLE H1, 399.7572012 MHz
Power 33 dB
continuously on
WALTZ-16 modulated
DATA PROCESSING
Line broadening 0.5 Hz
FT size 65536
Total time 38 min
166.305
163.489
156.005
144.673
130.222
134.920
130.025
128.795
127.793
127.664
127.262
103.475
87.741
77.486
77.168
76.849
66.822
58.633
56.378
48.826
40.014
21.730
220
200
180
160
140
120
100
80
60
40
20
0
ppm

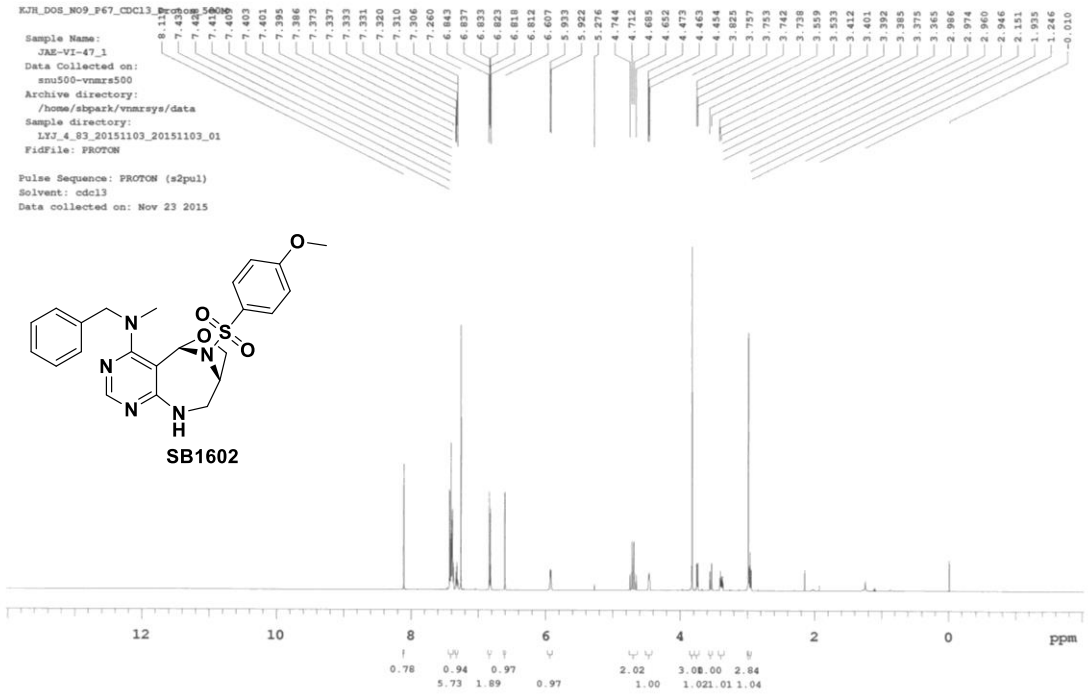
KJH_DOS_N09_P67_CDCl3_Proton_500M
Sample Name:
JAE-VI-47_1
Data Collected on:
snu500-vnmrs500
Archive directory:
/home/sbpark/vnmrsys/data
Sample directory:
LYJ_4_83_20151103_20151103_01
FidFile: PROTON
Pulse Sequence: PROTON (s2pul)
Solvent: cdcl3
Data collected on: Nov 23 2015
SB1602
ppm

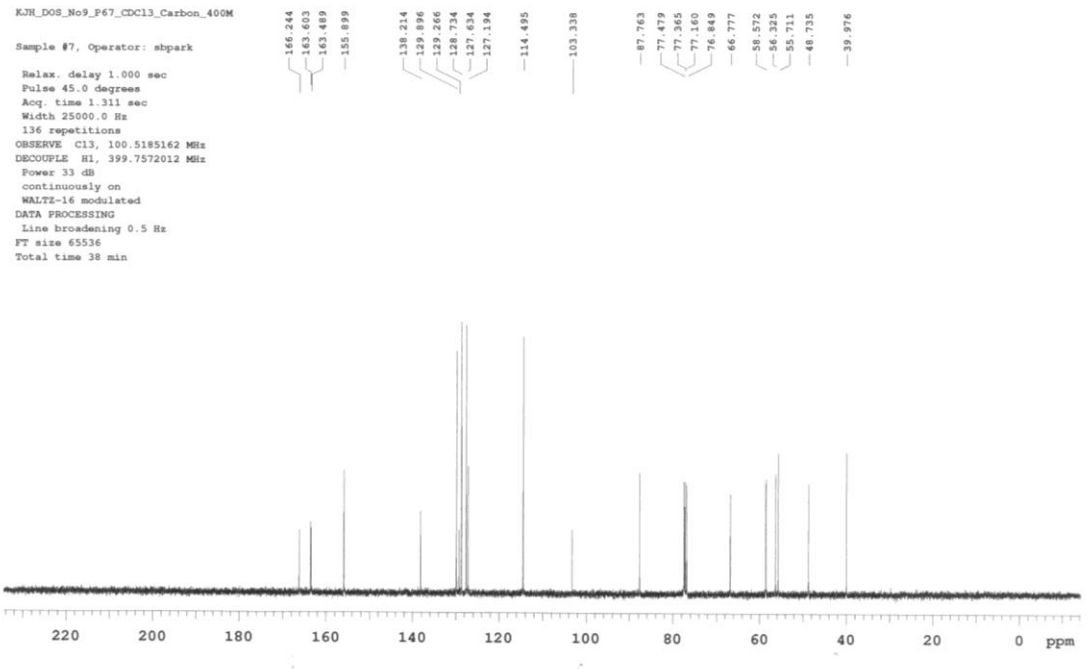
KJH_DOS_N09_P67_CDCl3_Carbon_400M
Sample #7, Operator: sbpark
Relax. delay 1.000 sec
Pulse 45.0 degrees
Acq. time 1.311 sec
Width 25000.0 Hz
136 repetitions
OBSERVE C13, 100.5185162 MHz
DECOUPLE H1, 399.7572012 MHz
Power 33 dB
continuously on
WALTZ-16 modulated
DATA PROCESSING
Line broadening 0.5 Hz
FT size 65536
Total time 38 min
ppm

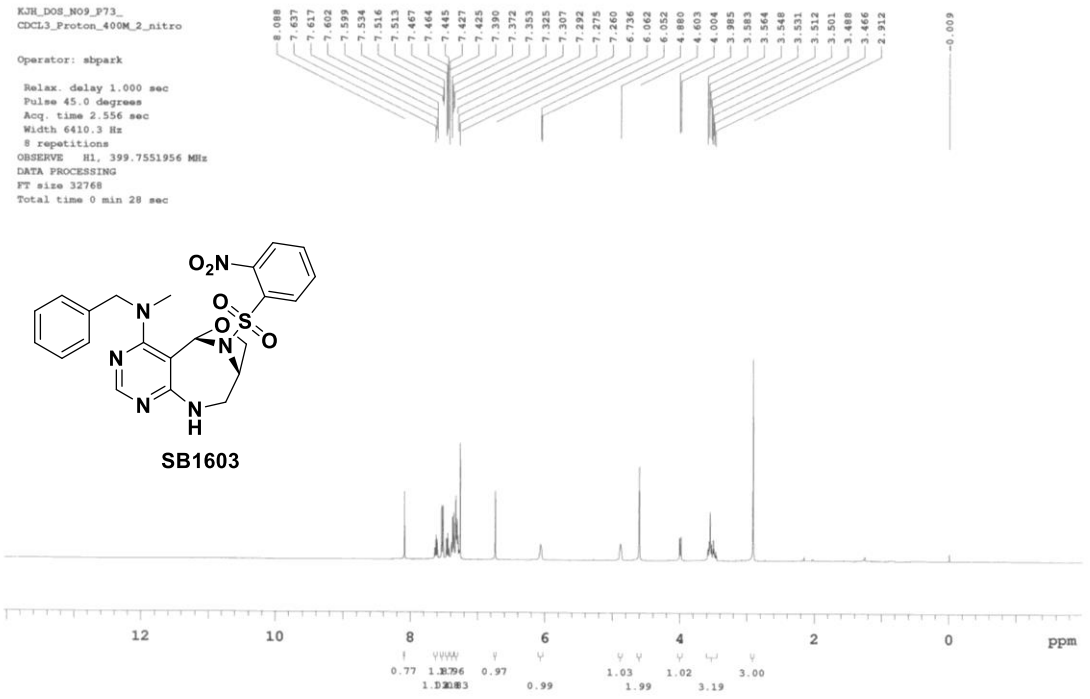
KJH_DOS_NO9_P73_
CDCL3_Proton_400M_2_nitro
Operator: sbpark
Relax. delay 1.000 sec
Pulse 45.0 degrees
Acq. time 2.556 sec
Width 6410.3 Hz
8 repetitions
OBSERVE H1, 399.7551956 MHz
DATA PROCESSING
FT size 32768
Total time 0 min 28 sec
SB1603
ppm

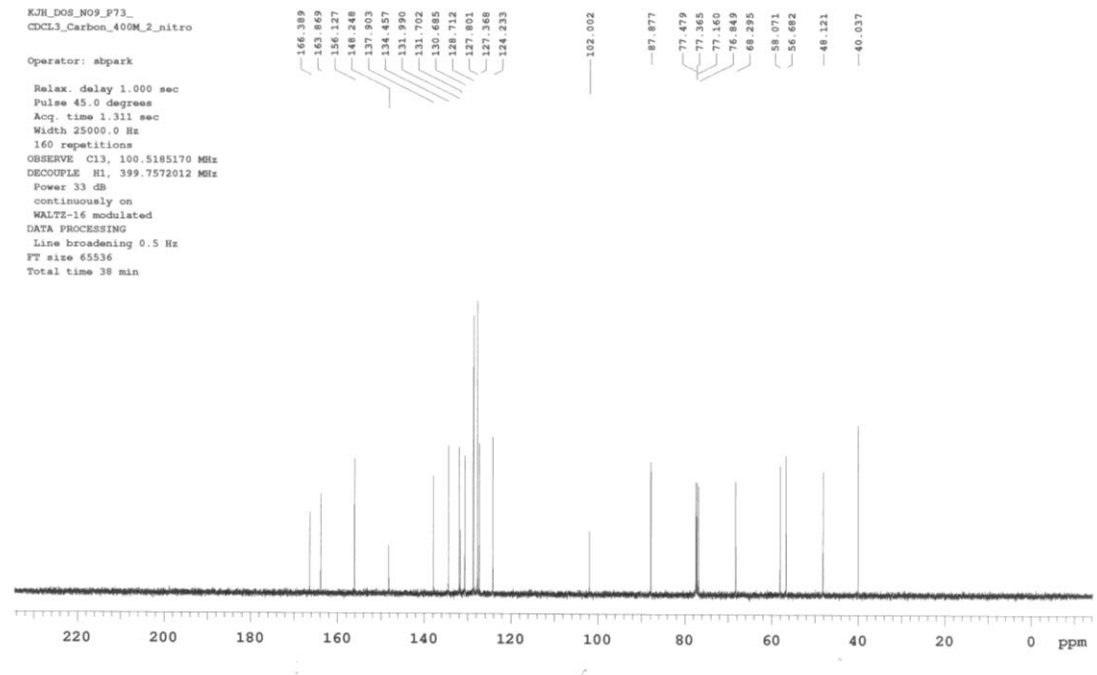
KJH_DOS_NO9_P73_
CDCL3_Carbon_400M_2_nitro
Operator: sbpark
Relax. delay 1.000 sec
Pulse 45.0 degrees
Acq. time 1.311 sec
Width 25000.0 Hz
160 repetitions
OBSERVE C13, 100.5185170 MHz
DECOUPLE H1, 399.7572012 MHz
Power 33 dB
continuously on
WALTZ-16 modulated
DATA PROCESSING
Line broadening 0.5 Hz
FT size 65536
Total time 38 min
ppm

15f

Sample Name:
JAE-III-107_1H
Data Collected on:
Agilent-NMR-vnmrs400
Archive directory:
/home/vnmr1/vnmrsys/data/sbpark
Sample directory:
JAE-III-107_1H_20150407_01
FidFile: PROTON_01

Pulse Sequence: PROTON (s2pul)
Solvent: cdcl3
Data collected on: Apr 7 2015

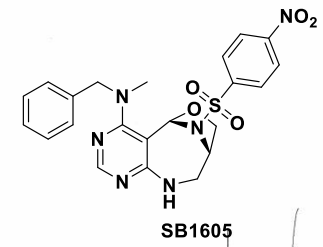

SB1605

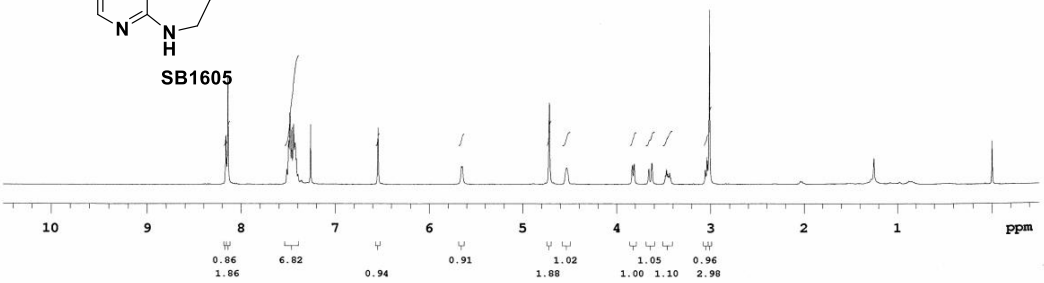

15f

Sample Name:
JAE-III-107_13C_20150407
Data Collected on:
Agilent-NMR-vnmrs400
Archive directory:
/home/vnmr1/vnmrsys/data/sbpark
Sample directory:
JAE-III-107_13C_20150407_20150407_01
FidFile: CARBON_01

Pulse Sequence: CARBON (s2pul)
Solvent: cdcl3
Data collected on: Apr 7 2015

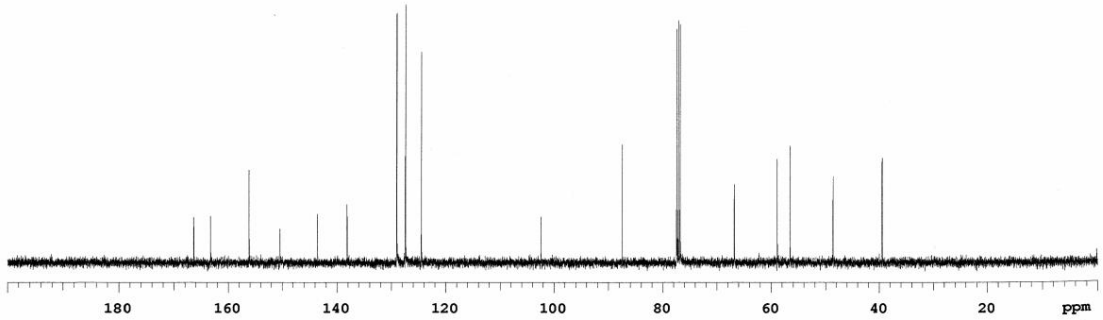

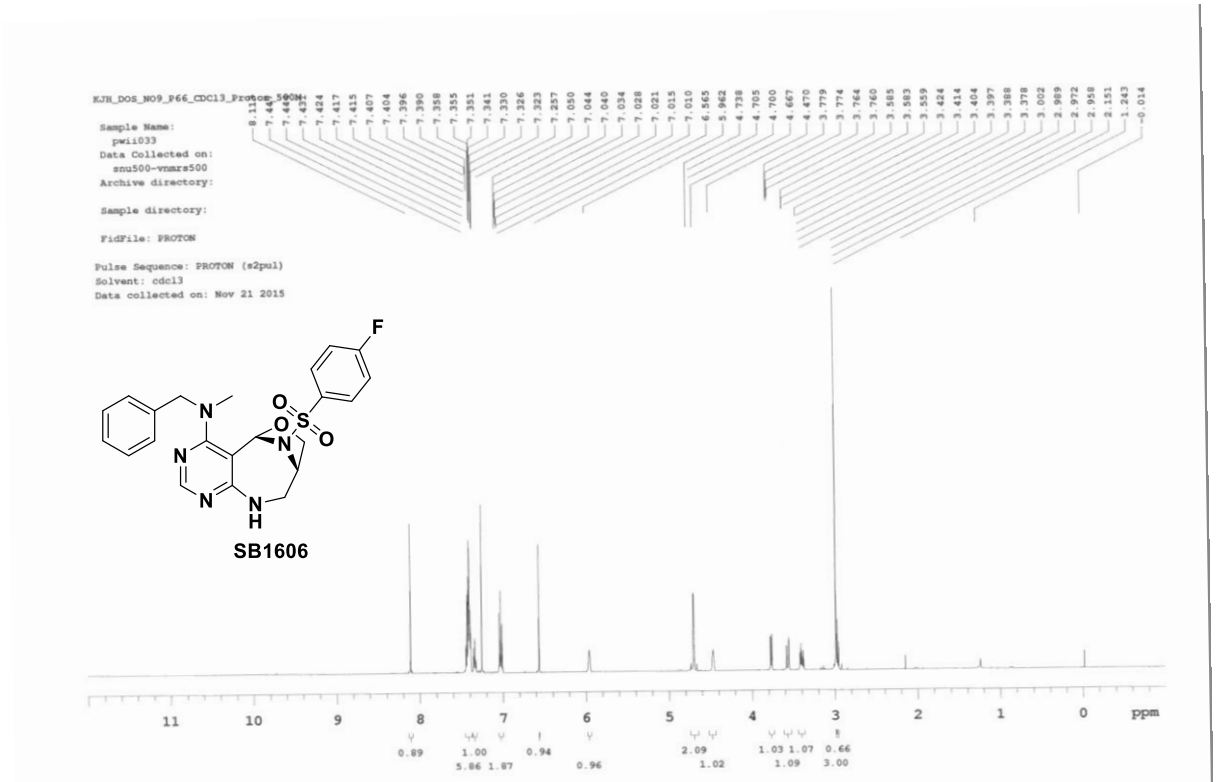
KJH_DOS_N09_P66_CDCl3_Proton_500M
Sample Name:
pwii033
Data Collected on:
snu500-vnmrs500
Archive directory:
Sample directory:
FidFile: PROTON
Pulse Sequence: PROTON (s2pul)
Solvent: cdcl3
Data collected on: Nov 21 2015
F
O
S
O
O
N
N
N
N
H
SB1606
11
10
9
8
7
6
5
4
3
2
1
0
ppm
0.89
1.00
5.86
1.87
0.94
0.96
2.09
1.02
1.03
1.07
1.09
0.66
3.00

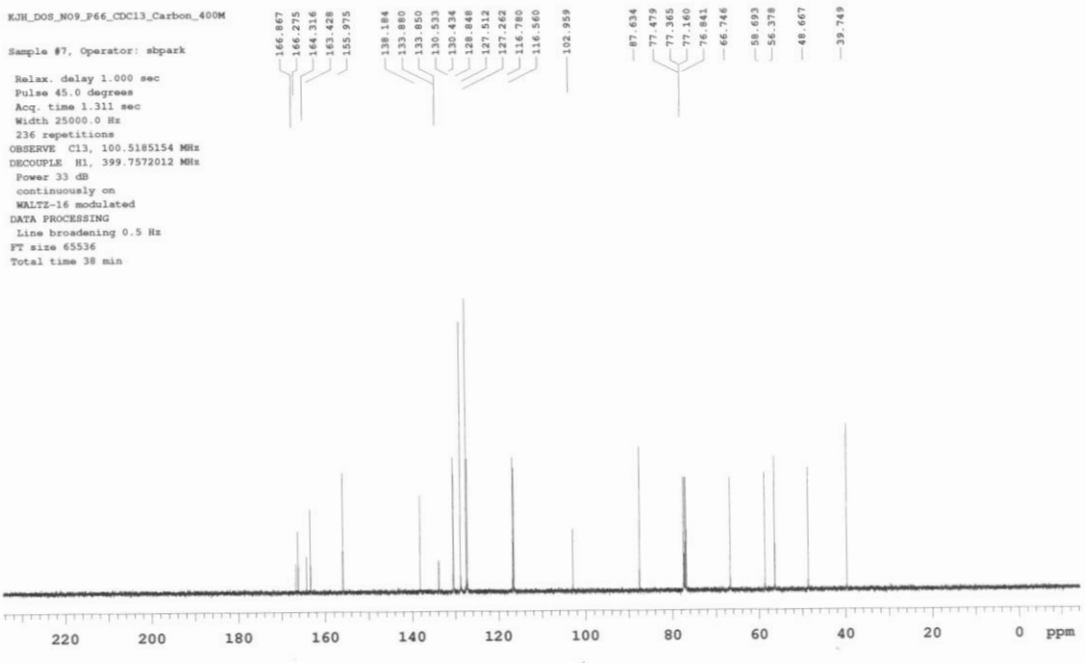
KJH_DOS_N09_P66_CDCl3_Carbon_400M
Sample #7, Operator: sbpark
Relax. delay 1.000 sec
Pulse 45.0 degrees
Acq. time 1.311 sec
Width 25000.0 Hz
236 repetitions
OBSERVE C13, 100.5185154 MHz
DECOUPLE H1, 399.7572012 MHz
Power 33 dB
continuously on
WALTZ-16 modulated
DATA PROCESSING
Line broadening 0.5 Hz
FT size 65536
Total time 38 min
166.867
166.275
164.316
163.428
155.975
138.184
133.880
133.850
130.533
130.434
128.848
127.512
127.262
116.780
116.560
102.959
87.634
77.479
77.365
77.160
76.841
66.746
58.693
56.378
48.667
39.749
220
200
180
160
140
120
100
80
60
40
20
0
ppm

KJH_DOS_No9_P65_CDCl3_Proton_400M

Sample #11, Operator: sbpark

Relax. delay 1.000 sec
Pulse 45.0 degrees
Acq. time 2.556 sec
Width 6410.3 Hz
8 repetitions
OBSERVE H1, 399.7551900 MHz
DATA PROCESSING
FT size 32768
Total time 0 min 28 sec

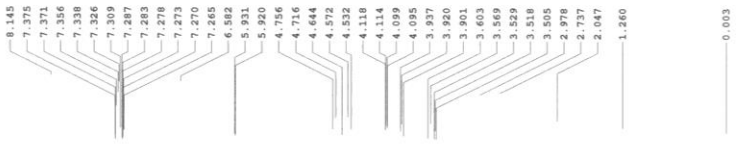

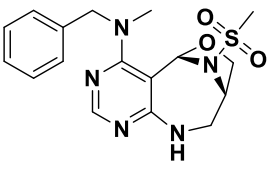

SB1607

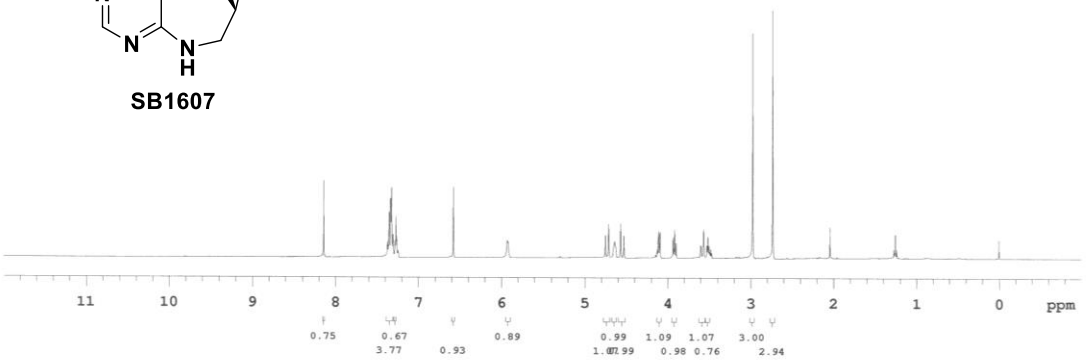

KJH_DOS_No9_P65_CDCl3_Carbon_400M

Sample #11, Operator: sbpark

Relax. delay 1.000 sec
Pulse 45.0 degrees
Acq. time 1.311 sec
Width 25000.0 Hz
136 repetitions
OBSERVE C13, 100.5185147 MHz
DECOUPLE H1, 399.7572012 MHz
Power 33 dB
continuously on
WALTZ-16 modulated
DATA PROCESSING
Line broadening 0.5 Hz
FT size 65536
Total time 38 min

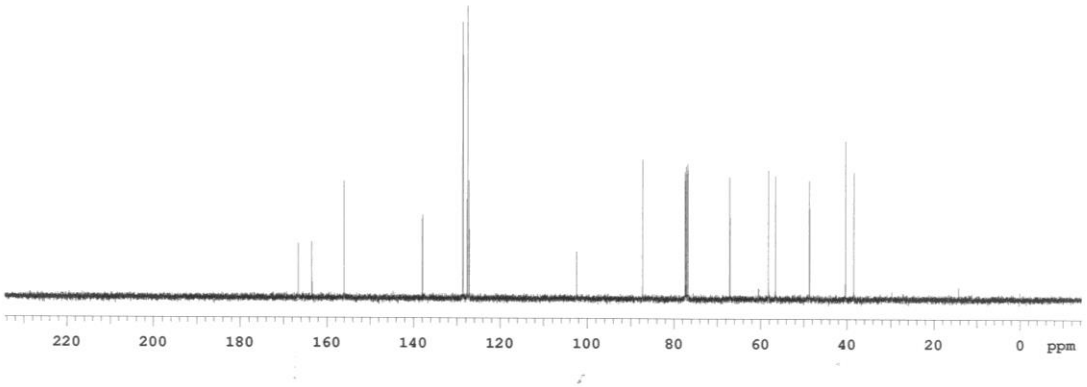

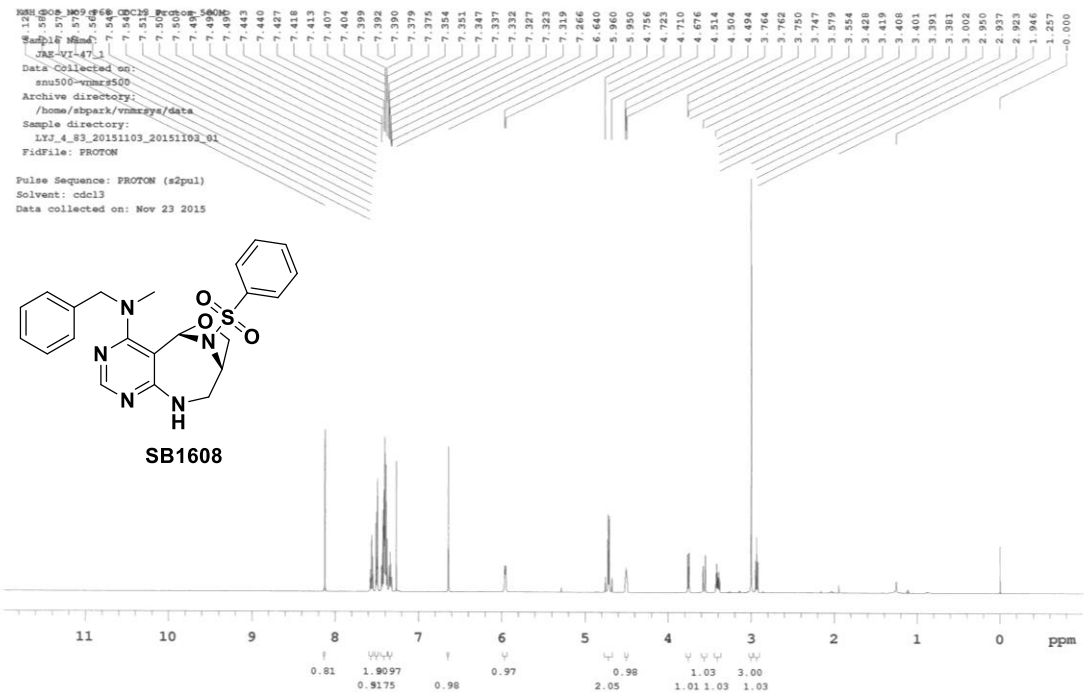
Sample Name:
JAE-VI-47_1
Data Collected on:
snu500-vnmrs500
Archive directory:
/home/sbpark/vnmrsys/data
Sample directory:
LYJ_4_83_20151103_20151103_01
FidFile: PROTON
Pulse Sequence: PROTON (s2pul)
Solvent: cdcl3
Data collected on: Nov 23 2015
SB1608
ppm
0.81
1.9097
0.9175
0.98
0.97
0.98
2.05
1.03
1.01
1.03
3.00
1.03

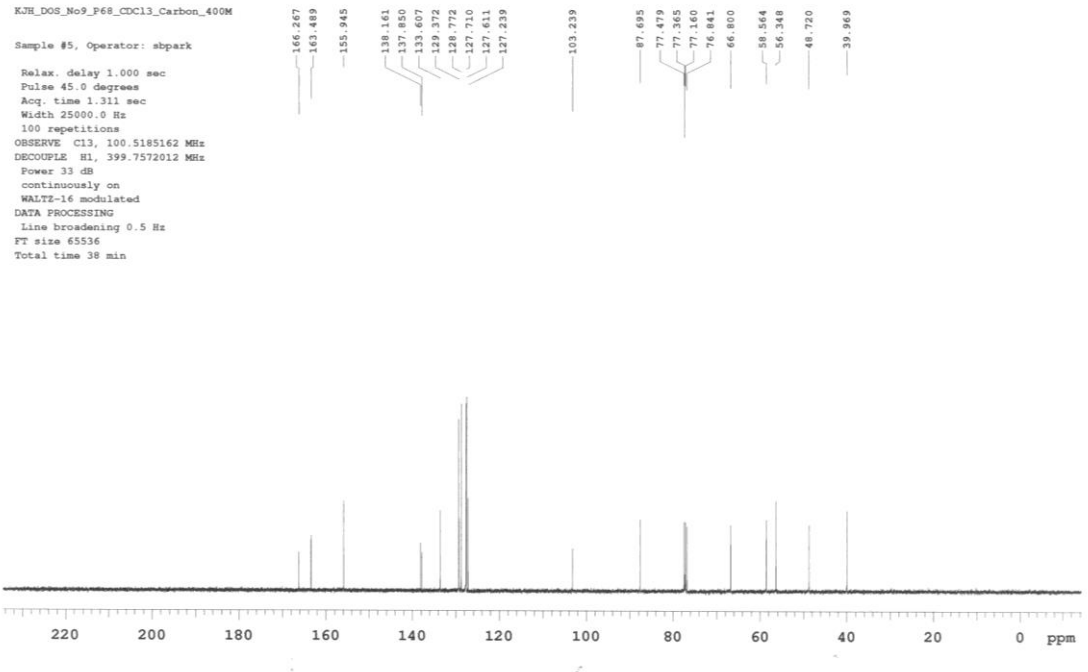
KJH_DOS_No9_P68_CDCl3_Carbon_400M
Sample #5, Operator: sbpark
Relax. delay 1.000 sec
Pulse 45.0 degrees
Acq. time 1.311 sec
Width 25000.0 Hz
100 repetitions
OBSERVE C13, 100.5185162 MHz
DECOUPLE H1, 399.7572012 MHz
Power 33 dB
continuously on
WALTZ-16 modulated
DATA PROCESSING
Line broadening 0.5 Hz
FT size 65536
Total time 38 min
166.267
163.489
155.945
138.161
137.850
133.607
129.372
128.772
127.710
127.611
127.239
103.239
87.695
77.479
77.365
77.160
76.841
66.800
58.564
56.348
48.720
39.969
ppm

KJH_DOS_No10_P86_CDCl3_Proton_400M

Sample #1, Operator: sbpark

Relax. delay 1.000 sec
Pulse 45.0 degrees
Acq. time 2.556 sec
Width 6410.3 Hz
8 repetitions
OBSERVE H1, 399.7551943 MHz
DATA PROCESSING
FT size 32768
Total time 0 min 28 sec

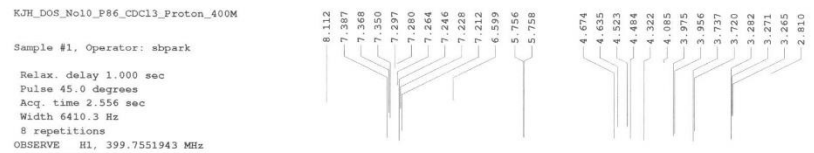

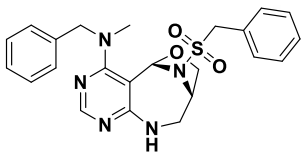

SB1609

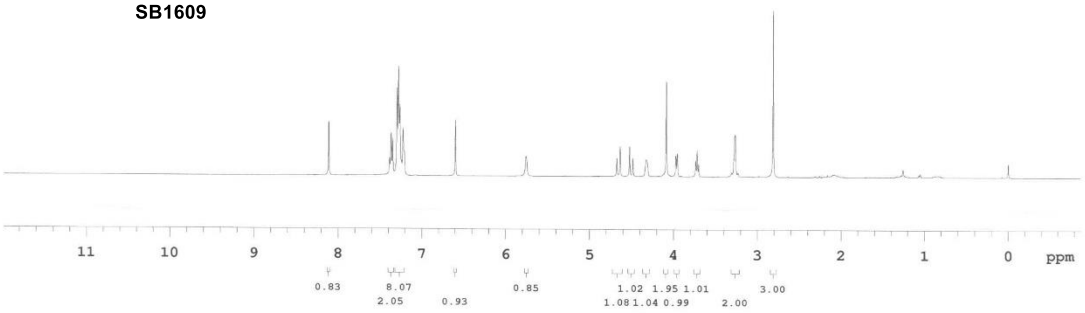

KJH_DOS_No10_P86_CDCl3_Carbon_400M

Sample #1, Operator: sbpark

Relax. delay 1.000 sec
Pulse 45.0 degrees
Acq. time 1.311 sec
Width 25000.0 Hz
98 repetitions
OBSERVE C13, 100.5185139 MHz
DECOUPLE H1, 399.7572012 MHz
Power 33 dB
continuously on
WALTZ-16 modulated
DATA PROCESSING
Line broadening 0.5 Hz
FT size 65536
Total time 38 min

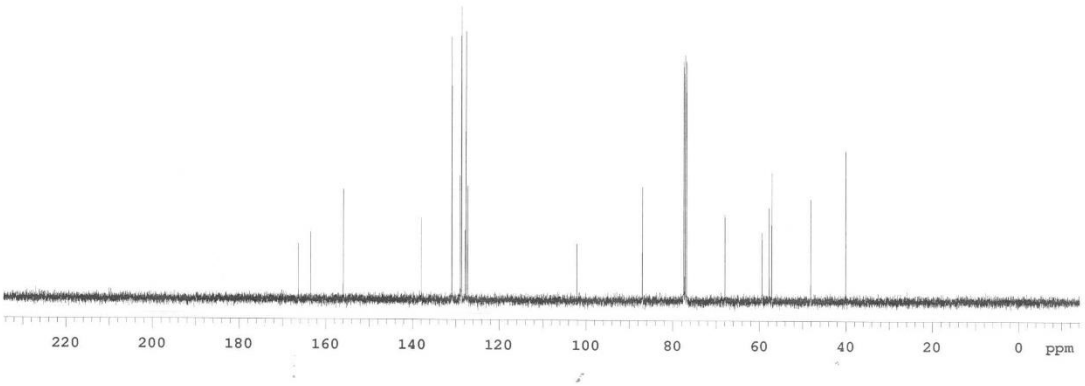

SBP_Pyridine at 350K / 1H

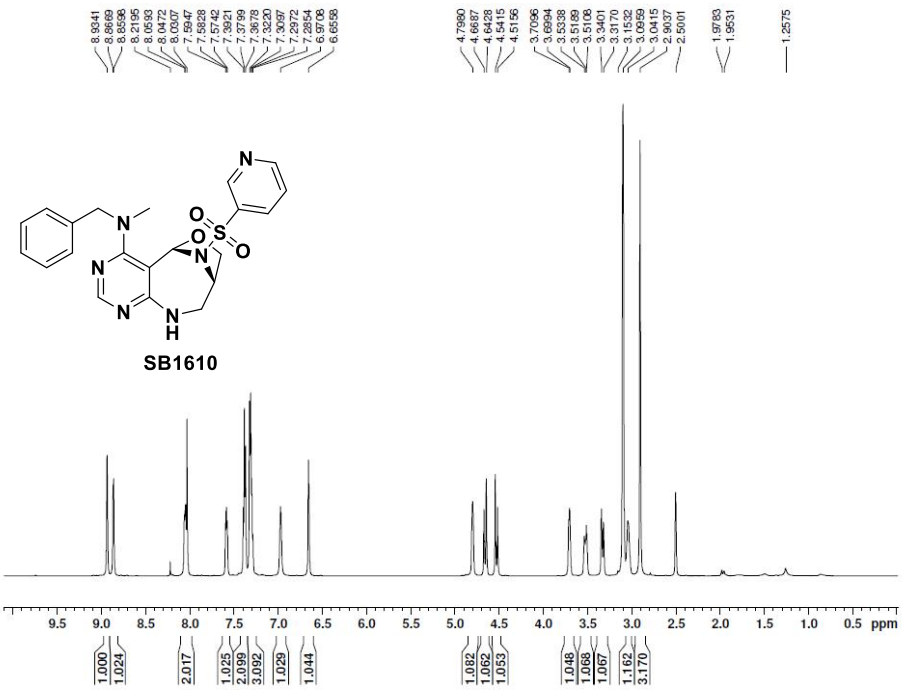

SB1610

서 울 대 학 교
SEOUL NATIONAL UNIVERSITY
기초과학공동기기원
핵자기공명연구실

```
Current Data Parameters
NAME      sep13-chem-psb
EXPNO                  1
PROCNO                 1

F2 - Acquisition Parameters
Date_           20160913
Time              13.02 h
INSTRUM             spect
PROBHD   Z8323_0178 (PA
PULPROG             zg30
TD                 65536
SOLVENT             DMSO
NS                     8
DS                     0
SWH           12019.230 Hz
FIDRES            0.366798 Hz
AQ              2.7262976 sec
RG                    57
DW                41.600 usec
DE                 6.50 usec
TE                350.0 K
D1            1.00000000 sec
TD0                    1
SFO1         600.1336008 MHz
NUC1                  1H
P1                 10.00 usec
PLW1         14.79100037 W

F2 - Processing parameters
SI                 65536
SF           600.1300041 MHz
WDW                   EM
SSB       0
LB                 0.50 Hz
GB        0
PC                 1.00
```

SBP_Pyridine at 350K /13C

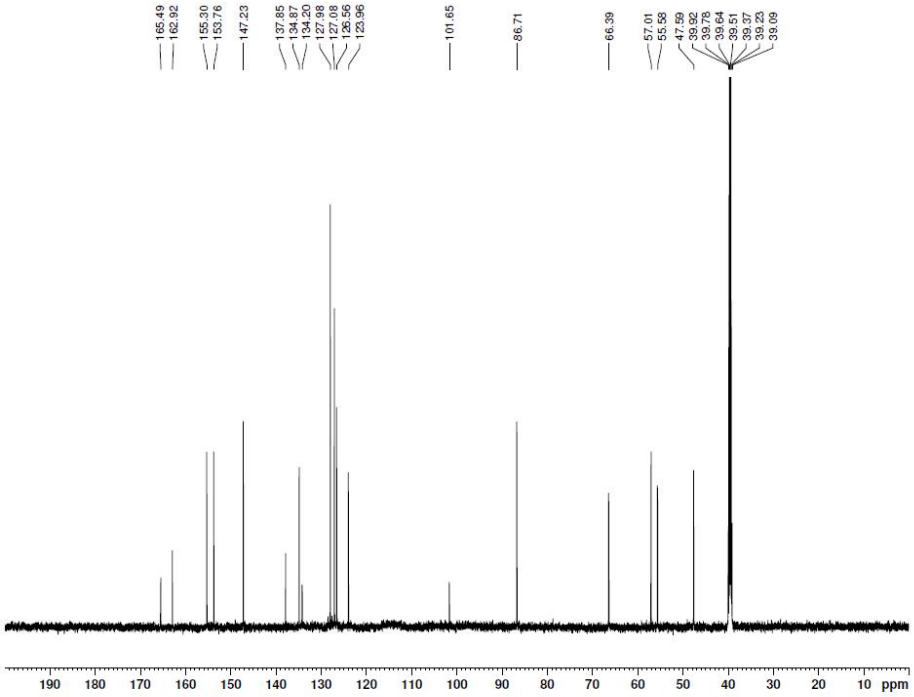

서 울 대 학 교
SEOUL NATIONAL UNIVERSITY
기초과학공동기기원
핵자기공명연구실

```
Current Data Parameters
NAME      sep13-chem-psb
EXPNO                  2
PROCNO                 1

F2 - Acquisition Parameters
Date_           20160913
Time              13.46 h
INSTRUM             spect
PROBHD   Z8323_0178 (PA
PULPROG          zgpg30
TD                 65536
SOLVENT             DMSO
NS                  1433
DS                     4
SWH           42613.637 Hz
FIDRES            1.300465 Hz
AQ              0.7689557 sec
RG                  2050
DW                11.733 usec
DE                 6.50 usec
TE                350.0 K
D1            1.00000000 sec
D11           0.03000000 sec
TD0                    1
SFO1         150.9194083 MHz
NUC1                  13C
P1                 12.00 usec
PLW1        257.04000854 W
SFO2         600.1342009 MHz
NUC2                  1H
CPDPRG[2          waltz16
PCPD2              70.00 usec
PLW2         13.48999977 W
PLW12         0.27531001 W
PLW13         0.13490000 W

F2 - Processing parameters
SI                 32768
SF           150.9029403 MHz
WDW                   EM
SSB       0
LB                 1.00 Hz
GB        0
PC                 1.00
```

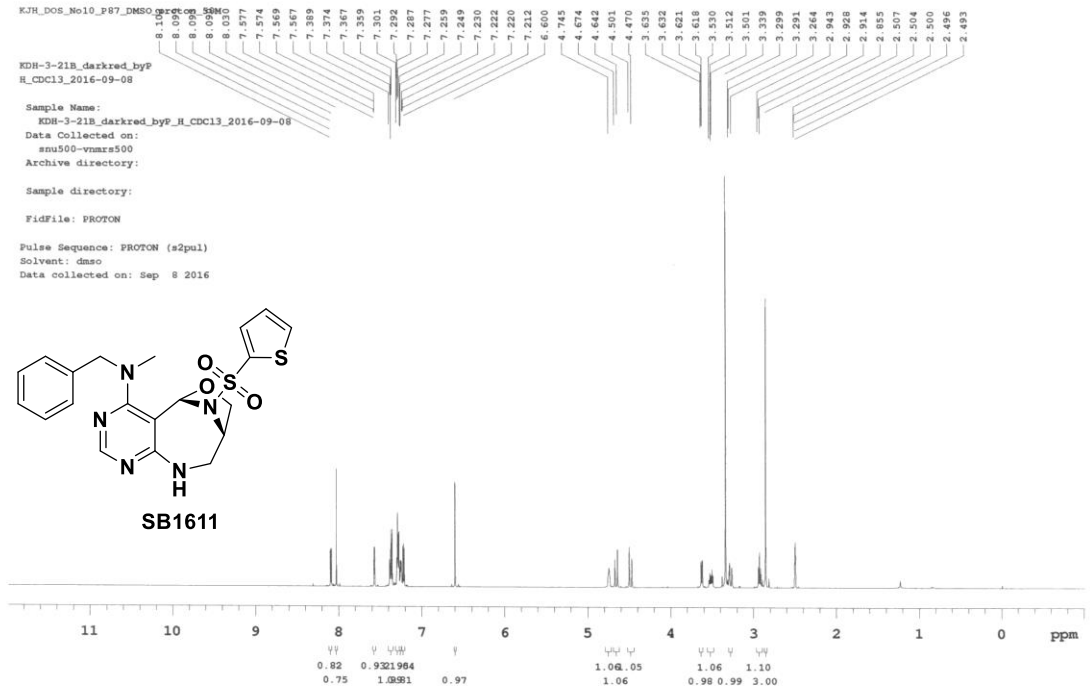
KDH-3-21B_darkred_byP
H_CDC13_2016-09-08
Sample Name:
KDH-3-21B_darkred_byP_H_CDC13_2016-09-08
Data Collected on:
snu500-vnmrs500
Archive directory:
Sample directory:
FidFile: PROTON
Pulse Sequence: PROTON (s2pul)
Solvent: dmso
Data collected on: Sep 8 2016
SB1611
ppm

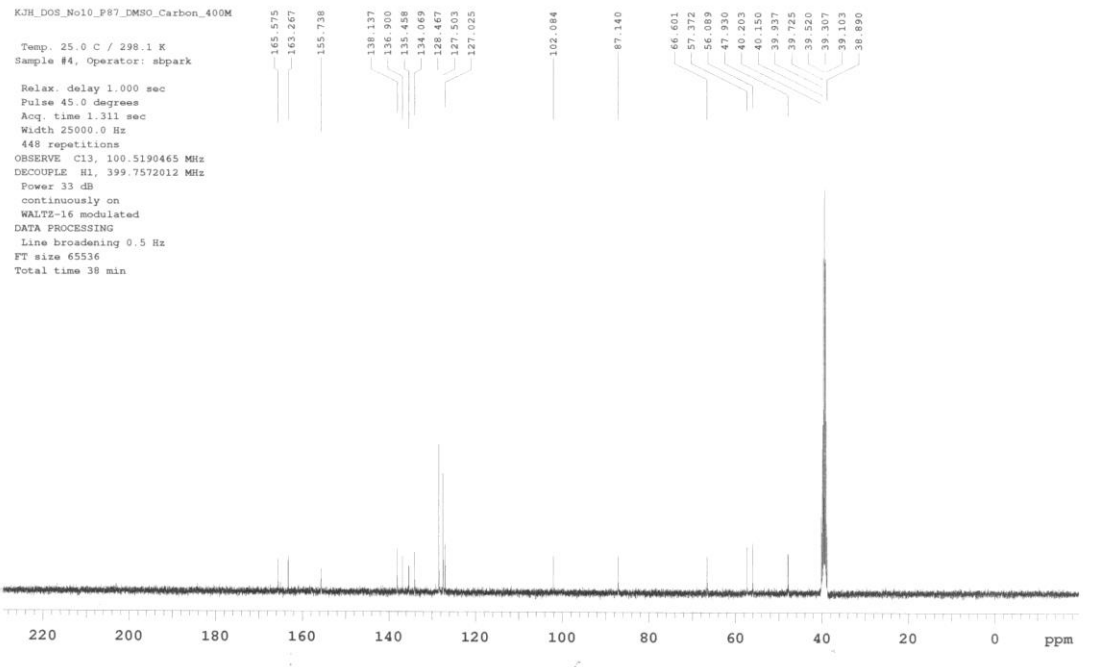
KJH_DOS_No10_P87_DMSO_Carbon_400M
Temp. 25.0 C / 298.1 K
Sample #4, Operator: sbpark
Relax. delay 1.000 sec
Pulse 45.0 degrees
Acq. time 1.311 sec
Width 25000.0 Hz
448 repetitions
OBSERVE C13, 100.5190465 MHz
DECOUPLE H1, 399.7572012 MHz
Power 33 dB
continuously on
WALTZ-16 modulated
DATA PROCESSING
Line broadening 0.5 Hz
FT size 65536
Total time 38 min
ppm

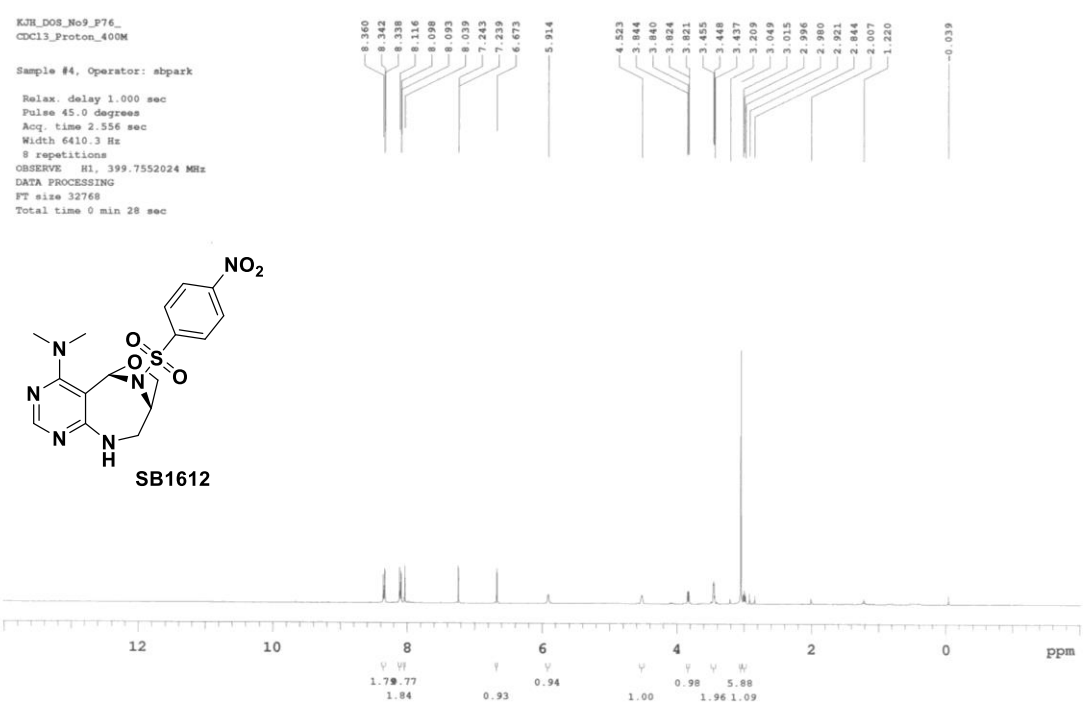
KJH_DOS_No9_P76_
CDCl3_Proton_400M
Sample #4, Operator: sbpark
Relax. delay 1.000 sec
Pulse 45.0 degrees
Acq. time 2.556 sec
Width 6410.3 Hz
8 repetitions
OBSERVE H1, 399.7552024 MHz
DATA PROCESSING
FT size 32768
Total time 0 min 28 sec
8.360
8.342
8.338
8.116
8.098
8.093
8.039
7.243
7.239
6.673
5.914
4.523
3.844
3.840
3.824
3.821
3.455
3.448
3.437
3.209
3.049
3.015
2.996
2.980
2.921
2.844
2.007
1.220
-0.039
NO2
O
S
N
H
SB1612
12
10
8
6
4
2
0
ppm
1.79
9.77
1.84
0.93
0.94
1.00
0.98
1.96
5.88
1.09

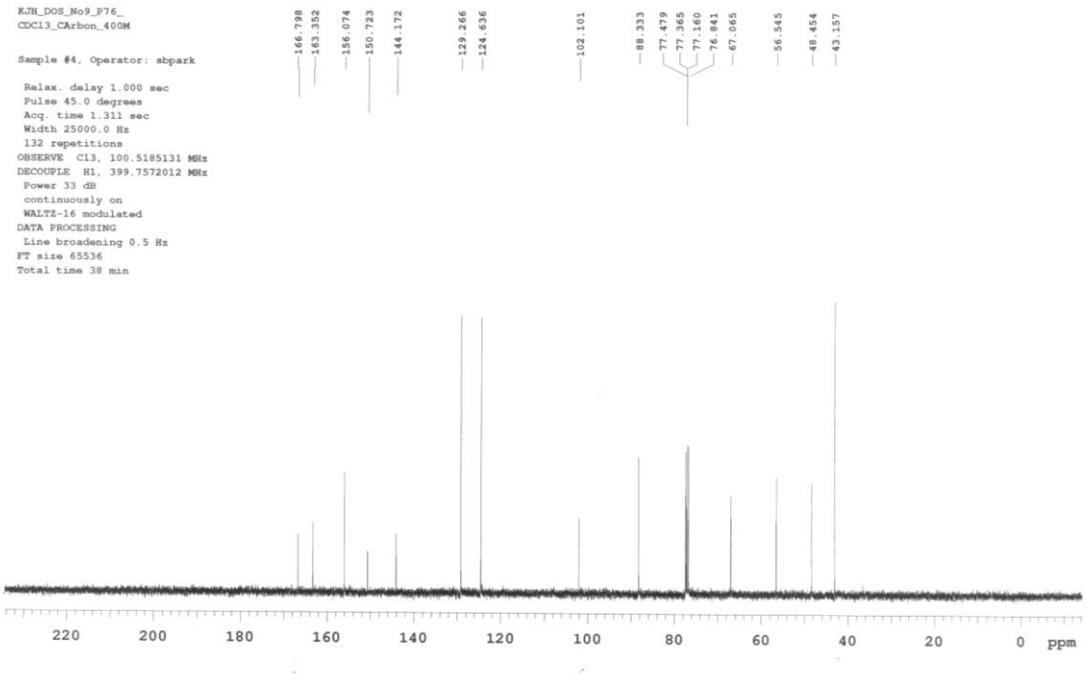
KJH_DOS_No9_P76_
CDCl3_CArbon_400M
Sample #4, Operator: sbpark
Relax. delay 1.000 sec
Pulse 45.0 degrees
Acq. time 1.311 sec
Width 25000.0 Hz
132 repetitions
OBSERVE C13, 100.5185131 MHz
DECOUPLE H1, 399.7572012 MHz
Power 33 dB
continuously on
WALTZ-16 modulated
DATA PROCESSING
Line broadening 0.5 Hz
FT size 65536
Total time 38 min
166.798
163.352
156.074
150.723
144.172
129.266
124.636
102.101
88.333
77.479
77.365
77.160
76.841
67.065
56.545
48.454
43.157
220
200
180
160
140
120
100
80
60
40
20
0
ppm

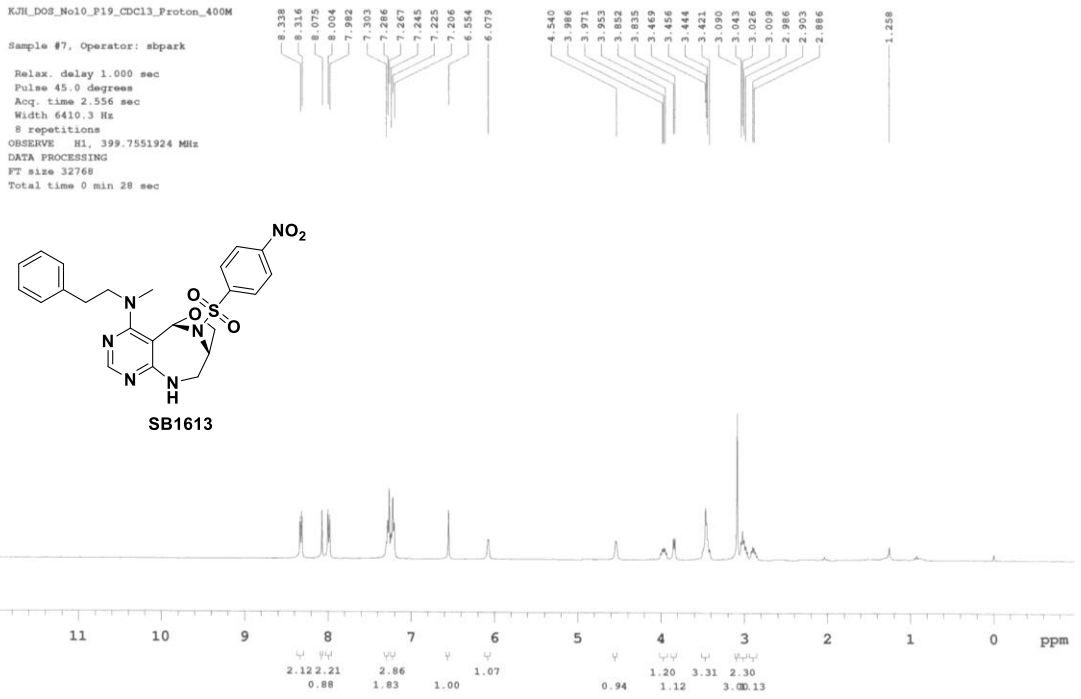
KJH_DOS_No10_P19_CDCl3_Proton_400M
Sample #7, Operator: sbpark
Relax. delay 1.000 sec
Pulse 45.0 degrees
Acq. time 2.556 sec
Width 6410.3 Hz
8 repetitions
OBSERVE H1, 399.7551924 MHz
DATA PROCESSING
FT size 32768
Total time 0 min 28 sec
8.338
8.316
8.075
8.004
7.982
7.303
7.286
7.267
7.245
7.225
7.206
6.554
6.079
4.540
3.986
3.971
3.953
3.852
3.835
3.469
3.456
3.444
3.421
3.090
3.043
3.026
3.009
2.986
2.903
2.886
1.258
NO2
N
O
S
O
O
N
N
N
N
H
SB1613
11
10
9
8
7
6
5
4
3
2
1
0
ppm
2.12
2.21
0.88
2.86
1.83
1.00
1.07
0.94
1.20
1.12
3.31
2.30
3.00
0.13

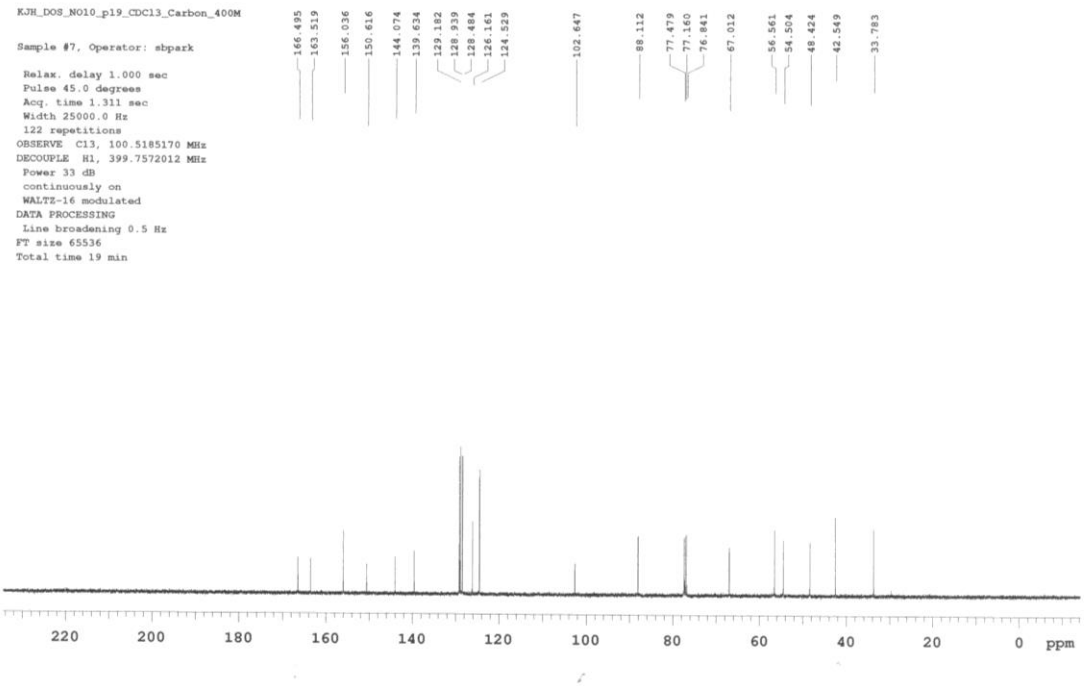
KJH_DOS_NO10_p19_CDCl3_Carbon_400M
Sample #7, Operator: sbpark
Relax. delay 1.000 sec
Pulse 45.0 degrees
Acq. time 1.311 sec
Width 25000.0 Hz
122 repetitions
OBSERVE C13, 100.5185170 MHz
DECOUPLE H1, 399.7572012 MHz
Power 33 dB
continuously on
WALTZ-16 modulated
DATA PROCESSING
Line broadening 0.5 Hz
FT size 65536
Total time 19 min
166.495
163.519
156.036
150.616
144.074
139.634
129.182
128.939
128.484
126.161
124.529
102.647
88.112
77.479
77.160
76.841
67.012
56.561
54.504
48.424
42.549
33.783
220
200
180
160
140
120
100
80
60
40
20
0
ppm

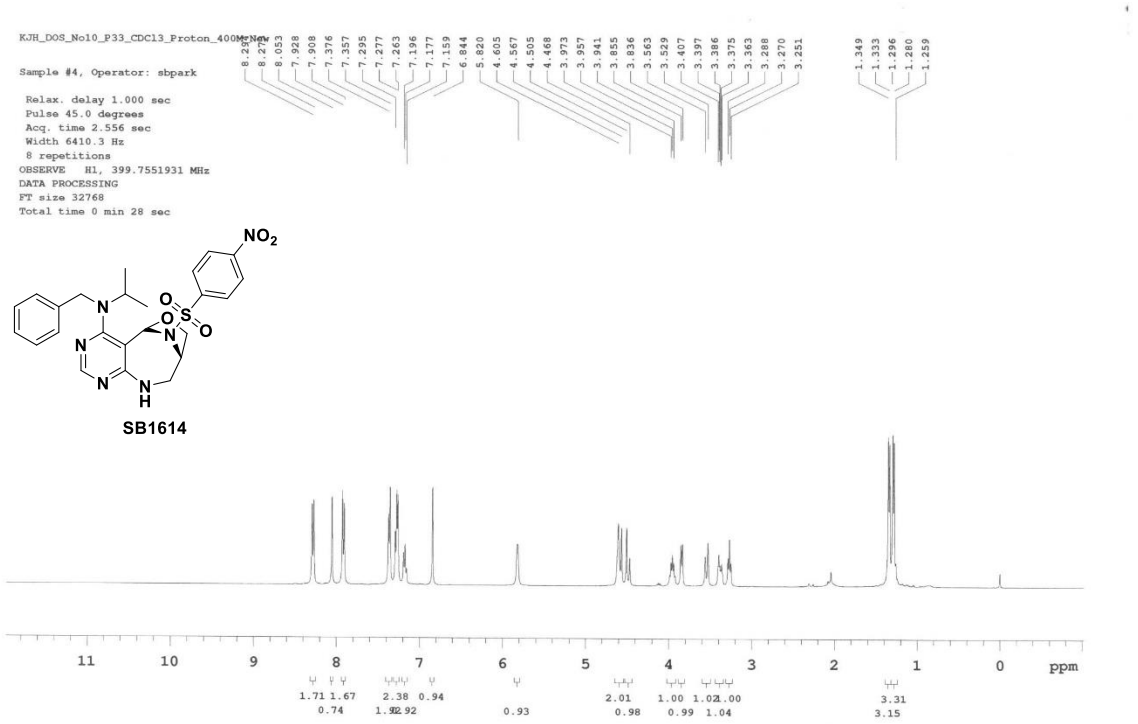
KJH_DOS_No10_P33_CDCl3_Proton_400MzNew
Sample #4, Operator: sbpark
Relax. delay 1.000 sec
Pulse 45.0 degrees
Acq. time 2.556 sec
Width 6410.3 Hz
8 repetitions
OBSERVE H1, 399.7551931 MHz
DATA PROCESSING
FT size 32768
Total time 0 min 28 sec
NO2
SB1614
ppm

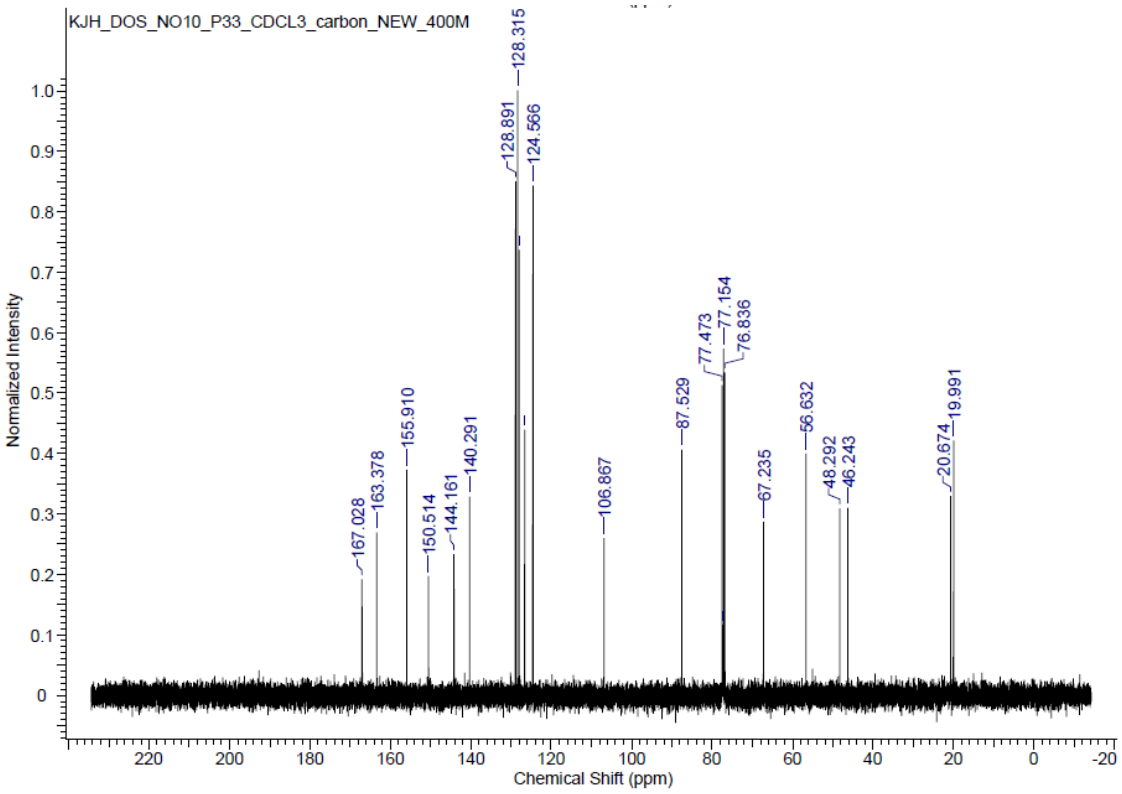
KJH_DOS_NO10_P33_CDCL3_carbon_NEW_400M
Normalized Intensity
Chemical Shift (ppm)
167.028
163.378
155.910
150.514
144.161
140.291
128.891
128.315
124.566
106.867
87.529
77.473
77.154
76.836
67.235
56.632
48.292
46.243
20.674
19.991

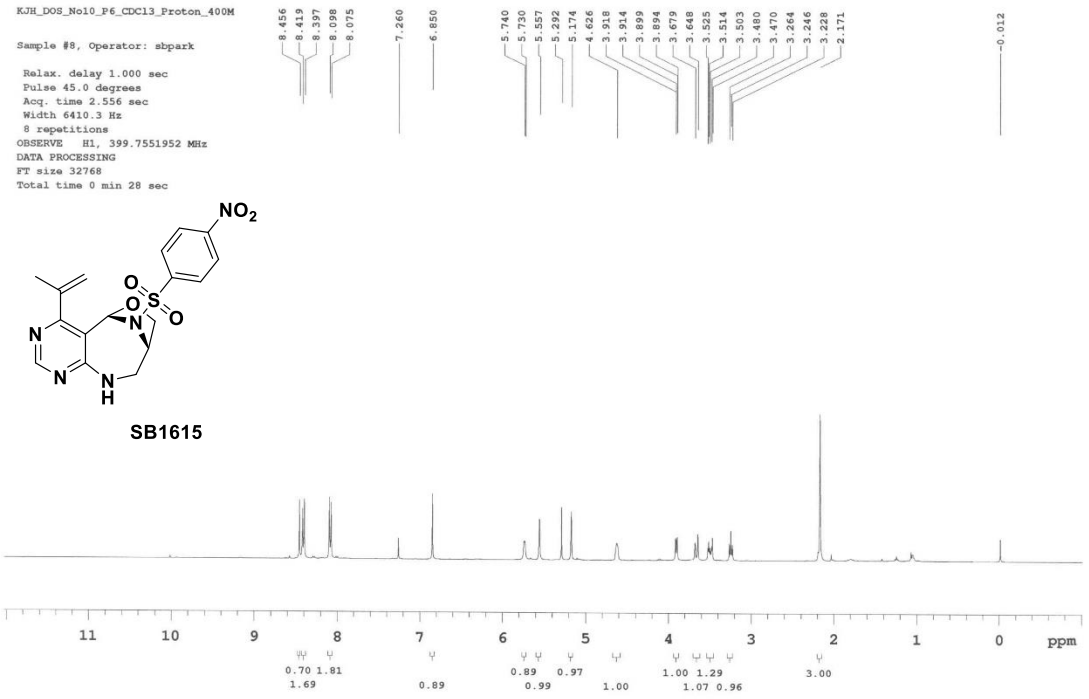
KJH_DOS_No10_P6_CDCl3_Proton_400M
Sample #8, Operator: sbpark
Relax. delay 1.000 sec
Pulse 45.0 degrees
Acq. time 2.556 sec
Width 6410.3 Hz
8 repetitions
OBSERVE H1, 399.7551952 MHz
DATA PROCESSING
FT size 32768
Total time 0 min 28 sec
8.456
8.419
8.397
8.098
8.075
7.260
6.850
5.740
5.730
5.557
5.292
5.174
4.626
3.918
3.914
3.899
3.894
3.679
3.648
3.525
3.514
3.503
3.480
3.470
3.264
3.246
3.228
2.171
0.012
NO2
O
S
O
O
N
N
N
H
SB1615
11
10
9
8
7
6
5
4
3
2
1
0
ppm
0.70 1.81
1.69
0.89
0.89 0.97
0.99
1.00
1.00 1.29
1.07 0.96
3.00

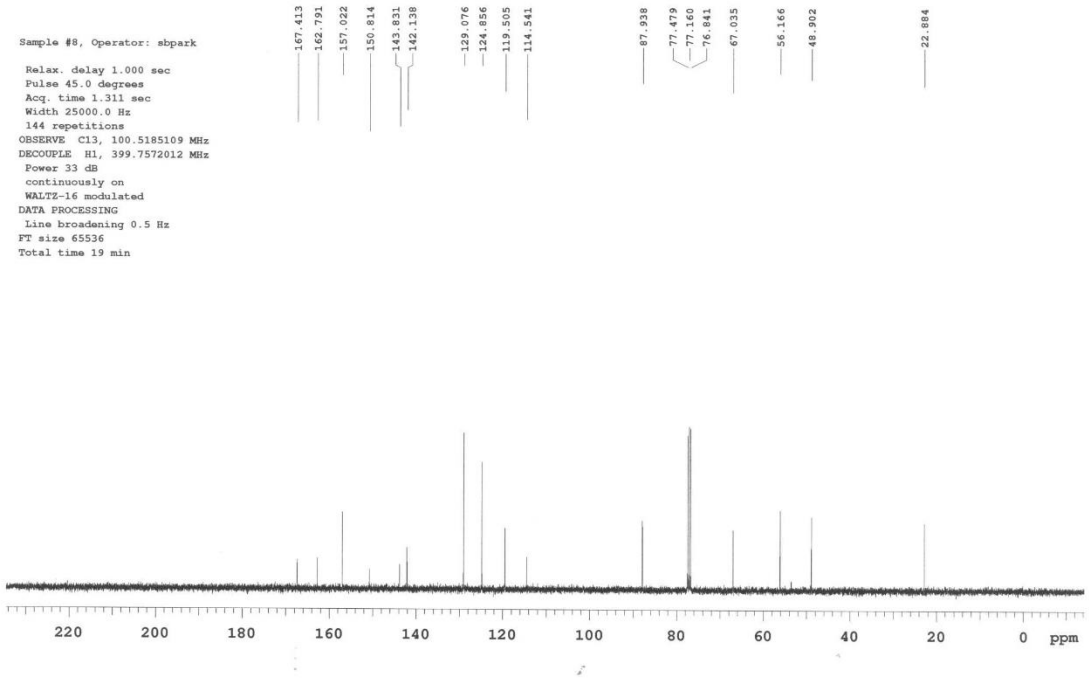
Sample #8, Operator: sbpark
Relax. delay 1.000 sec
Pulse 45.0 degrees
Acq. time 1.311 sec
Width 25000.0 Hz
144 repetitions
OBSERVE C13, 100.5185109 MHz
DECOUPLE H1, 399.7572012 MHz
Power 33 dB
continuously on
WALTZ-16 modulated
DATA PROCESSING
Line broadening 0.5 Hz
FT size 65536
Total time 19 min
167.413
162.791
157.022
150.814
143.831
142.138
129.076
124.856
119.505
114.541
87.938
77.479
77.160
76.841
67.035
56.166
48.902
22.884
220
200
180
160
140
120
100
80
60
40
20
0
ppm

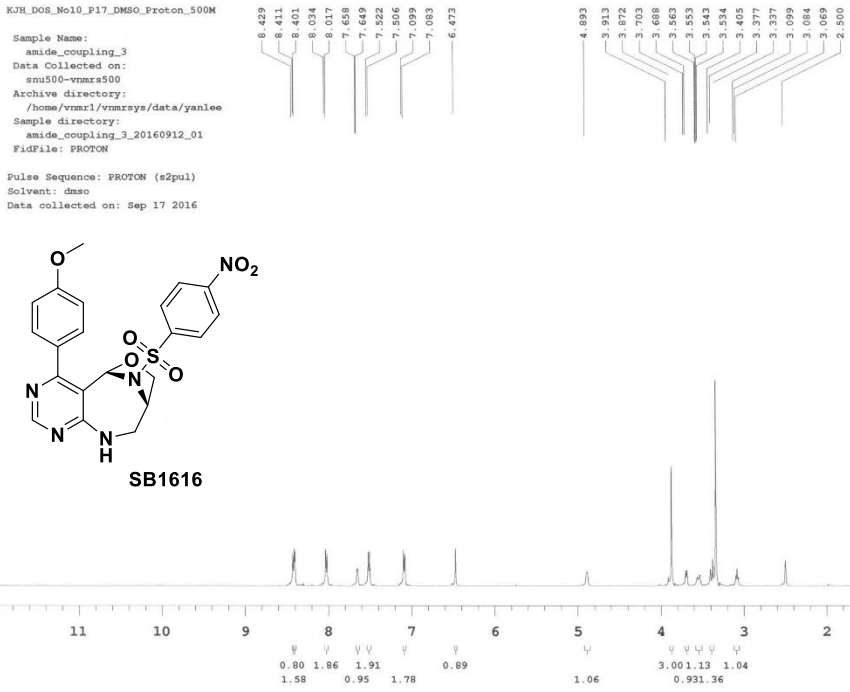
KJH_DOS_No10_P17_DMSO_Proton_500M
Sample Name:
amide_coupling_3
Data Collected on:
snu500-vnmrs500
Archive directory:
/home/vnmrl/vnmrsys/data/yanlee
Sample directory:
amide_coupling_3_20160912_01
FidFile: PROTON
Pulse Sequence: PROTON (s2pul)
Solvent: dmso
Data collected on: Sep 17 2016
8.429
8.411
8.401
8.034
8.017
7.658
7.649
7.522
7.506
7.099
7.083
6.473
4.893
3.913
3.872
3.703
3.688
3.563
3.553
3.543
3.534
3.405
3.377
3.337
3.099
3.084
3.069
2.500
O
NO2
O
S
O
O
N
N
N
N
H
SB1616
11
10
9
8
7
6
5
4
3
2
1
0
ppm
0.80
1.86
1.91
0.89
3.00
1.13
1.04
1.58
0.95
1.78
1.06
0.93
1.36

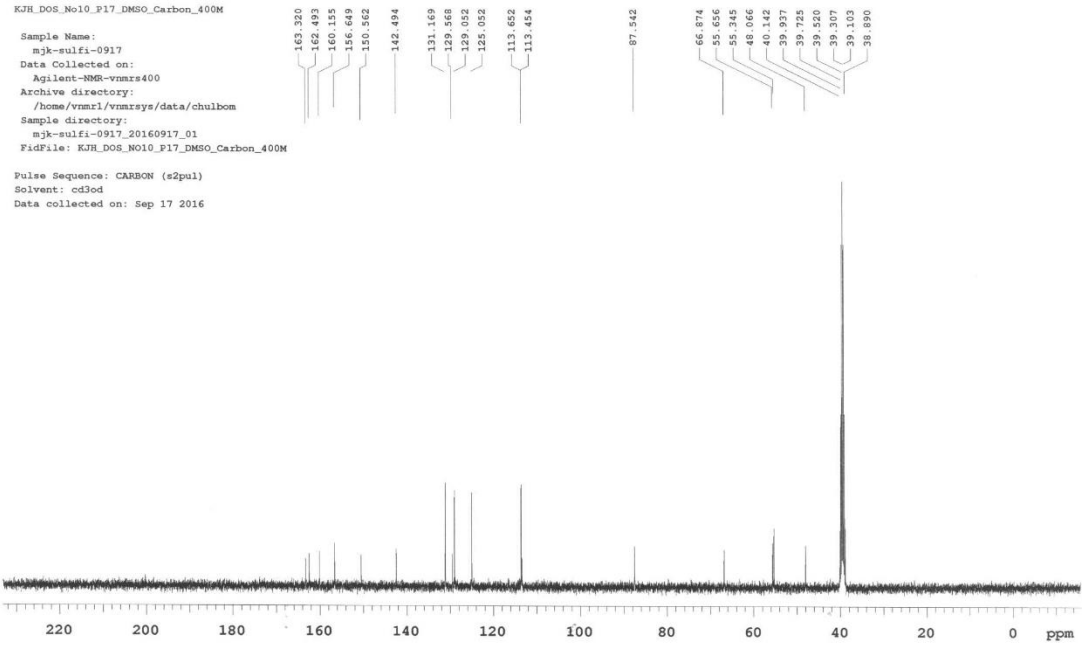
KJH_DOS_No10_P17_DMSO_Carbon_400M
Sample Name:
mjk-sulfi-0917
Data Collected on:
Agilent-NMR-vnmrs400
Archive directory:
/home/vnmrl/vnmrsys/data/chulbom
Sample directory:
mjk-sulfi-0917_20160917_01
FidFile: KJH_DOS_NO10_P17_DMSO_Carbon_400M
Pulse Sequence: CARBON (s2pul)
Solvent: cd3od
Data collected on: Sep 17 2016
163.320
162.493
160.155
156.649
150.562
142.494
131.169
129.568
129.052
125.052
113.652
113.454
87.542
66.874
55.656
55.345
48.066
40.142
39.937
39.725
39.520
39.307
39.103
38.890
220
200
180
160
140
120
100
80
60
40
20
0
ppm

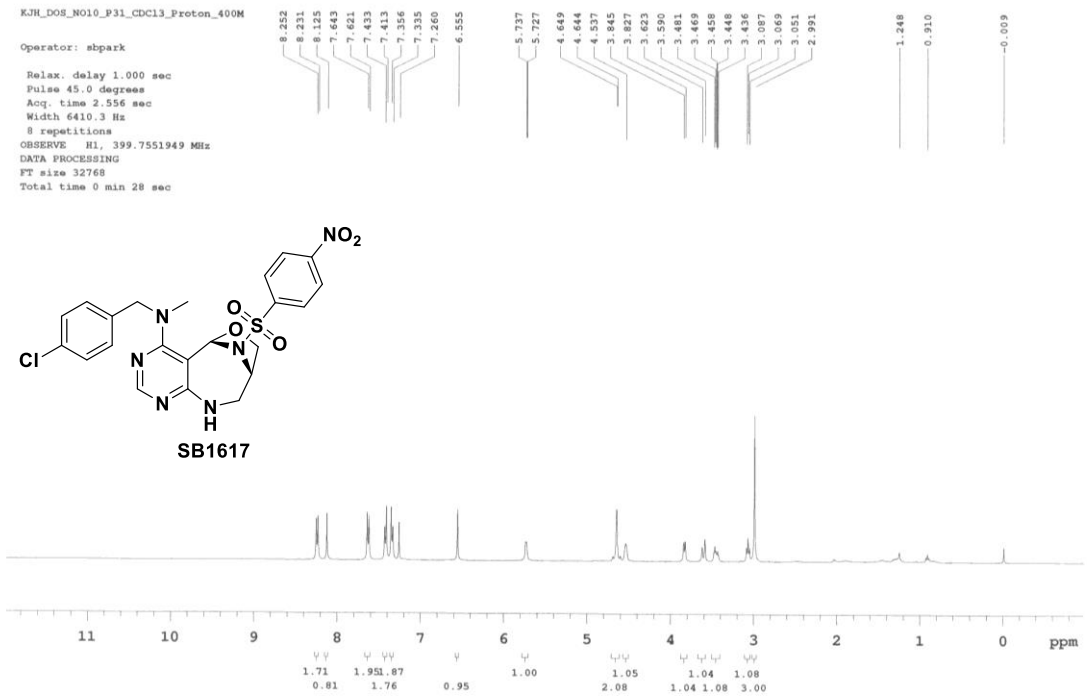
KJH_DOS_NO10_P31_CDC13_Proton_400M
Operator: sbpark
Relax. delay 1.000 sec
Pulse 45.0 degrees
Acq. time 2.556 sec
Width 6410.3 Hz
8 repetitions
OBSERVE H1, 399.7551949 MHz
DATA PROCESSING
FT size 32768
Total time 0 min 28 sec
8.252
8.231
8.125
7.643
7.621
7.433
7.413
7.356
7.335
7.260
6.555
5.737
5.727
4.649
4.644
4.537
3.845
3.827
3.623
3.590
3.481
3.469
3.458
3.448
3.436
3.087
3.069
3.051
2.991
1.248
0.910
0.009
NO2
Cl
N
O
S
O
O
N
N
N
N
H
SB1617
11
10
9
8
7
6
5
4
3
2
1
0
ppm
1.71
0.81
1.95
1.76
1.87
0.95
1.00
1.05
2.08
1.04
1.04
1.08
3.00

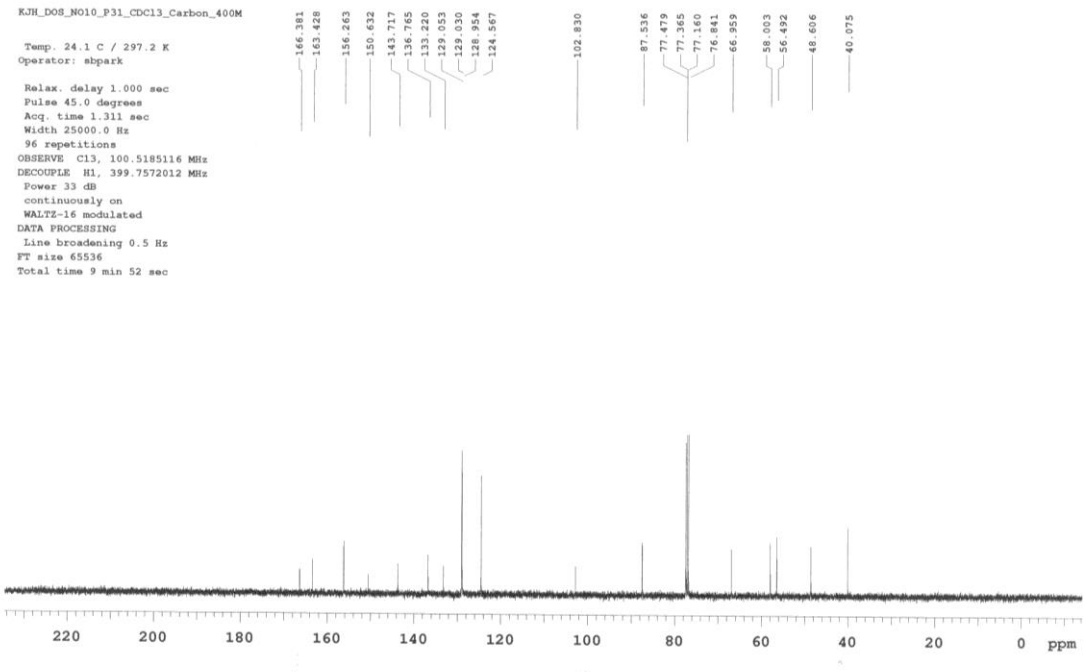
KJH_DOS_NO10_P31_CDC13_Carbon_400M
Temp. 24.1 C / 297.2 K
Operator: sbpark
Relax. delay 1.000 sec
Pulse 45.0 degrees
Acq. time 1.311 sec
Width 25000.0 Hz
96 repetitions
OBSERVE C13, 100.5185116 MHz
DECOUPLE H1, 399.7572012 MHz
Power 33 dB
continuously on
WALTZ-16 modulated
DATA PROCESSING
Line broadening 0.5 Hz
FT size 65536
Total time 9 min 52 sec
166.381
163.428
156.263
150.632
143.717
136.765
133.220
129.053
129.030
128.954
124.567
102.830
87.536
77.479
77.365
77.160
76.841
66.959
58.003
56.492
48.606
40.075
220
200
180
160
140
120
100
80
60
40
20
0
ppm

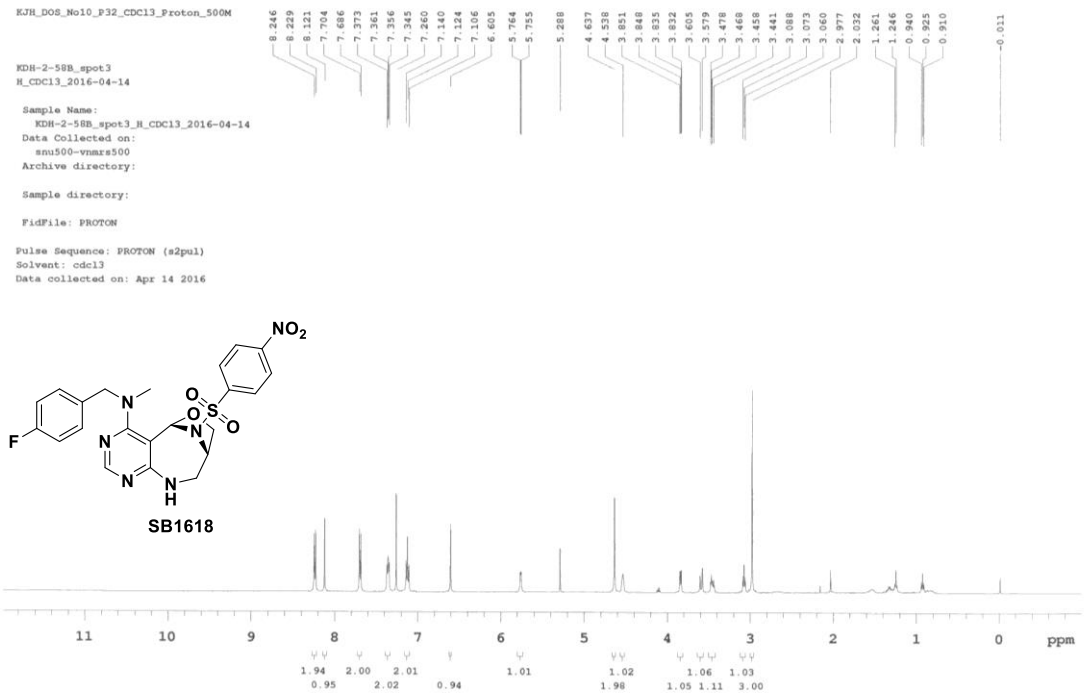
KJH_DOS_No10_P32_CDCl3_Proton_500M
KDH-2-58B_spot3
H_CDCl3_2016-04-14
Sample Name:
KDH-2-58B_spot3_H_CDCl3_2016-04-14
Data Collected on:
snu500-vnmrs500
Archive directory:
Sample directory:
FidFile: PROTON
Pulse Sequence: PROTON (s2pul)
Solvent: cdcl3
Data collected on: Apr 14 2016
8.246
8.229
8.121
7.704
7.686
7.373
7.361
7.356
7.345
7.260
7.140
7.124
7.106
6.605
5.764
5.755
5.288
4.637
4.538
3.851
3.848
3.835
3.832
3.605
3.579
3.478
3.468
3.458
3.441
3.088
3.073
3.060
2.977
2.032
1.261
1.246
0.940
0.925
0.910
-0.011
NO2
O
S
O
O
N
N
N
N
H
F
SB1618
11
10
9
8
7
6
5
4
3
2
1
0
ppm
1.94
2.00
2.01
1.01
1.02
1.06
1.03
0.95
2.02
0.94
1.98
1.05
1.11
3.00

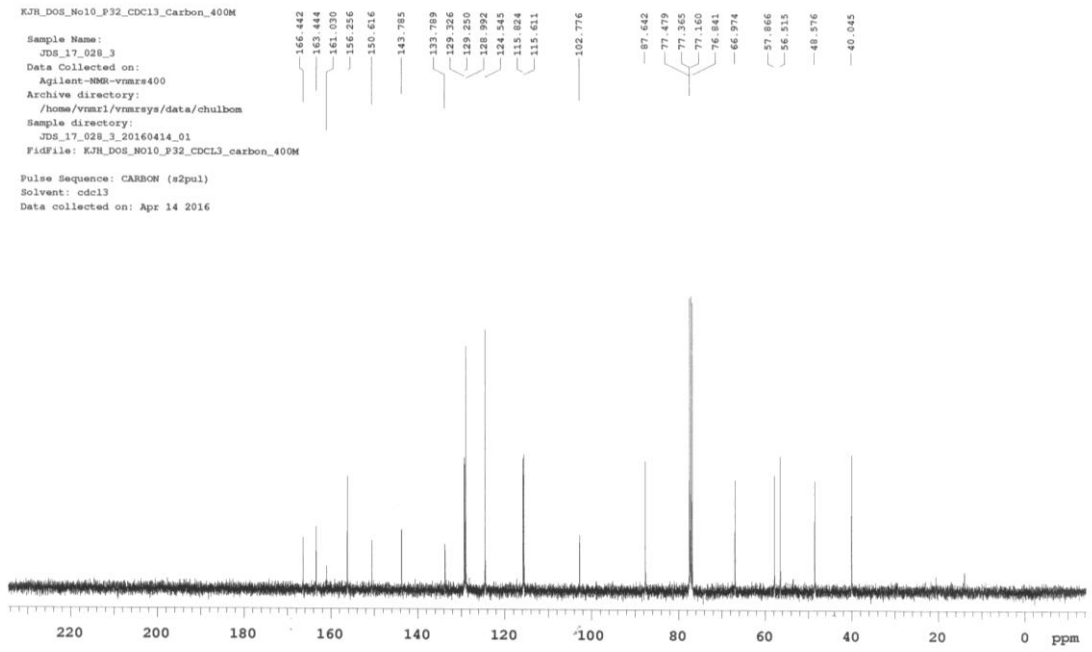
KJH_DOS_No10_P32_CDCl3_Carbon_400M
Sample Name:
JDS_17_028_3
Data Collected on:
Agilent-NMR-vnmrs400
Archive directory:
/home/vnmr1/vnmrsys/data/chulbom
Sample directory:
JDS_17_028_3_20160414_01
FidFile: KJH_DOS_NO10_P32_CDCL3_carbon_400M
Pulse Sequence: CARBON (s2pul)
Solvent: cdcl3
Data collected on: Apr 14 2016
166.442
163.444
161.030
156.256
150.616
143.785
133.789
129.326
129.250
128.992
124.545
115.824
115.611
102.776
87.642
77.479
77.365
77.160
76.841
66.974
57.866
56.515
48.576
40.045
220
200
180
160
140
120
100
80
60
40
20
0
ppm

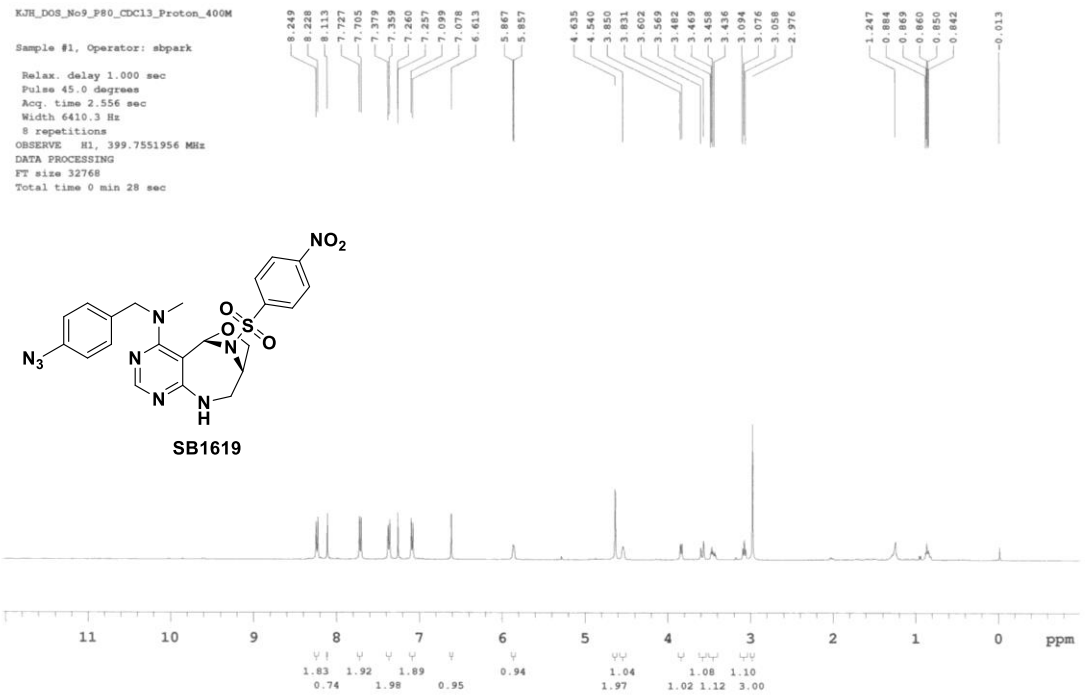
KJH_DOS_No9_P80_CDCl3_Proton_400M
Sample #1, Operator: sbpark
Relax. delay 1.000 sec
Pulse 45.0 degrees
Acq. time 2.556 sec
Width 6410.3 Hz
8 repetitions
OBSERVE H1, 399.7551956 MHz
DATA PROCESSING
FT size 32768
Total time 0 min 28 sec
8.249
8.228
8.113
7.727
7.705
7.379
7.359
7.260
7.257
7.099
7.078
6.613
5.867
5.857
4.635
4.540
3.850
3.831
3.602
3.569
3.482
3.469
3.458
3.436
3.094
3.076
3.058
2.976
1.247
0.884
0.869
0.860
0.850
0.842
-0.013
NO2
N3
SB1619
11
10
9
8
7
6
5
4
3
2
1
0
ppm
1.83
1.92
1.89
0.94
1.04
1.08
1.10
0.74
1.98
0.95
1.97
1.02
1.12
3.00

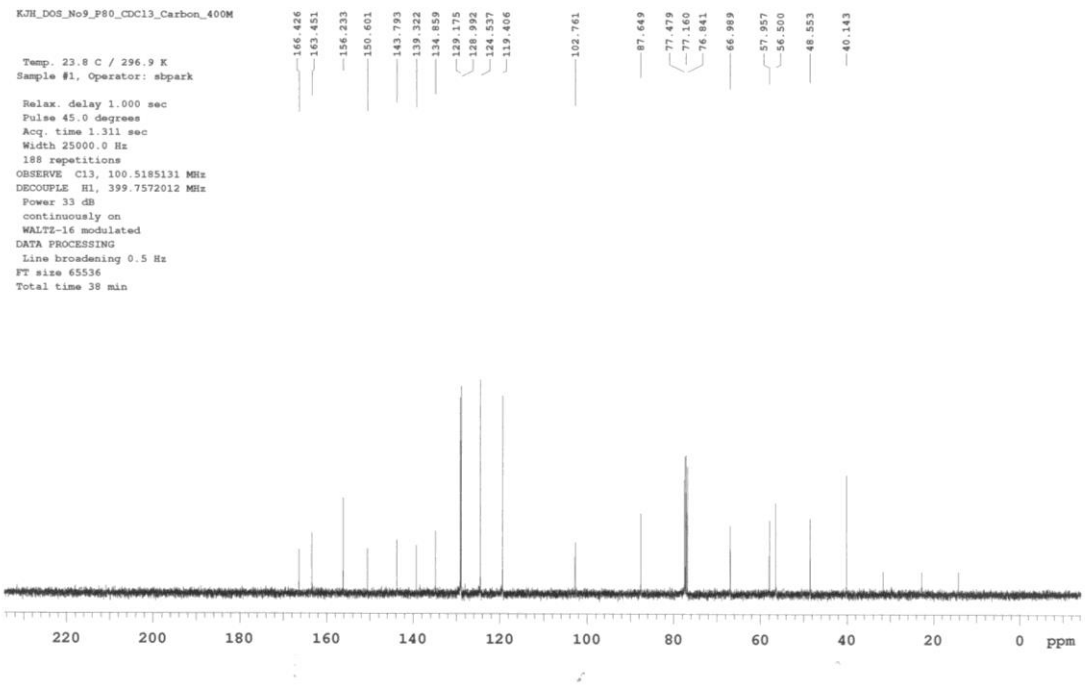
KJH_DOS_No9_P80_CDCl3_Carbon_400M
Temp. 23.8 C / 296.9 K
Sample #1, Operator: sbpark
Relax. delay 1.000 sec
Pulse 45.0 degrees
Acq. time 1.311 sec
Width 25000.0 Hz
188 repetitions
OBSERVE C13, 100.5185131 MHz
DECOUPLE H1, 399.7572012 MHz
Power 33 dB
continuously on
WALTZ-16 modulated
DATA PROCESSING
Line broadening 0.5 Hz
FT size 65536
Total time 38 min
166.426
163.451
156.233
150.601
143.793
139.322
134.859
129.175
128.992
124.537
119.406
102.761
87.649
77.479
77.160
76.841
66.989
57.957
56.500
48.553
40.143
220
200
180
160
140
120
100
80
60
40
20
0
ppm

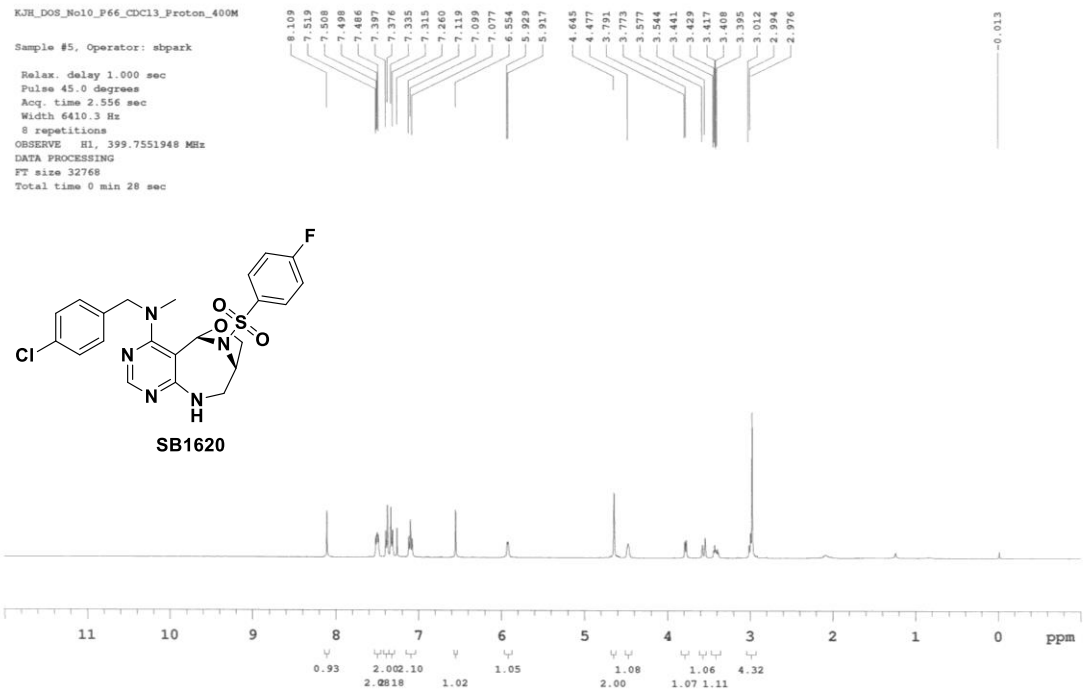
KJH_DOS_No10_P66_CDCl3_Proton_400M
Sample #5, Operator: sbpark
Relax. delay 1.000 sec
Pulse 45.0 degrees
Acq. time 2.556 sec
Width 6410.3 Hz
8 repetitions
OBSERVE H1, 399.7551948 MHz
DATA PROCESSING
FT size 32768
Total time 0 min 28 sec
SB1620
ppm

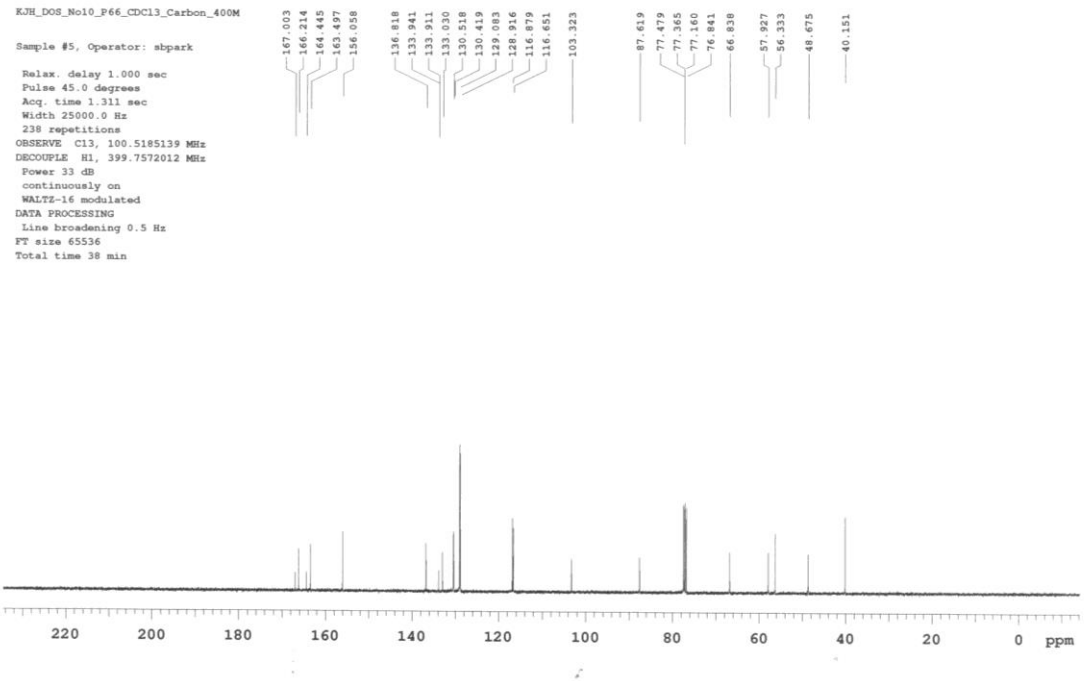
KJH_DOS_No10_P66_CDCl3_Carbon_400M
Sample #5, Operator: sbpark
Relax. delay 1.000 sec
Pulse 45.0 degrees
Acq. time 1.311 sec
Width 25000.0 Hz
238 repetitions
OBSERVE C13, 100.5185139 MHz
DECOUPLE H1, 399.7572012 MHz
Power 33 dB
continuously on
WALTZ-16 modulated
DATA PROCESSING
Line broadening 0.5 Hz
FT size 65536
Total time 38 min
ppm

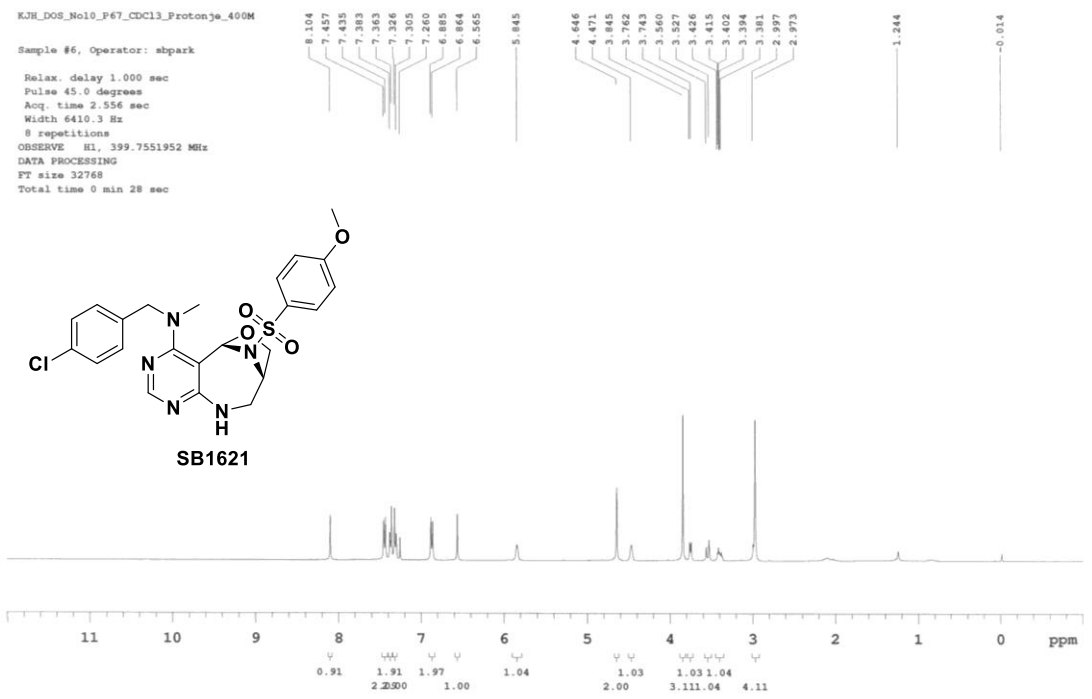
KJH_DOS_No10_P67_CDCl3_Protonje_400M
Sample #6, Operator: sbpark
Relax. delay 1.000 sec
Pulse 45.0 degrees
Acq. time 2.556 sec
Width 6410.3 Hz
8 repetitions
OBSERVE H1, 399.7551952 MHz
DATA PROCESSING
FT size 32768
Total time 0 min 28 sec
8.104
7.457
7.435
7.383
7.363
7.326
7.305
7.260
6.885
6.864
6.565
5.845
4.646
4.471
3.845
3.762
3.743
3.560
3.527
3.426
3.415
3.402
3.394
3.381
2.997
2.973
1.244
0.014
SB1621
11
10
9
8
7
6
5
4
3
2
1
0
ppm
0.91
1.91
1.97
1.04
1.03
1.03
1.04
1.00
2.00
3.11
4.11

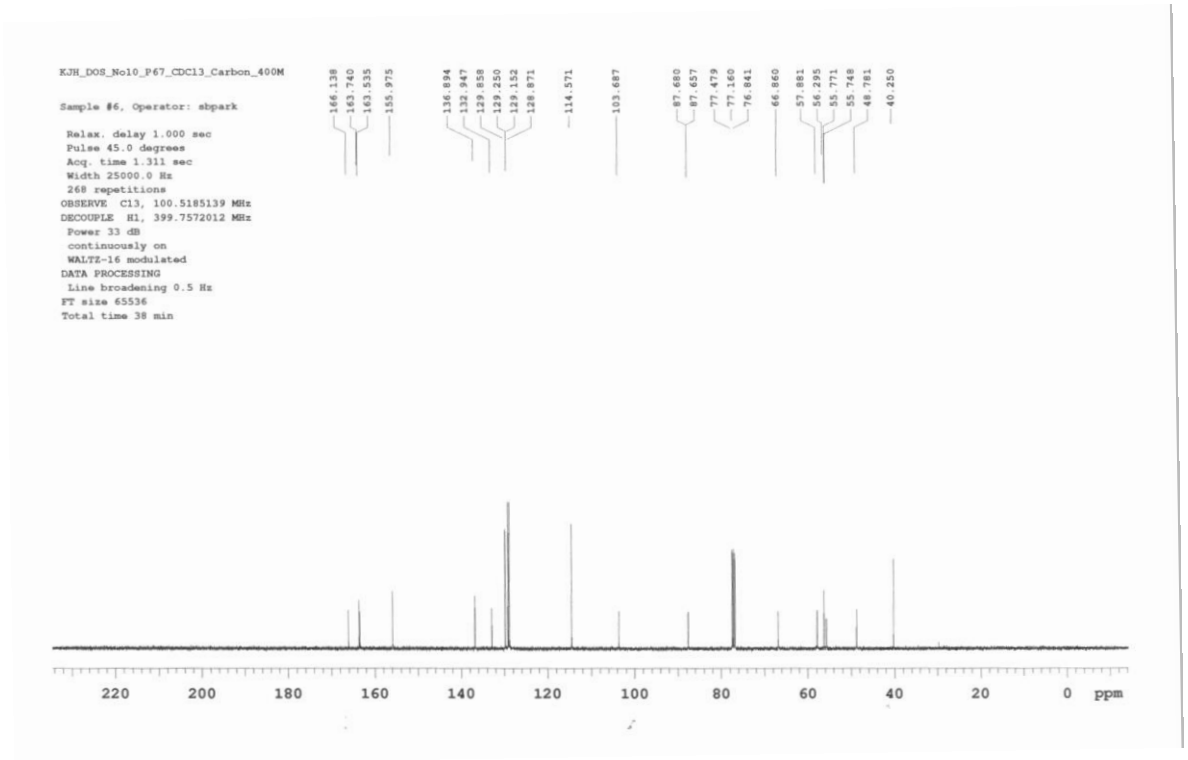
KJH_DOS_No10_P67_CDCl3_Carbon_400M
Sample #6, Operator: sbpark
Relax. delay 1.000 sec
Pulse 45.0 degrees
Acq. time 1.311 sec
Width 25000.0 Hz
268 repetitions
OBSERVE C13, 100.5185139 MHz
DECOUPLE H1, 399.7572012 MHz
Power 33 dB
continuously on
WALTZ-16 modulated
DATA PROCESSING
Line broadening 0.5 Hz
FT size 65536
Total time 38 min
166.138
163.740
163.535
155.975
136.894
132.947
129.858
129.250
129.152
128.871
114.571
103.687
87.680
87.657
77.479
77.160
76.841
66.860
57.881
56.295
55.771
55.748
48.781
40.250
220
200
180
160
140
120
100
80
60
40
20
0
ppm

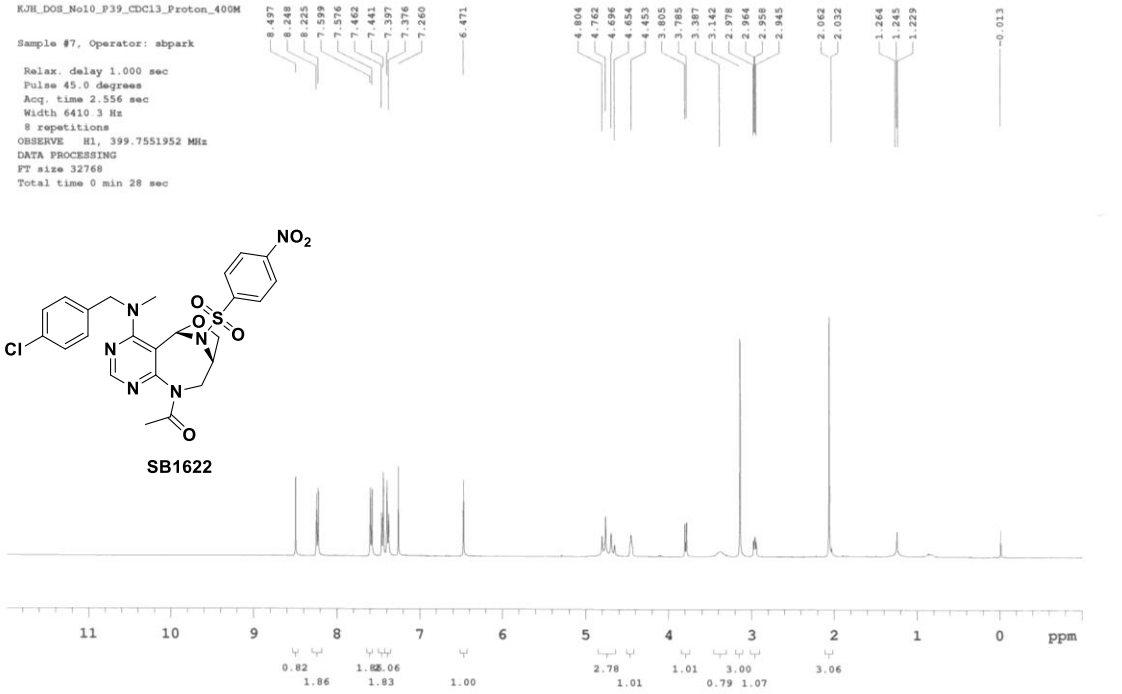
KJH_DOS_No10_P39_CDCl3_Proton_400M
Sample #7, Operator: sbpark
Relax. delay 1.000 sec
Pulse 45.0 degrees
Acq. time 2.556 sec
Width 6410.3 Hz
8 repetitions
OBSERVE H1, 399.7551952 MHz
DATA PROCESSING
FT size 32768
Total time 0 min 28 sec
8.497
8.248
8.225
7.599
7.576
7.462
7.441
7.397
7.376
7.260
6.471
4.804
4.762
4.696
4.654
4.453
3.805
3.785
3.387
3.142
2.978
2.964
2.958
2.945
2.062
2.032
1.264
1.245
1.229
0.013
NO2
Cl
O
S
N
SB1622
11
10
9
8
7
6
5
4
3
2
1
0
ppm
0.82
1.86
1.06
1.83
1.00
2.78
1.01
1.01
3.00
0.79
1.07
3.06

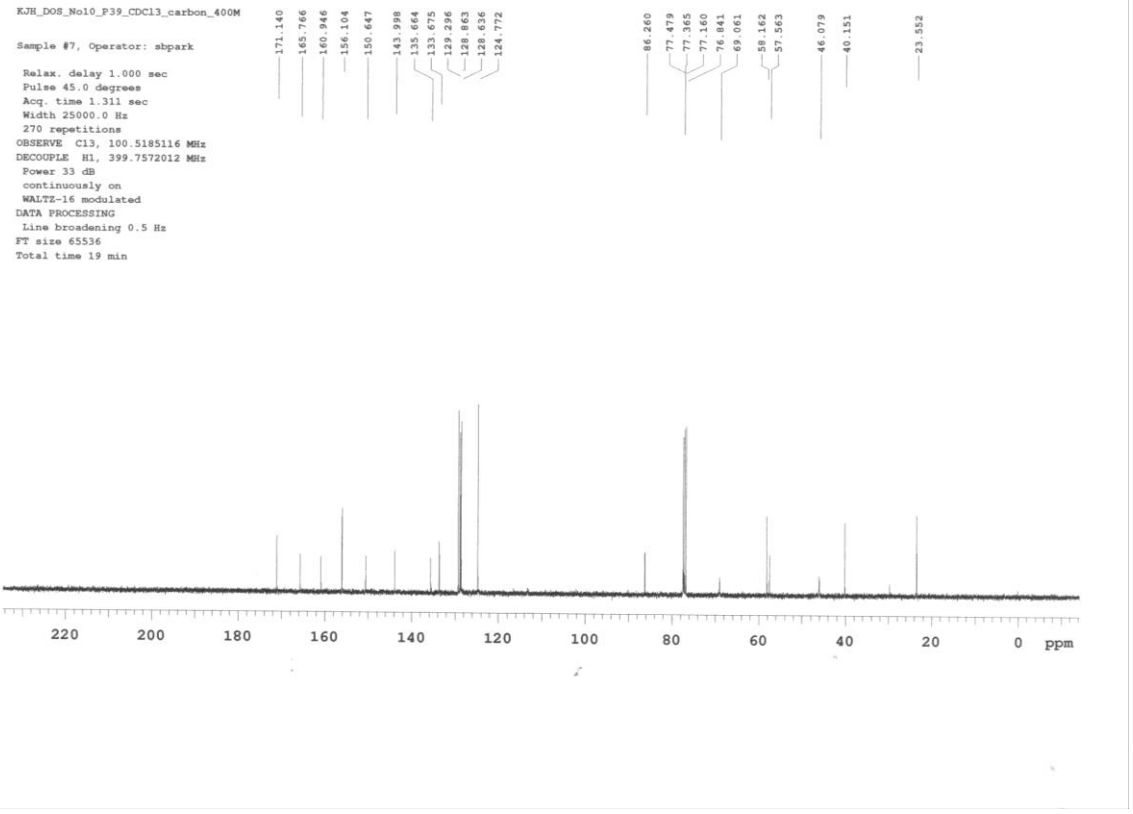
KJH_DOS_No10_P39_CDCl3_carbon_400M
Sample #7, Operator: sbpark
Relax. delay 1.000 sec
Pulse 45.0 degrees
Acq. time 1.311 sec
Width 25000.0 Hz
270 repetitions
OBSERVE C13, 100.5185116 MHz
DECOUPLE H1, 399.7572012 MHz
Power 33 dB
continuously on
WALTZ-16 modulated
DATA PROCESSING
Line broadening 0.5 Hz
FT size 65536
Total time 19 min
171.140
165.766
160.946
156.104
150.647
143.998
135.664
133.675
129.296
128.863
128.636
124.772
86.260
77.479
77.365
77.160
76.841
69.061
58.162
57.563
46.079
40.151
23.552
220
200
180
160
140
120
100
80
60
40
20
0
ppm

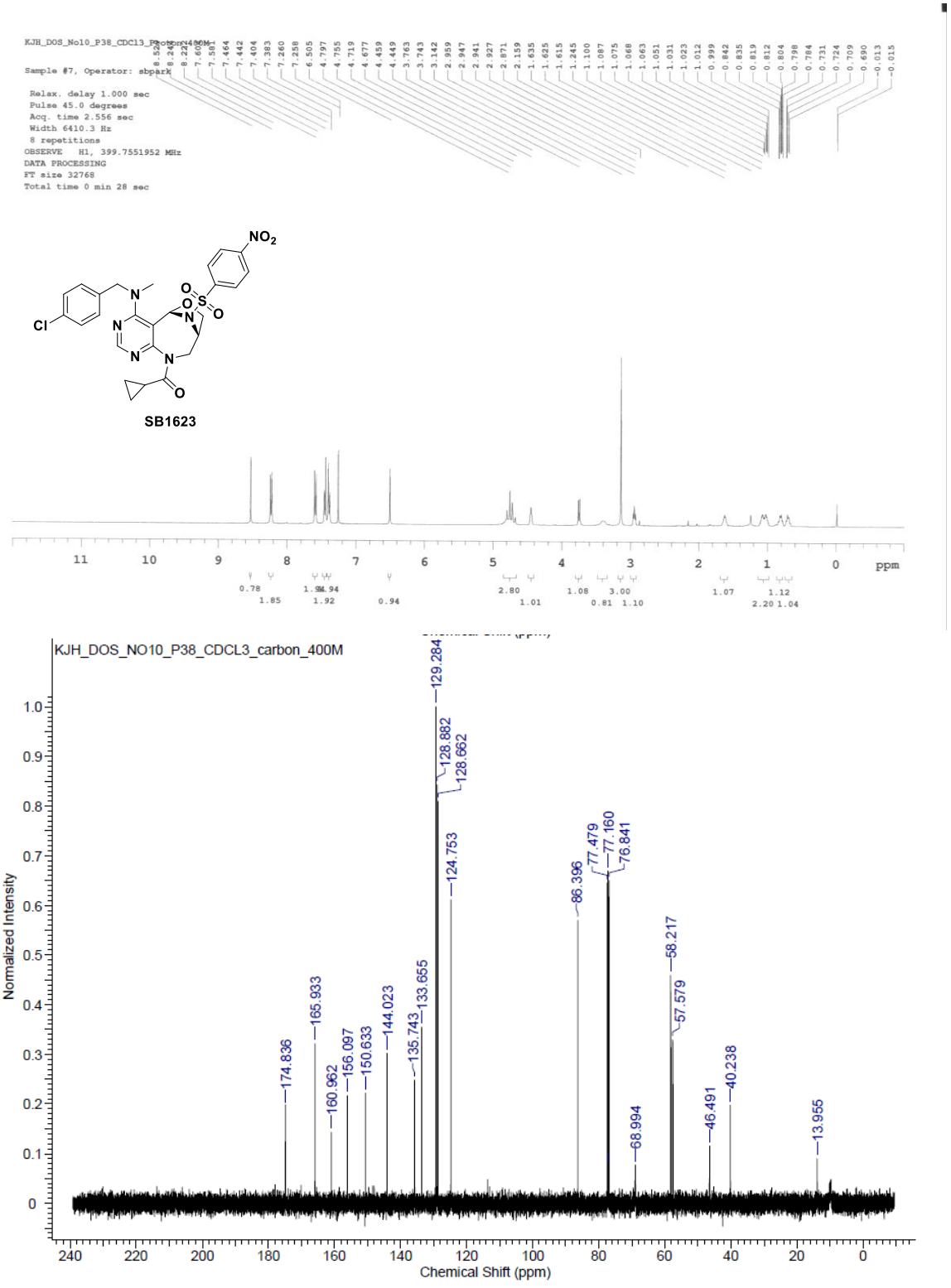
Sample #7, Operator: sbpark
Relax. delay 1.000 sec
Pulse 45.0 degrees
Acq. time 2.556 sec
Width 6410.3 Hz
8 repetitions
OBSERVE H1, 399.7551952 MHz
DATA PROCESSING
FT size 32768
Total time 0 min 28 sec
SB1623
ppm
KJH_DOS_NO10_P38_CDCL3_carbon_400M
Normalized Intensity
Chemical Shift (ppm)
129.284
128.882
128.662
124.753
86.396
77.479
77.160
76.841
58.217
57.579
46.491
40.238
13.955
68.994
174.836
165.933
160.962
156.097
150.633
144.023
135.743
133.655

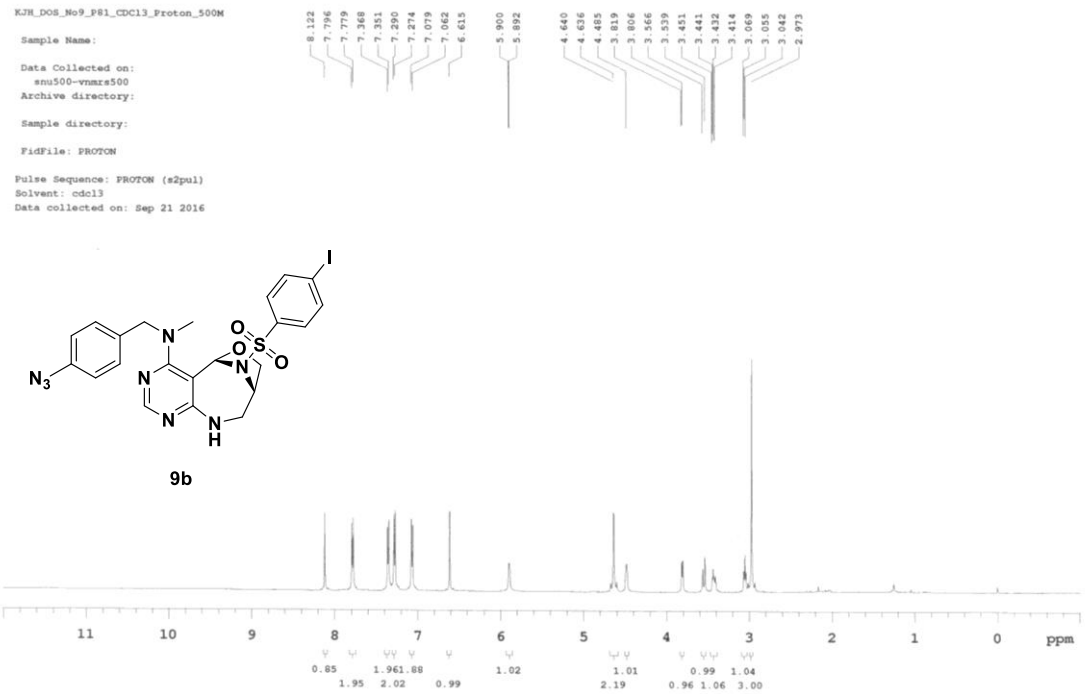
KJH_DOS_No9_P81_CDCl3_Proton_500M
Sample Name:
Data Collected on:
snu500-vnmrs500
Archive directory:
Sample directory:
FidFile: PROTON
Pulse Sequence: PROTON (s2pul)
Solvent: cdcl3
Data collected on: Sep 21 2016
8.122
7.796
7.779
7.368
7.351
7.290
7.274
7.079
7.062
6.615
5.900
5.892
4.640
4.636
4.485
3.819
3.806
3.566
3.539
3.451
3.441
3.432
3.414
3.069
3.055
3.042
2.973
I
N
O
S
O
O
N
O
N3
N
N
N
H
9b
11
10
9
8
7
6
5
4
3
2
1
0
ppm
0.85
1.95
1.96
2.02
1.88
0.99
1.02
1.01
2.19
0.99
0.96
1.06
1.04
3.00

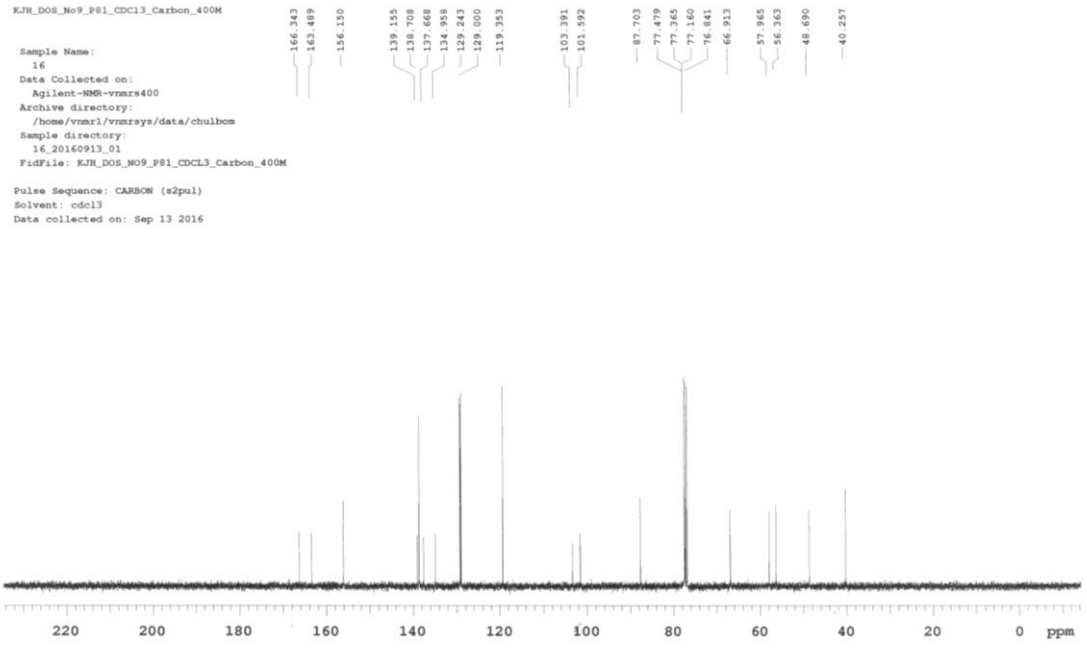
KJH_DOS_No9_P81_CDCl3_Carbon_400M
Sample Name:
16
Data Collected on:
Agilent-NMR-vnmrs400
Archive directory:
/home/vnmrl/vnmrsys/data/chulbom
Sample directory:
16_20160913_01
FidFile: KJH_DOS_NO9_P81_CDCL3_Carbon_400M
Pulse Sequence: CARBON (s2pul)
Solvent: cdcl3
Data collected on: Sep 13 2016
166.343
163.489
156.150
139.155
138.708
137.668
134.958
129.243
129.000
119.353
103.391
101.592
87.703
77.479
77.365
77.160
76.841
66.913
57.965
56.363
48.690
40.257
220
200
180
160
140
120
100
80
60
40
20
0
ppm

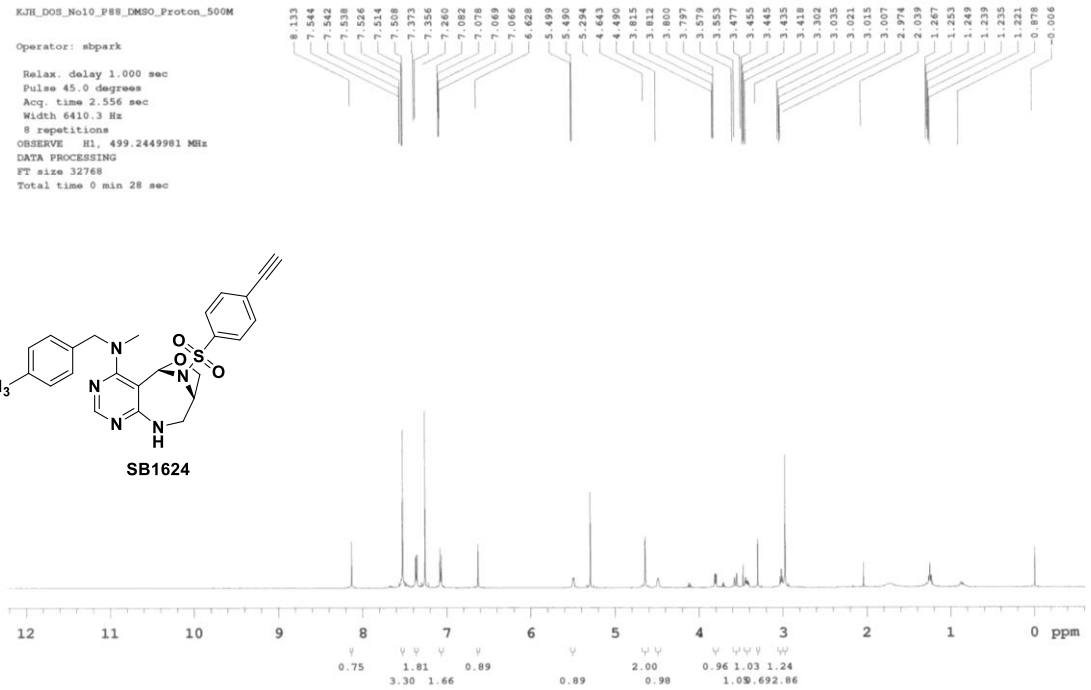
KJH_DOS_No10_P88_DMSO_Proton_500M
Operator: sbpark
Relax. delay 1.000 sec
Pulse 45.0 degrees
Acq. time 2.556 sec
Width 6410.3 Hz
8 repetitions
OBSERVE H1, 499.2449981 MHz
DATA PROCESSING
FT size 32768
Total time 0 min 28 sec
SB1624
ppm

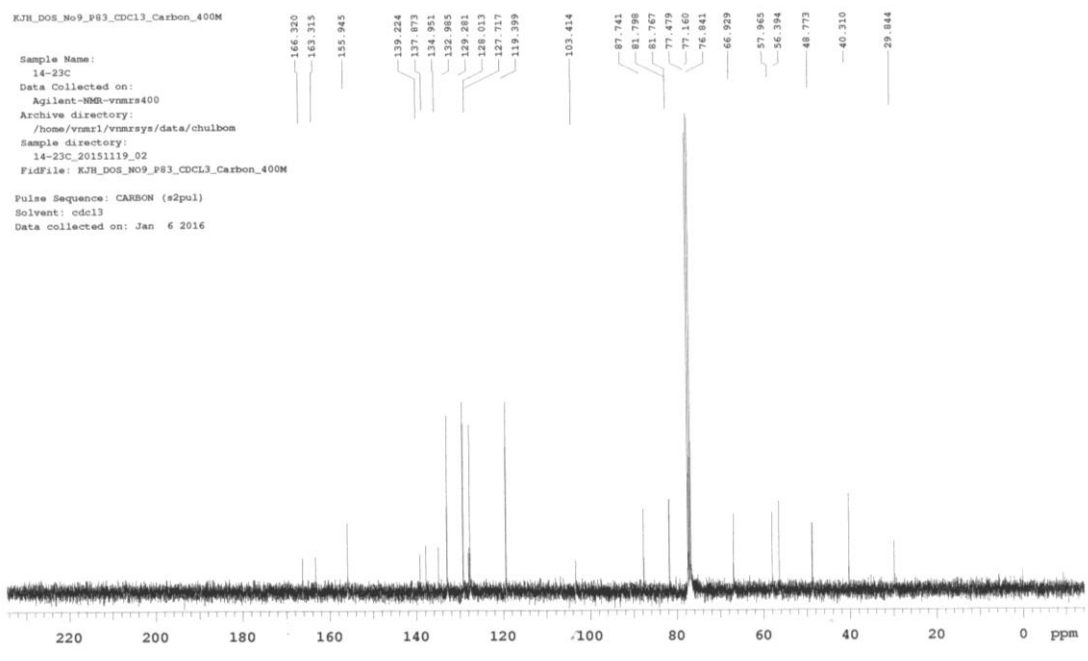
KJH_DOS_No9_P83_CDCl3_Carbon_400M
Sample Name:
14-23C
Data Collected on:
Agilent-NMR-vnmrs400
Archive directory:
/home/vnmr1/vnmrsys/data/chulbom
Sample directory:
14-23C_20151119_02
FidFile: KJH_DOS_NO9_P83_CDCL3_Carbon_400M
Pulse Sequence: CARBON (s2pul)
Solvent: cdcl3
Data collected on: Jan 6 2016
ppm

References

[1] H. Park, J. Ha, J. Y. Koo, J. Park, S. B. Park, *Chem. Sci.* **2017**, *8*, 1127–1133.

[2] P. Kranz, F. Neumann, A. Wolf, F. Classen, M. Pompsch, T. Ocklenburg, J. Baumann, K. Janke, M. Baumann, K. Goepelt, H. Riffkin, E. Metzen, U. Brockmeier, *Cell Death & Disease* **2017**, *8*, e2986.

[3] C. Kilkenny, W. J. Browne, I. C. Cuthill, M. Emerson, D. G. Altman, *PLoS Biol.* **2010**, *8*, e1000412.

[4] a) B. Y. Choi, B. G. Jang, J. H. Kim, B. E. Lee, M. Sohn, H. K. Song, S. W. Suh, *Brain Res.* **2012**, *1481*, 49–58; b) B. Y. Choi, S. H. Lee, H. C. Choi, S. K. Lee, H. S. Yoon, J. B. Park, W. S. Chung, S. W. Suh, *Transl. Res.* **2019**, *207*, 1–18.

[5] T. M. Kauppinen, Y. Higashi, S. W. Suh, C. Escartin, K. Nagasawa, R. A. Swanson, *J. Neurosci.* **2008**, *28*, 5827–5835.

[6] J. Tsenter, L. Beni-Adani, Y. Assaf, A. G. Alexandrovich, V. Trembovler, E. Shohami, *J. Neurotrauma* **2008**, *25*, 324–333.

[7] H. Ghazale, N. Ramadan, S. Mantash, K. Zibara, S. El-Sitt, H. Darwish, F. Chamaa, R. M. Boustany, S. Mondello, W. Abou-Kheir, J. Soueid, F. Kobeissy, *Behav. Brain Res.* **2018**, *340*, 1–13.

[8] H. Tak, M. M. Haque, M. J. Kim, J. H. Lee, J. H. Baik, Y. Kim, D. J. Kim, R. Grailhe, Y. K. Kim, *Plos One* **2013**, *8*, e81682.

[9] J. Kim, H. Kim, S. B. Park, *J. Am. Chem. Soc.* **2014**, *136*, 14629–14638.

[10] a) J. Park, M. Koh, J. Y. Koo, S. Lee, S. B. Park, *ACS Chem. Biol.* **2016**, *11*, 44–52; b) H. Park, J. Y. Koo, Y. V. Srikanth, S. Oh, J. Lee, J. Park, S. B. Park, *Chem. Commun. (Camb)* **2016**, *52*, 5828–5831.

[11] J. Kim, J. Jung, J. Koo, W. Cho, W. S. Lee, C. Kim, W. Park, S. B. Park, *Nat. Commun.* **2016**, *7*, 13196.